FACULDADE DE ENGENHARIA DA UNIVERSIDADE DO PORTO

Person Authentication in Hazardous Work Environments: Exploring ECG and Respiration Signals as a continuous biometric method

Mafalda Alexandra Faria Ferreira

Mestrado em Engenharia Eletrotécnica e de Computadores

Supervisor: João Paulo Cunha

August 9, 2023

Resumo

Nos últimos anos, têm sido feitos avanços significativos no desenvolvimento de métodos biométricos mais seguros e confiáveis, que envolvem a medição e análise das características físicas ou comportamentais de um indivíduo. Uma tendência emergente nesse domínio é a utilização de características fisiológicas como traços biométricos, com os *wearable devices* desempenhando um papel fundamental na aquisição desses sinais de forma não invasiva e confortável. Esses dispositivos oferecem a possibilidade de monitorar a saúde de um indivíduo durante as atividades diárias, tornando-os altamente relevantes no mundo automatizado moderno.

Esta tese de mestrado explora a aplicação de *wearable devices* na aquisição de sinais fisiológicos e seu papel no reconhecimento individual, particularmente em contextos de saúde e segurança. Especificamente, o foco é um processo de identificação humana baseado no eletrocardiograma (ECG), bem como a investigação se há vantagem na integração de sinais de respiração com sinais de ECG para fins de identificação em ambientes de trabalho de alto risco, como bombeiros, por exemplo. Nessas situações, os trabalhadores frequentemente precisam usar equipamentos de proteção (como luvas, capacetes, óculos, roupas à prova de fogo, entre outros) que inviabilizam métodos de identificação mais tradicionais, como digitar códigos ou leitura de impressões digitais. Nesse contexto, a utilização de sinais biológicos medidos continuamente por *wearable devices* constitui uma alternativa viável. Para garantir a praticidade de uma futura utilização em *wearable devices* com capacidades de processamento limitadas, são examinados modelos de classificação baseados em métodos tradicionais de *machine learning*.

A pesquisa inclui a aquisição de um conjunto de dados de 24 pessoas, submetido e aprovado pela comissão de ética da instituição INESC TEC. Além disso, também inclui a validação dos sinais coletados, tanto de respiração quanto de ECG, pelo dispositivo VitalSticker produzido no INESC TEC. Além disso, foi realizado um estudo envolvendo diferentes algoritmos de *machine learning* aplicados ao conjunto de dados coletados. Como entrada para os algoritmos utilizados, o conjunto de dados foi dividido em grupos de 24, 10 e 5 pessoas, fornecendo dados de respiração e ECG em todos eles. Os resultados demonstram que o classificador Support Vector Machine supera os outros métodos nos casos em que apenas os sinais de ECG são utilizados, e o classification Random Forest nos casos em que é utilizada a combinação dos sinais de ECG com a respiração. Os resultados revelam que os sinais de ECG isoladamente apresentam alta *accuracy* no processo de identificação, alcançando 86% de *accuracy* com o conjunto de dados de 10 pessoas. A avaliação predominante de 10 pessoas é devida a ser o número mais próximo de indivíduos designados para compor uma equipe responsável por um trabalho de alto risco. No entanto, quando combinados com os sinais de respiração, os valores de *accuracy* aumentam, atingindo 91% com o mesmo conjunto de dados de 10 pessoas, apoiando a hipótese de que a combinação dos sinais de ECG com a respiração seja vantajosa com os dados adquiridos nesta pesquisa.

Este trabalho destaca a importância dos *wearable devices* na melhoria das medidas de segurança, ressaltando os problemas e as oportunidades relacionados à coleta de sinais fisiológicos e sua utilização em ambientes de trabalho de alto risco.

Abstract

In recent years, significant advancements have been made in the development of more secure and reliable biometric methods, which involve measuring and analyzing an individual's physical or behavioral characteristics. An emerging trend in this field is the use of physiological features as biometric traits, with wearable devices playing a crucial role in non-invasively and comfortably acquiring these signals. These devices offer the possibility of monitoring an individual's health during daily activities, making them highly relevant in the modern automated world.

This master's thesis explores the application of wearable devices in acquiring physiological signals and their role in individual recognition, particularly in health and safety contexts. Specifically, the focus is on a human identification process based on electrocardiogram (ECG), as well as investigating whether there is an advantage in integrating respiratory signals with ECG signals for identification purposes in high-risk work environments, such as firefighters. In such environments, workers often need to wear protective equipment (such as gloves, helmets, goggles, fire-resistant suits, among others) that make more traditional identification methods, like typing codes or fingerprint reading, ineffective. In this context, the continuous measurement of biological signals by wearable devices offers a viable alternative. To ensure the feasibility of future use in wearable devices with limited processing capabilities, classification models based on traditional machine learning methods are examined.

The research involves acquiring a dataset of 24 individuals, which was submitted to and approved by the ethics committee of the INESC TEC institution. Additionally, it also includes validating the collected respiratory and ECG signals using the VitalSticker device developed at INESC TEC. Furthermore, a study involving different machine learning algorithms applied to the collected dataset was conducted.As input to the algorithms used, the dataset was divided into groups of 24, 10, and 5 individuals, with both respiratory and ECG data provided in all of them. The results demonstrate that the Support Vector Machine classifier outperforms other methods when using only ECG signals, and the Random Forest classifier when combining ECG with respiratory signals. The findings reveal that ECG signals alone exhibit high accuracy in the identification process, achieving 86% accuracy with the 10-person dataset. The predominant evaluation of 10 individuals is due to it being the closest number of designated individuals for a high-risk work team. However, when combined with respiratory signals, the accuracy values increases, reaching 91% with the same 10-person dataset, supporting the hypothesis that combining ECG and respiratory signals is advantageous with the data acquired in this research.

This research highlights the importance of wearable devices in enhancing safety measures, addressing the issues and opportunities related to collecting physiological signals and their utilization in high-risk work environments.

Acknowledgements

I conclude this stage of my life with this work, which challenged me as a student and future professional. The development of this work was only possible with the collaboration of exceptional people to whom I offer my sincere gratitude.

In the first place, I want to express my deep gratitude for the opportunity to collaborate with great people at INESC TEC. I thank my supervisor, João Paulo Cunha, and Duarte Dias, for their invaluable guidance, support, and expertise throughout my work. They helped me be more critical and encouraged me to pursue more and more. In particular, I would like to thank Francisco and Vitor for their direct assistance on my work and Rute and Beatriz for all the help with my integration. The fantastic work environment they brought to the group and the encouragement they gave me when I needed it was invaluable.

To all the participants in my study, I want to thank you for taking the time to join me in this project and be a part of it. I am thankful for the patience, kind words, and advice I received.

I would like to express my sincere thanks and appreciation to my family for their unwavering love, encouragement, and support throughout my academic journey. Their belief in me has been a constant source of strength and motivation. Without their support and love, my journey would never have been so fulfilling. A special thanks to my grandmother for all she taught me. Unfortunately, she could not be here at the end of this journey, but I hope she would be proud.

Finally, I would like to express my gratitude and appreciation to my dear friends who have been a beacon of support during my academic years. A bigger thank you for all the moments that we lived together that will forever be kept with me. I feel safe in their friendship and treasure the moments of laughter and respite we had together.

Mafalda Alexandra Faria Ferreira

Contents

List of Figures

List of Tables

Abbreviations and symbols

ANN	Artificial Neural Networks
BLE	Bluetooth Low-Energy
CNN	Convolution Neural Networks
CSI	Channel State Information
EMD	Empirical Mode Decomposition
ECG	Electrocardiography
FWPT	Fuzzy Packet Wavelet Transformation
GBDT	Gradient Boosting Decision Tree
HR	Heart Rate
IoT	Internet of Things
KNN	K-Nearest Neighbour
LoRa	Long Range radio
ML	Machine Learning
NN	Neural Network
PCA	Principle Component Analysis
PPE	Personal Protective Equipmen
SVM	Support Vector Machine
WHD	Wearable Health Device

Chapter 1

Introduction

1.1 Context

Wearable health devices are an emerging technology not only for clinical markets but also for accessing the well-being of a person. These devices measure and monitor different physiological signals in scenarios such as an individual's daily activities or even hazardous scenarios. The principal advantages of these devices for the aforementioned cases are the low computational effort and the low energy consumption requirements. Moreover, the small size of these devices and the integration of textiles and electronics becomes another benefit for the user's comfort.

In hazardous working environments where safety is paramount, implementing biometric identification methods becomes crucial, particularly for professionals in industries such as oil and gas maintenance, emergency interventions, and industrial firefighting. These environments often involve high temperatures and necessitate Personal Protective Equipment (PPE) clothing, making conventional identification techniques impractical.

PPE is the equipment worn to minimize exposure to hazards that cause serious workplace injuries and illnesses, and it is classified into four categories of protection: eye and face, hand, body, respiratory, and hearing. There are PPE levels of clothing, which means a individual can use some of this clothing to protect one of the four categories or all of them, at figure 1.1 there are some examples of them. Dangerous situations lead us to re-think physiological biometrics requiring a vital human signal, namely their electrocardiogram (ECG) or respiration signal, as an option for authenticating a subject.

The inherent risks associated with these professions highlight the need for stringent access control measures in hazardous or high-security facilities. In such scenarios, traditional identification methods like face, fingerprint, or retina recognition may prove incompatible or unreliable due to the inability to expose a part of the body while wearing PPE clothing. To address these challenges, physiological biometric technologies that leverage vital human signals have become increasingly relevant. These technologies utilize physiological signals such as electrocardiogram (ECG) and respiration, which can be acquired even when the individual is wearing full-body PPE attire. Employing these vital signs as authentication mechanisms significantly reduces the risk of

forgery, as these signals are inherently unique to each individual and challenging to replicate or copy.

With industry 5.0, the main paradigm "is the shift of focus from technology-driven progress to a thoroughly human-centric approach"[1]. The human-machine collaboration in hazardous environments emphasizes the importance of specialized human interventions while ensuring optimal performance and efficiency. By implementing physiological biometric identification methods, rigorous access control can be maintained, allowing only qualified personnel with verified vital signals to access hazardous or high-security areas. This advanced authentication approach enhances security and enables seamless operations in environments where traditional identification methods would be impractical or incompatible.

Human authentication is the ability to verify that a user is indeed the individual they claim to be within a specific system, granting or denying privileges accordingly. On the other hand, identification refers to possessing unique characteristics that set an individual apart from others. The authentication process implies that exists an identification process as well. [2]

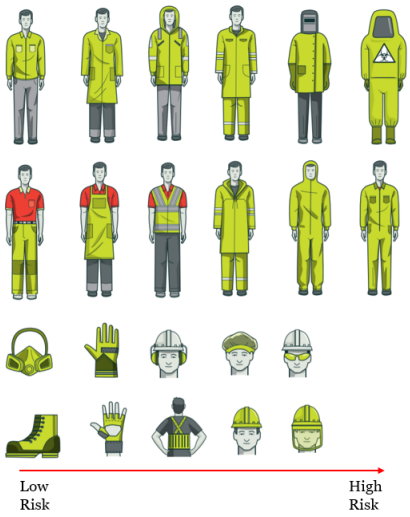

Figure 1.1: Examples of PPE clothing [3]

Electrocardiography (ECG) is a physiological biometric technique that gives information about the heart's structure and operation. ECG signals are a recent and less used method of biometric identification, but literature confirmed that fiducial ECG features and heartbeat waveform are possible approaches for human identification. Consequently, these signals correspond to an option when the traditional identity recognition methods are unreliable, or their acquisition is unfeasible, but the use of electrodes is possible. Additionally, ECG biometric systems can continuously monitor the identity [4] and the health of the users, because this signal is unique and intrinsic to each individual. Wearable devices are more than suitable to monitor ECG continuously, and combined with an identification algorithm can easily provide authentication information, working as a biometric continuous method.

On the other hand, at an exploratory level, it would be interesting to verify the role and benefit of using respiration signals in the identification and monitoring of an individual operating in hazardous scenarios. The respiration signals are another important vital indicator for human beings. There are a few studies about their contribution to identifying a subject. However, respiration signals as a complement to ECG data might increase the performance of classifying methods. Wearable devices can acquire both of these types of signals.

1.2 Motivation

In a world where technology is always around us, the better way to use it is to help someone or facilitate our lives. The possibility of monitoring and making the work of professionals easier with wearable devices has made this topic grow in recent years.

The real-time monitoring of professionals engaged in hazardous occupations holds great potential for enhancing their work efficiency and ensuring their well-being. Wearable devices equipped with sensors can provide valuable insights into vital signs, enabling timely interventions and preventing potential health risks. This capability not only contributes to the improvement of working conditions but also promotes the overall safety and productivity of professionals.

Moreover, wearable devices provide a unique chance to improve authentication processes with minimal user intervention. These devices can provide a safe and seamless authentication mechanism by gathering essential signals such as ECG and other physiological data. Continuous real-time transmission of these signals enables the creation of robust identification systems capable of reliably recognising individuals. This technology eliminates the need for traditional authentication methods such as passwords or physical tokens, expediting the authentication process while increasing security.

Combining the benefits of wearable technology, real-time capture of biometric signals, and continuous transmission for authentication purposes could revolutionise how people are authenticated. This innovative approach has the potential to provide faster, more secure, and user-friendly authentication experiences, improving efficiency and convenience in various domains.

Given these considerations, this research aims to investigate the possibilities of wearable devices and vital signal-based authentication systems. This study intends to contribute to developing efficient, secure, and non-intrusive authentication systems for a wide range of applications by investigating the integration of real-time vital signals and continuous transmission.

1.3 Objetives

This master's thesis aims to contribute to advancing wearable technology for continuous signal acquisition and improving the reliability of human identification systems based on biometric data. Particularly, in working enviroments where workers often need to wear protective equipment and are not able to remove it to be identificated. The focus will be on studying and assisting in improving the bioemtrics capabilities of the wearable device produced by INESC TEC, VitalSticker

[5]. This device collects ECG and respiration signals, and the objective is to enhance its accuracy for more precise data acquisition.

This works starts by acquiring a 24 subjects dataset, after its design, submission and approval by the institutional Ethics committee. With the data collected, a study will be perfomed to comprove the VitalSticker device signal quality against Medical Certificated devices (for the ECG and the respiration signals). Additionally, a ECG-driven human identification approach will be implemented and compare it to the related literature [4]. Furthermore, this research will look into the relationship between respiration patterns and biometric identification and develop appropriate feature extraction and merging approaches to investigate the eventual benefit of the combination between ECG and respiration data. It will be used tradicional machine learning approaches for the identification process with the data collected.

To summarise, the following are the dissertation's objectives:

- Study and comprove the signal quality of the wearable device produced by INESCTEC, VitalSticker, which collects ECG and respiration signals.
- Acquire Electrocardiogram (ECG) and Respiration signals from VitalSticker device.
- Develop an ECG-based human identification, using the data acquired with VitalSticker
- Investigate the potential benefits of incorporating respiration data alongside ECG signals in the human identification system.
- Conduct research and training on machine learning approaches to develop a robust biometric classification method

1.4 Contributions

This section outlines the contributions made in this research, which focuses on leveraging wearable devices for human identification based on electrocardiogram (ECG) and respiration signals acquired by VitalSticker device.

This master's thesis made also a significant contribution by co-authoring an article titled 'VitalSticker: A novel multimodal physiological wearable patch device for health monitoring' [5], which focused on the wearable device used in this research. This article was successfully accepted at the renowned ENBENG 2023 conference, highlighting its academic and scientific significance. The acceptance and presentation of this work in the conference proceedings emphasises the recognition and importance of the wearable device research. It attests to the developments and insights achieved by using this device, as well as establishing its significance in the sector. The article's collective effort displays the commitment to advance the understanding and application of wearable technology in real-world applications. The accepted paper can be depicted in appendix C.

1.5 Document Structure

The document structure of this master's thesis is organized into several chapters, each contributing to a comprehensive presentation of the research. The first chapter (1) serves as the introduction, providing the necessary context and motivation for the study. It outlines the objectives to be achieved throughout the thesis.

The second chapter (2), titled "State of the Art," establishes a solid foundation and understanding of the current state of the technology areas relevant to this research. It includes thoroughly examining the field's accomplishments and trends, establishing the framework for the succeeding chapters.

Chapter 3, focuses on the methodology employed in this research. It begins by describing the signal acquisition process and provides detailed insights into the dataset collected. It also delves into signal validation and analysis techniques, presenting a systematic approach to handling and interpreting the collected signals.

In Chapter 4, the emphasis shifts towards the performance evaluation of the machine learning classifiers for human identification. This chapter examines the classifiers' effectiveness and tests their capacity to reliably classify individuals based on biometric signals, ECG and Respiration.

Finally, Chapter 5 has the study's conclusion, summarizing the key findings and insights derived from the research. Moreover, it offers valuable suggestions for potential future work in the field of biometric identification using vital human signals, paving the way for further advancements and innovation in this area.

Chapter 2

State of the Art

The perspective of monitoring the human health, identification processes of professionals working in hazardous situations, like firefighters, leads to the combination of wearable devices and biometric recognition areas. This section provides state of the art in these two areas and discusses typical vital signal processing and possible classification procedure for identifying subjects.

2.1 Wearable Devices for physiological monitoring in hazardous scenarios

The modernization and automation of the world require more specialized people to do the maintenance of machines or places that might have a high level of danger. Nowadays, the combination of this factor and the requirement for workers' well-being in risky professions are significant factors for the industry. The better way to achieve these specifications is to monitor continuously the employees' health to assure their safety and protection. Additionally, guaranteeing the security of the restricted places they need to work on is another crucial factor to have in account. If besides transmitting vital parameters from the users, was possible to control the access of restricted and dangerous areas, that might be a huge help to companies leading with these recent problems.

Wearable devices can be a solution to the problems described previously. According to the International Data Corporation, the wearable shipment volume is expected to grow 12.4% and reached approximately 637.1 million units in 2024 [6].

Therefore, wearable health devices are increasingly helping self-tracking as well as providing data to health professionals. These devices include electronics in small dimensions that are easily adaptable and have the advantage of minimising discomfort and interference with daily human activities. Use different sensors which can detect and analyse the physical and physiological status of the human body [7]. Additionally, wearable devices have the benefit of having a lower cost, higher processing speed and mobility and sensibility while the data is being collected. It represent an advantage when used in hazardous scenarios, because it does not cause any impediment for workers to perform their tasks.

Wearable devices can have various forms, from wristwatches, ear devices, adhesive patches, or even t-shirts with embedded electronics, which help create the concept of smart textiles. The materials used to develop these devices need to be flexible and have a large diversity of sizes and shapes to be more customised for individuals. A good fit to the human body improves the quality of the signal collected and also reduces the noise from the measurement [8].

2.1.1 Generic system architecture

The generic architecture of wearable health device (WHD) systems can be expressed in Figure 2.1. This architecture might be used in the future for an advanced phase of this dissertation. This picture separates the different phases of how the process of collecting the vital signal works with a wearable device.

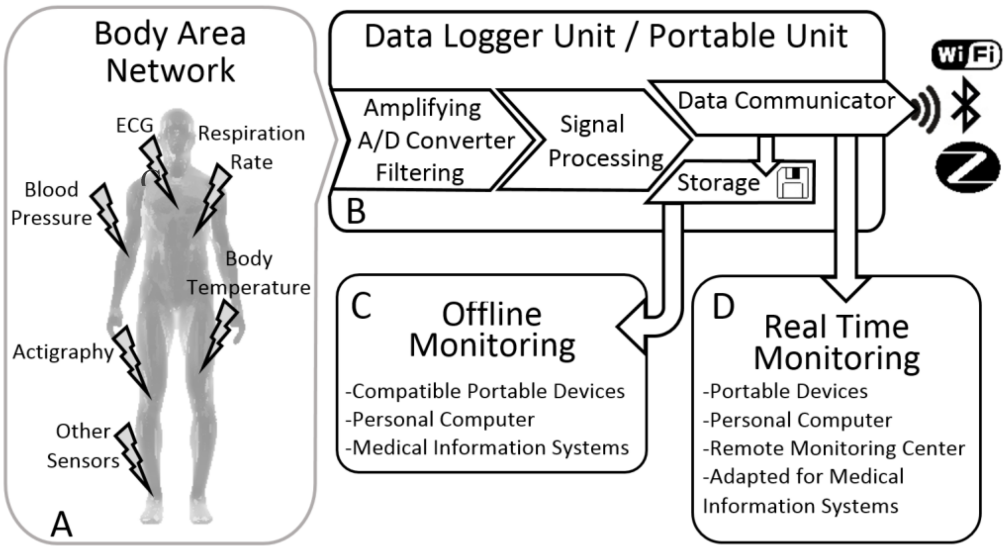

Figure 2.1: Architecture of wearable devices system [9]

The first phase (A - 2.1) designed for Body Area Network (BAN) involves low-cost, low-power consumption, and small sensor nodes. The nodes are responsible for capturing the signals, pre-processing them, and also have communication capabilities. Second phase (B- 2.1) is where the vital signals are received. The portable unit is responsible for amplifying or filtering the signals collected and transforming them into digital ones. Additionally, the portable unit also extracts the features from the vital parameters. Furthermore, the raw data received can be transmitted or stored in a local memory to be processed or used after (C- 2.1 – offline monitoring).

The principal wireless protocols for transmitting the data acquired are Bluetooth, Wi-fi, ZigBee, and LoRa (Long Range radio). They differ mostly in the maximum range and data rate transmission and also power consumption. The LoRa is the one with more maximum range, the Wi-fi is the one with the maximum data rate, and finally, the Bluetooth has less power consumption. The lower requirements of power consumption and cost of Bluetooth make them an ideal candidate to be used in wearable devices. Moreover, Bluetooth Low-Energy (BLE) is a recent technology that

consumes even less power, is also of short-range frequency, and enables incorporation in small devices, like wearable devices [9].

Real-time monitoring (phase D) is another feature associated with the use of wearable devices. This offers the possibility of people monitoring themselves while they perform daily activities, because with the data transmission via Bluetooth, they have free and easy access to their vital signals [9].

2.1.2 Vital Parameters

Wearable devices can be comfortable and noninvasive when continuously monitoring a human's vital signals. Some physiological signals they can measure are body, temperature, heartbeat, respiration rate, and blood pressure. These signals are useful for fitness monitoring and medical diagnosis.

This section describes how the process of acquiring some vital signals from wearable devices works. More particularly, the ECG and respiration signals because they will be used in the following stages of this dissertation.

2.1.2.1 Electrocardiogram

As it was mentioned before, an electrical sensor in a wearable device is capable of collecting heart activity. To obtain electrocardiography in used skin electrodes that capture the depolarisation from the heart. This process conventionally uses 12 electrodes and an electrode gel. However, this can be done with two electrodes on the chest which offers a more practical way to integrate into wearable devices[8]. Wearable devices can measure a simple heart rate and an ECG waveform, depending on the sensor and the quality of the signal collected. The literature defends that exist three types of devices that acquired heart activity: (1) Heart Rate (HR) – devices that collect R-peaks but not the entire ECG waveform; (2) R-R interval – devices that acquired the time difference between R-peaks in ECG signals; (3) ECG – devices that can collect the ECG waveform. In figure 2.2 is possible to visualise some of the wearable devices described [9].

An electrocardiogram (ECG) is a physiological signal that measures the contraction and recovery of the heart. ECG uses electrodes attached to the skin of a person to describe the activity of the heart and provide information about the heart rate, rhythm, and morphology[4]. The contraction of the heart muscle generates electrical currents which represent the polarization and depolarization of the heart. The electrodes measure that current, and the signal resulting is called ECG.

A normal ECG consists of a P wave, a QRS complex, and a T wave (Figure 2.3). This information is the key to ECG-based biometrics. The first wave (P) results from the depolarisation of the heart and starts with the atrial contraction. The QRS complex is the combination of the Q, R, and S waves, and results from the depolarisation of the ventricles that came before their contraction. This complex has the largest amplitude of the waveform and depends on the heart rate, so the lower the heartbeat is, the wider the QRS complex [10]. Additionally, the temporal distances QR and RS are asymmetric and can change with the heart rate or respiration [4]. Finally, the T wave

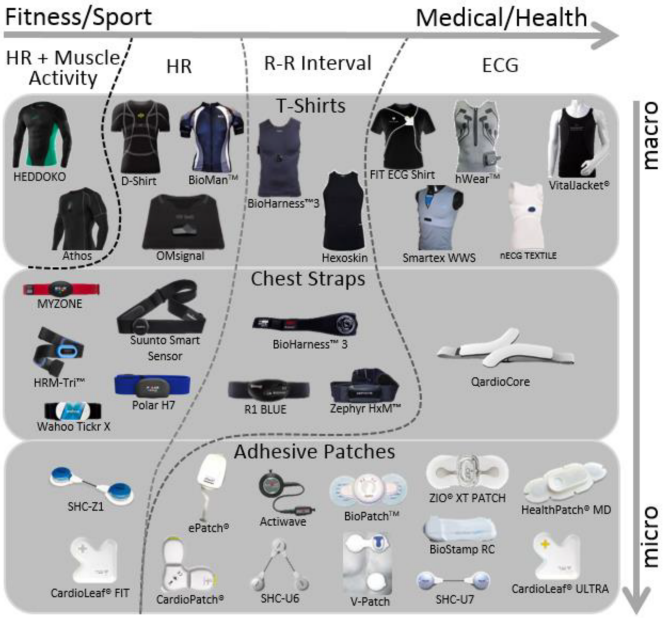

Figure 2.2: Heart activity trackers divided [9]

represents the repolarization of the ventricles and occurs approximately 300 milliseconds after the QRS complex. Following the T wave, the U wave occurs as a low-amplitude wave that may not always be visible. ECG is a valuable tool for diagnosing cardiac diseases for being painless, easy to measure, and non-surgical[10]. Figure 2.3 and table 2.1 show the format of a ECG waveform and the its features with a brief description of them.

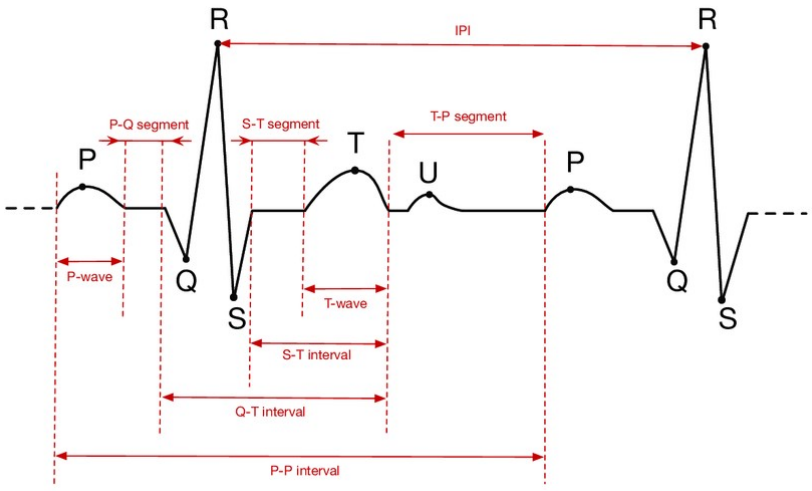

Figure 2.3: ECG waveform and fiducial points [11]

Feature	Description	Duration
RR interval	The RR interval represents the duration between two consecutive R-waves (ventricular depolarization) on the ECG waveform.	0.6-1.2s
P wave	P-wave represents atrial depolarization	80-120ms
PR interval	The PR interval represents the duration from the beginning of the P-wave to the start of the QRS complex, reflecting the time taken for the electrical signal to travel from the atria to the ventricles.	120-200ms
QRS complex	The QRS complex represents ventricular depolarization, indicating the contraction of the ventricles.	70-120ms
ST interval	The ST interval represents the time between the end of the QRS complex and the beginning of the T-wave. It reflects the early phase of ventricular repolarization	120ms
T wave	The T-wave represents ventricular repolarization, indicating the recovery of the ventricles.	< 250ms
QT interval	The QT interval represents the total duration of ventricular depolarization and repolarization. It is measured from the beginning of the QRS complex to the end of the T-wave.	420ms
U wave	The U-wave is a small and often subtle waveform that follows the T-wave.	<100ms

Table 2.1: ECG features [12] [13] [14]

2.1.2.2 Respiration signal

The sensors capable of collecting respiration signals can do it by measuring the flow of breath, the pressure in the chest, and the expansion or contraction of the abdomen during breathing. Most sensors, in contact with skin, detect the body's volume or pressure change. For that, the wearable device must be as comfortable as possible and have a high level of sensibility. Some examples of sensor technologies are acoustic, resistive, inductive, acceleration, pressure, electromyography, impedance, and infrared. The materials used to measure this type of signal must be conductive or dielectric. After acquiring the signal, to remove interference and noise from the body motion, it is usually used band-pass filters [8].

The respiration signal represents the breathing process, including a pattern of inhalation and exhalation. Inspiration or inhalation involves the contraction of the diaphragm and the expansion of the chest cavity or abdomen because of the increased airflow drawn into the lungs. Opposite in the expiration or exhalation occurs the relaxation of the diaphragm and the chest cavity returns to a rest position. In this phase, the airflow into the lung decrease. The respiration rate is an essential parameter for health monitoring. This parameter refers to the number of breaths taken in a minute and indicates the frequency of the respiration signal and the pace of the breathing cycle.

Figure 2.4 presents a recording of human breathing, representing an example of the respiration signal that can be captured from a wearable device.

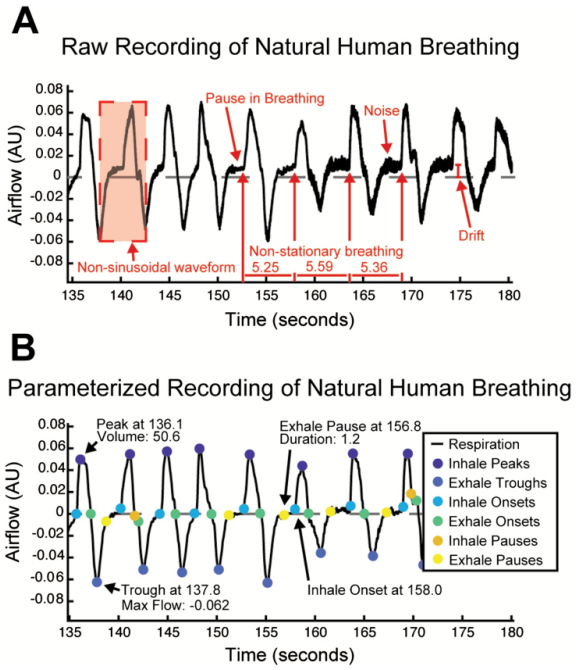

Figure 2.4: (A) Human respiration signal (B) The same respiration signal after removing drift and noise, and estimating features with BreathMetrics [15]

2.2 Biometrics recognition methods

Biometrics is the measurement of unique physiological characteristics for identification purposes that can be used for digital authentication and access control. Biometric technology makes signing into accounts and security protocols quicker and easy for the user and much harder for possible attacks. However, there is a risk of fraud or identity theft with the increased use of biometric data.

Biometric data can be derived from an individual's intrinsic characteristics (biometric recognition) that include anatomical (such as the face, fingerprints, and iris), physiological (electrocardiogram, electroencephalogram, photoplethysmogram), and behavioral traits (the way of walk)[16].

The principal advantages of biometric security are the considerable difficulty of hacking because of the extreme complexity and randomness of biometric data, which is fast and easy to obtain from the user, and always available wherever a person is without additional authentication devices. These factors make biometric recognition a good choice for cases like public security, military operations, healthcare or commercial applications, remote access, or even travel control. In hazardous scenarios, where the workers need to use PPE clothing, physiological biometrics are increasingly gaining importance, because there are the best and sometimes the unique way to restrict access to diverse areas. This type of biometric security will guarantee not only the monitoring of the individuals but also prevent unwanted people to enter private and reserved places.

The first technologies to be explored in the field of biometrics were fingerprint, retina, face, iris, and voice recognition. The principal and more robust recognition techniques are face and fingerprint recognition, and the last one is considered the most mature, with algorithms that obtain the best accuracy levels[4]. However, there are many drawbacks to both of them that introduce

variability to the features and compromise the ability of the classifier. Some factors are the modifications in a person's facial expressions depending on her emotional state, the person's age, and also the environment, because the algorithms are highly influenced by, for example, illumination. Furthermore, in the case of fingerprint recognition, the use of synthetic material or unconstrained environments compromises the acquiring data process which leads to the rejection of the inputs[4]. The most widely used methods with good performance require an algorithm with high complexity at the computational level.

Figure 2.5 presents a comprehensive overview of the speed rates associated with various biometric methods, as documented in the literature. The analysis reveals that fingerprint and hand geometry exhibit relatively slower speeds among the considered methods, while iris recognition stands out as the fastest method available.

Biometric Method Type	Speed Rate (SR)
Facial Recognition	3-30 seconds
Speech Recognition	5-30 seconds
Vein Pattern Recognition	2-40 seconds
Hand Geometry Recognition	≈0.6 seconds-10 minutes
Iris Recognition	2-5 seconds
Signature Recognition	3-5 seconds
Fingerprint Recognition	20 seconds-1 minute and 45 seconds
Face + Fingerprint Recognition	≈5 minutes
Retina Recognition	6-15 seconds

Figure 2.5: Speed Rate (SR) range values for some state-of-the-art biometrictechniques [4]

2.2.1 Electrocardiogram biometry

In order to overcome aspects that can affect the algorithm to identify a subject that was aforementioned, the ECG was introduced as an option for biometrics. ECG, besides providing liveliness detection, confers information to identify a subject[4].

ECG signals present a variability intra-subject and inter-subject. The first is mainly explored for health statistics and monitoring while, the second is useful to distinguish individuals in biometric recognition. Both variabilities fall in the heart geometry, amplitude, and duration between the fiducial points, cardiac conditions, or electrode characteristics and placement [17]. This inter-subject variability confers the ECG information on identity and guarantees that the ECG signal is difficult to steal and mimic which represents a high-security measure to use for recognition[4], [16].

The goal of the ECG biometric methods is to recognize a person in less time as possible with a fewer computational cost to use in wearable devices[4]. With the advance of the years, the heartbeats needed to ensure a good classification and identification of a subject using ECG tend to be less. It started with the information extracted from 10 heartbeats and an accuracy of 98%, but with a high computational cost and a complex implementation [18]. However, recently is,

already possible to achieve an accuracy of 97.5% with a only two heartbeats and with a method computational simpler and embedded in a small device [4].

For biometric identification systems using ECG signals, the following steps are usually covered: (1) preprocessing of ECG data; (2) feature extraction; (3) classification process [19].

The acquisition process is susceptible to noise and interference, and the ECG data depend on the characteristics and placement of the electrodes. Because of that, there is a need for preprocessing of the data. In approaches for on-the-person signals, the most used techniques to remove noise and interferences are using bandpass, lowpass, highpass, and notch filters[17].

(1) Preprocessing: In order to facilitate the calculation of PQRST points and the filtering/smoothing of signals in the context of ECG analysis, it is essential to perform a preprocessing step on the raw ECG signal [20]. The raw signal often contains different types of noise, including baseline drift, high-frequency noises, and interference from external components. These noise types can be caused by muscle movements, external interferences, and other activities [20].

Preprocessing plays a crucial role due to the susceptibility of ECG signals to noise interference [17]. The term "artefact" is commonly used to describe non-natural components that can disrupt ECG signals. Artefacts result from electrical disturbances caused by factors such as electrical noise within the body, external sources, improper placement of electrodes, or hardware malfunctions [21]. It is important to note that the placement of electrodes influences the amplitude and shape of the ECG waveform, with greater distances between electrodes resulting in weaker signal acquisition [17].

Removing artefacts is essential to interpret the heart's waveform accurately. ECG signals exhibit various types of noise sources and artefacts [17]. These include:

- **Powerline interference (AC interference):** This interference arises from the sinusoidal current of the acquisition equipment's energy source, potentially altering the electrical frequency (typically 50Hz in Europe). Consequently, the interference appears as high-frequency noise and a thickened ECG line in the signal. Causes of this interference may include disconnected electrodes or electromagnetic interference generated by the power supply [21][22].

- **Baseline wonder:** This noise is caused by patient breathing or movements and dirty or loosely attached electrodes. It leads to low-frequency undulations in the signal baseline, posing challenges in detecting signal peaks [21][22].

- **Electromyographic interference:** Electromyographic signals are induced by the electric impulses used by muscles to contract. These signals can interfere with the collection of ECG signals, resulting in high-frequency, high-amplitude peaks or short-term bursts [21][22].

- **Electrode movement:** Patient movements can alter the skin impedance around the electrodes, causing high-amplitude artefacts in the signal[22].

- **Lead reversal:** This interference refers to the incorrect placement of electrodes, such as reversing leads, which can lead to inaccurate measurements of potentials[21].

By employing appropriate preprocessing techniques, such as using band-pass filters, and applying mean filters for signal smoothing [20], it is possible to address these sources of noise and artefacts. This approach enhances the quality and reliability of subsequent stages of ECG signal analysis in the study.

(2) Feature Extraction: Feature extraction from ECG signals can be accomplished using fiducial points and non-fiducial features. Fiducial point extraction employs temporal features such as the duration of heartbeat waves, time intervals between fiducial points, peak amplitudes, and morphological features [19]. On the other hand, non-fiducial feature extraction involves statistical and transformation techniques[23].

A robust QRS recognition algorithm is crucial in analysing ECG waveforms using various instruments. The erroneous detection of the QRS complex can result in unnecessary data transmission and excessive memory storage of captured ECG segments [24]. However, detecting the QRS complex poses challenges due to its variability and multiple types of noise in the ECG signal. The Pan-Tompkins Algorithm is a commonly used and efficient algorithm for QRS detection. It employs digital filters to mitigate the influence of muscle noise, electrode motion, powerline interference, baseline wander, and high-frequency characteristics of T-waves while simultaneously improving the signal-to-noise ratio [24]. The choice of this algorithm for the dissertation is motivated by its utilisation of integer arithmetic, low memory consumption, and minimal computational time. Consequently, it can be implemented as a real-time filter on the microcontroller (BGM220P) for signal acquisition.

The Pan Tompkins algorithm [24] performs real-time QRS detection by applying processing steps to a digital signal obtained from an analogue-to-digital converter. The algorithm initiates with a bandpass filter to suppress low-pass interference, muscle noise, and T-wave interference. The bandpass filter consists of cascaded low-pass and high-pass filters. Subsequently, the ECG signal undergoes differentiation to extract QRS-complex slope information. The differentiated signal is squared and passed through a moving-window integrator to derive waveform information. The integration window spans 30 samples (150ms). The rising edge of the integrated waveform corresponds to the QRS complex, with the duration representing the width of the QRS complex. The algorithm dynamically adjusts thresholds and limits for the RR interval periodically, accommodating inter-patient variability and changes in ECG morphology within a single patient.

In the Pan-Tompkins algorithm [24], the identification of fiducial points (peaks) relies on changes in signal direction within a specific time interval. It first detects the QRS complex and the corresponding RR interval. The identification of the T-wave occurs when the maximum slope between two consecutive RR intervals is half that of the preceding QRS waveform. This algorithm accurately utilises the ECG signal, with only a 0.675% failure rate in detecting the fiducial points. With the extraction of the principal peaks of an ECG waveform (P, QRS and T), it is possible to calculate time intervals and wave amplitudes that can be included as features to include in the classification algorithm.

Other feature extraction techniques that have been utilised include the Discrete Wavelet Transform (DWT), Continuous Wavelet Transform (CWT), Discrete Cosine Transform (DCT), S-Transform

(ST), and Discrete Fourier Transform (DFT). However, most of these techniques demonstrate a considerable degree of complexity and are time-consuming when it comes to noise removal during the feature extraction process. In contrast, the Pan-Tompkins algorithm necessitates less computational effort while attaining enhanced efficiency [13].

Overall, the combination of preprocessing techniques and the Pan Tompkins Algorithm offers a comprehensive approach to reliable ECG signal analysis, ensuring accurate detection of fiducial points and enhancing the overall interpretation of ECG waveform.

(3) Classification Process: The last step in biometric systems is the identification process, consisting in use of classification methods, such as machine learning models. Some those methods based on the closest distance between samples [25] or classifiers based on distance such as, K-Nearest Neighbour (KNN) or Support Vector Machine (SVM) classifiers [26] [4] which have been widely explored by the literature. In addition, other methods learn the non-linear relations between the input samples. Some examples of that are the Neural Networks (NN) for the QRS detection [27], and the Convolution Neural Networks (CNN) [28] [29]. Another possible option proposed in [19] is a Cascaded CNN composed of the combination of an F-CNN (CNN for feature extraction of heartbeats) and M-CNN (CNN for biometric comparison).

2.2.2 Respiration biometry

Recently, respiration signals have been used as a vital parameter in biometric recognition. This signal like the ECG signal can be measured using different wearable devices and does not require extra effort for the individual to be collected.

Researchers discovered that the breathing pattern is influenced by sex and the thoracoabdominal motion by age [30], but generally breathing movements do not vary significantly with increasing age [31]. Additionally, in the literature, it was found studies that defend the existence of unique characteristics from the respiration signals which makes it possible to identify different subjects from these kinds of signals.

Some methods are free from the involvement of the user and use the Wi-fi infrastructure to recognize unique physiological characteristics of an individual in the user's respiratory motions. Existing studies indicated that respiration motions can distinguish humans without any extra information. The method described in [32] is non-intrusive and can use any Wifi mobile device to automatically identify a user. The process of extracting the features was based on the waveform morphology analysis and Fuzzy Wavelet Packet Transformation (FWPT) of the respiratory signals in Channel State Information (CSI) readings from Wi-fi devices. The interference and noise presented in the data were mitigated with an Empirical Mode Decomposition (EMD) based filter. Furthermore, with a deep learning algorithm, they were able to identify the legitimate user and the existence of spoofing attacks. The results they obtained achieved a 95% authentication success rate, a 92% of accuracy in detecting spoofing attacks, and less than a 5% false positive rate. Another method using Wi-fi devices was described in [33]. The researchers also used CSI of Wi-fi signals to sense human respiration and then were capable of identifying a subject with 97.5% of accuracy for 11 users in different scenarios.

In [34] the combination of respiratory signature extraction feature with machine learning classifiers make it possible to authenticate the identity of a subject. For the separation of the individual's characteristics, a dynamic segmentation algorithm was used, and after a diagonalization of the eigematrices algorithm to isolate the different breathing patterns. Finally, it was used the k-nearest neighbour (KNN) and the support vector machine (SVM) for subject authentication. With these two Machine Learning (ML) classifiers, the accuracy obtained was 97.5% for a two-subject and 98.33% for a single-subject experiment. The SVM algorithm was also used in [35] for the same purpose. Another possible ML algorithm used in other approaches for identifying a subject using respiration patterns was an artificial neural network (ANN) that acquired the data from a knitted piezoresistive smart chest band [36].

Approaches utilizing radar for identifying authentication are other options presented in the literature [37], [38], [39]. Radar has the advantage of not requiring direct contact with the body or an intentional engagement of the individual in the authentication system [39]. Biotag [38] is a continuous user verification system that uses a low-cost Radio Frequency Identification (RFID) technology to find unique physiological signals of the individual's respirations motions. In this method, the extraction of the characteristic with biometric information was based on the waveform morphology analysis and the fuzzy wavelet packet transformation of the respirations signals. The respiration signals showed different amplitudes and patterns from person to person, so the features extracted were generally effective for identifying a user and always available independently of the source of the RFID used for measurements. Additionally, for the classification process, they adapted the gradient boosting decision tree (GBDT) and achieved a 95.2% and 94.8% on verification accuracy on random attack and imitation attack scenarios [38].

Another study has captured the breathing patterns from the post-physiological activity and sedentary conditions to defend the existence of unique features in the breath movement that confers identity to a person using radar. Even when the breath pattern changes, for example, after a short time exercising, it changes consistently for each individual and permits his recognition [39].

Finally, in [40] was developed a wearable mask to track respiration in free-living conditions. With Principle Component Analysis (PCA) algorithms, they identified unique respirations patterns of the user. The wearable device communicated via wireless and was capable of measuring health information such as respiratory volume, waveform, exhalation peak flow rate, and also recognize an individual from his respiration pattern.

The studies mentioned confirm that respiratory patterns can be a good biometric for continuous user verification.

2.3 Conclusion

In conclusion, this section has provided an overview of the state of the art, highlighting the methodologies and techniques employed to capture the signal and process it in the context of this master

thesis. Furthermore, it introduced the wearable device utilised, a small electronic device capable of acquiring electrocardiogram (ECG) and respiration signals in real time. The device offers portability, practicality and utilises the Bluetooth Low Energy (BLE) communication protocol.

The collection of the ECG signal involved a two-electrode setup, enabling high-quality waveform extraction beyond just obtaining the heart rate. The collected ECG signal underwent various signal processing techniques to ensure accurate analysis. These techniques included the application of bandpass and low-pass filters, effectively filtering and removing noise and artefacts typically present in raw ECG signals. Additionally, the Pan-Tompkins algorithm was employed to locate crucial fiducial points within the ECG waveform, facilitating identifying and analysing of distinct features.

Regarding the respiration signal, the wearable device measured the impedance between the two electrodes, enabling the capture of the respiration waveform. Subsequently, a Butterworth filter was applied to the acquired signal to eliminate unwanted noise and ensure signal fidelity. By detecting peaks and valleys within the respiration waveform, essential parameters such as inspiration and expiration amplitude and duration were extracted, providing valuable insights into the individual's respiratory pattern.

According to current literature, each person's ECG and respiratory signals display unique features, and this master thesis focuses on human identification utilising these signals. To achieve this system, a machine learning (ML) classifier will be used, using the gathered signals and their relevant attributes to construct an identification model.

The subsequent chapters will describe the full implementation and assessment of the suggested technique, reflecting on its feasibility and efficacy.

Chapter 3

Dataset and Signal Quality Validation

3.1 Signal Acquisition Setup

In order to capture accurate physiological data from a group of individuals, a hardware setup was employed to acquire electrocardiogram (ECG) and respiration signals. This section provides an overview of the hardware components utilized, their specifications, and their relevance to the research objectives.

3.1.1 Hardware

The ECG and respiration signals were captured using the wearable device called VitalSticker [5] (Figure 3.2), designed and produced by INESCTEC, capable of precise measurements.

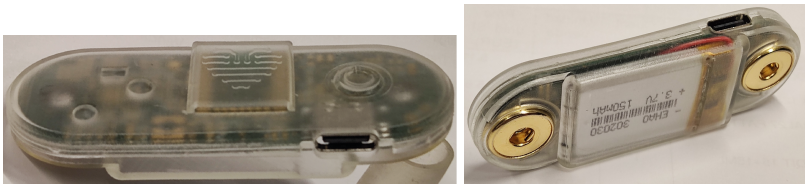

(a) Front view (b) Back view

Figure 3.1: The wearable device VitalSticker [5]

The sensors employed in the measurements of ECG and respiration utilize a peripheral with programmable gain amplifiers and high-resolution 24-bit analogue-to-digital converters (ADC). This peripheral can measure high-quality lead ECGs with two contacts and a customizable virtual right leg (RL) driver reference. Additionally, it features a module for measuring respiration impedance that enables the acquisition of a respiration waveform. The sampling rate for both signals was set at 250 Hz and the measurement range was +/- 350mV [5], ensuring high-fidelity data acquisition. In the process of obtaining accurate physiological signals, a 2-electrode setup was utilized. This setup employed a bipolar chest lead configuration to measure the participants' electrocardiogram (ECG) signals. The two electrodes were carefully positioned on the anterior chest region, as shown in Figure 3.2a, or inside a thoracic band also positioned in the chest region

(Figure 3.2b). They were placed strategically to ensure accurate signal acquisition and capture the heart's electrical activity. It is important to note that although this bipolar chest lead design using two electrodes provides helpful information about cardiac electrical activity, it is a simplified version compared to the conventional 12-lead ECG method. The 12-lead ECG system considered the industry standard in clinical practices, provides a more comprehensive evaluation by including additional electrode placements on various body parts [41].

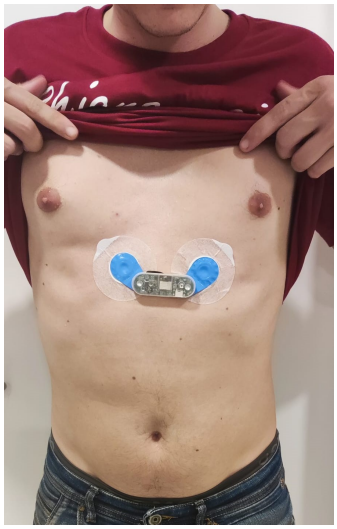

(a) VitalSticker with electrodes

(b) VitalSticker with the thoracic band

Figure 3.2: A visual representation of the VitalSticker device in use

In addition to measuring the electrocardiogram (ECG) signals, the experimental setup allowed for the simultaneous acquisition of respiration data using the impedance method. The impedance method measures the electrical impedance changes brought about by the expansion and contraction of the chest during respiration [42]. The electrode placements were selected to ensure accurate capture of variations in chest volume. Applying a small alternating current through one electrode and measuring the resulting voltage through the other electrode made it possible to assess the

impedance changes in the chest. These impedance changes were then used to derive a respiration waveform, reflecting the participants' breathing patterns. It is important to note that the respiration waveform acquired through the impedance method provides valuable information about the respiratory rate and pattern [42].

During the experiment, the electrodes were adequately positioned and adhered to minimize the likelihood of artefacts or signal interference. The participants were instructed to relax their breathing while seated and to refrain from any vigorous activity that could affect the accuracy of the respiration waveform. The recorded signals were subsequently processed and analyzed to extract relevant parameters, such as heart rate, respiration rate, wave morphology, and other ECG/respiration characteristics of interest.

Before the data collection phase, meticulous calibration and setup procedures were carried out to ensure the accuracy and reliability of the acquired signals. The ECG electrodes were carefully checked for proper adhesion, and impedance levels were verified to be within acceptable ranges. Furthermore, a median filter was implemented in the VitalSticker device to preprocess the ECG signal to remove the baseline wander from the raw data (a more detailed explanation of this filter will be in section 3.3.1). The device also incorporated noise reduction filters to mitigate the effects of body movement and electromagnetic interference, reducing the impact of principal noises.

3.1.2 Bluetooth communication

To ensure seamless data acquisition, a Bluetooth-based transmission system (Bluetooth 5.2 Low Energy (BLE) communication) was utilized to wirelessly transmit the acquired signals from the sensors to the data collection device, such as a computer. This wireless communication method provided several advantages, including convenience, mobility, and reduced participant discomfort during the data collection.

Precautions were taken to minimize signal loss, interference, and latency associated with Bluetooth transmission to ensure the transmitted data's reliability and integrity. These measures involved maintaining proximity between the sensors and the data collection device and selecting Bluetooth modules with robust signal transmission capabilities. Furthermore, an auxiliary buffer was implemented in the Bluetooth stack to prevent data loss, guaranteeing the availability of the primary buffer for receiving new data sent by the sensors. The buffer size had 99 bytes for ECG and respiration signals, accommodating 33 samples at a transmission frequency of 7.6Hz [5].

3.2 Dataset and Data Collecting Protocol

3.2.1 Ethics Approval Process

The study was conducted according to ethical guidelines and obtained INESCTEC's ethics committee's approval. Before participating in the study, all participants provided informed consent by signing a consent form. These forms comprehensively detailed the study's objectives, procedures, and guaranteed the confidentiality and anonymity of participants' data. Additionally, participants

were explicitly informed of their right to withdraw from the study at any point without without consequences.

For further reference, the appendix section (B) includes the collection protocol, the informed consent for study participation form, and the email correspondence containing the proposal approval from the ethics committee at INESC TEC. These documents serve as concrete evidence of the ethical procedures followed throughout the study, ensuring the protection of participants' rights and upholding the integrity of the research process.

3.2.2 Dataset Collection Process

The dataset was collected from a group of twenty-four (24) healthy individuals (without respiratory or cardiac problems), consisting of fourteen (14) women and ten (10) men, with ages ranging from 20 to 62. The data collection procedure involved participants assuming a sitting posture while wearing the VitalSticker wearable device, which consisted of two certified electrodes and a thoracic band. In addition to the sitting posture, data was recorded while participants engaged in activities such as walking, including ascending and descending stairs. These conditions were chosen to assess participants' physiological responses in different contexts. The recordings were conducted in the morning and afternoon sessions of 3 minutes for each participant, allowing for an exploration of potential variations in the signals throughout the day. Table 3.1 and 3.2 resumes the participant demographics information and the dataset characteristics, respectively.

Table 3.1: Participant Demographics

Participant Demographics			
Number of participants:	24	F	14
		M	10
Range of age:	[20-62] years		
Duration:	3 min		

Table 3.2: Dataset Characteristics

Dataset Characteristics	
Sample Frequency:	250 Hz
Material used:	Electrodes Thoracic band

The VitalSticker wearable device was used for capturing ECG and respiration signals. It operated at a sampling rate of 250 Hz, as mentioned in section section 3.1.1, and the recorded data was stored in CSV format.

After the recording sessions, participants were asked to provide feedback regarding their comfort level while wearing the VitalSticker device. An analysis of the collected data revealed interesting insights. The average comfort rating for the thoracic band was higher than that for the

electrodes. This observation is depicted in figure 3.3, which presents a graphical representation of the comfort ratings. The comparison between electrode comfort and band comfort provides valuable information regarding the participants' subjective experience during the data collection process.

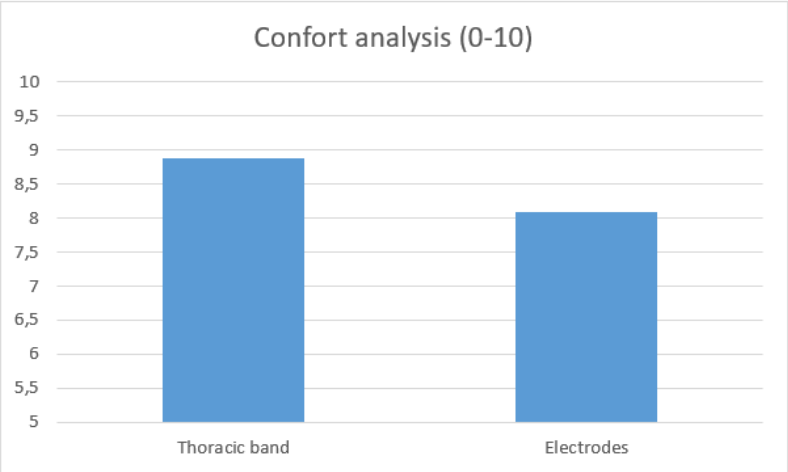

Figure 3.3: Comfort analysis between electrodes and thoracic band

As already mentioned, the collection process involved the utilization of electrodes and a thoracic band. While the subjects thought the thoracic band had a higher level of comfort (figure 3.3), the signal quality did not outperform the electrodes. Consequently, the signal obtained with the electrodes was chosen for subsequent analysis and classification throughout this dissertation. The decision was made because the electrodes provided a slightly superior signal to the band. It is worth noting that this disparity in signal quality could be attributed to the band being a prototype, and the electrodes integrated into it had lower quality than those with gel application.

Simultaneously with the main experiment, parallel research was conducted to confirm the reliability of the respiration signal collected by the VitalSticker device. A small group of five individuals participated in this validation study. The setup used for the main experiment, which included the VitalSticker wearable device with electrodes and a thoracic band, was employed for respiration signal acquisition. A CPAP/APAP device (Figure 3.4) that can measure respiratory signals was used to establish a baseline and compare the signal quality. This machine is widely used in clinical settings to monitor respiration during sleep, particularly for individuals with sleep apnea. It was the ideal reference for verifying the respiratory signal obtained from the VitalSticker device due to its medical-grade capability and established reliability. The CPAP/APAP machine recorded the respiration signals of the participants while they slept, capturing a range of breathing patterns and dynamics. A comprehensive assessment of the signal quality was achieved by comparing the respiration signals acquired by the VitalSticker with those obtained from the CPAP/APAP machine. This validation study played a vital role in ensuring the reliability and accuracy of the respiration signals captured by the VitalSticker device, enhancing the credibility of the findings related to respiratory analysis in the main experiment (section 3.3.2 will provide more information about this

comparison).

Figure 3.4: CPAP/APAP respiratory machine and nose mask

3.3 Signal Analysis

This study aims to identify and authenticate a small group of people based on their ECG and respiration signals. Initially, the analysis focused solely on the ECG signal, as numerous studies have already demonstrated its effectiveness in this context (Chapter 2). However, including the respiration signal aims to investigate its potential contribution to the identification/authentication processes.

Signal analysis is crucial to extracting meaningful information from the collected physiological signals. One of the primary reasons for conducting signal analysis is to address the presence of everyday noises typically captured during signal collection, such as baseline wander, muscle movements, and other interferences. These noises can hinder the accuracy and reliability of the signals, making preprocessing and signal quality validation essential steps in the analysis process.

In this study, the signals analysed are the ECG and respiration signals. The ECG signal provides valuable insights into the heart's electrical activity, while the respiration signal reflects breathing patterns. Both signals are relevant to the research objectives, as they can contribute to the accurate identification/authentication of individuals with the unique characteristics of each individual that they provide.

Before validating the quality of the acquired data, extracting relevant features from the signals is essential after the processing phase. These steps are crucial for the subsequent classification process using machine learning algorithms. By extracting meaningful features and ensuring the quality of the signals, the classification algorithm can effectively distinguish and classify individuals based on their ECG and respiration signals. These steps will be explained in the following sections.

3.3.1 Signal processing and feature extraction

ECG signal

Signal processing

A series of processing steps were performed in the ECG signal to ensure the quality and reliability of the acquired physiological signals. A median filter was incorporated within the firmware of the employed wearable device (VitalSticker) to eliminate the baseline wander present in the collected signal [5], as mentioned in the previous section. This particular filter was selected due to its ability to preserve the waveform integrity of the signal without introducing significant computational overhead. Alternative filters such as high-pass filters (FIR, IIR), Wavelet transform, and mean filters were considered. However, they either required excessive computational resources or introduced additional artefacts to the signal waveform, which could adversely affect the subsequent feature extraction process.

The implemented median filter utilizes a sliding window with 150 samples, which is approximately the number of samples from the P wave to the T wave passing through the QRS point of the ECG waveform. It calculates the median value within this window and subtracts it from all other signal elements. As a result, the filtered signal is centred around zero, effectively removing the baseline wander typically present in the ECG waveform without compromising its integrity. Figure 3.5 illustrate the function of the filter. The amplitude shown in Figure 3.5a is provided directly from the devices in bits. After applying the filter, a conversion to mV units was performed according to the characteristics of the ADC system in VitalSticker device [5], as can be observed in Figure 3.5b.

After the signal acquisition, a thorough analysis and processing were performed. Noise removal techniques were applied to the raw physiological signal to mitigate noise and artefacts, including filtering and artefact removal. The BioSPPy toolbox [43] [44], implemented in Python, was employed for signal filtering using a bandpass and FIR filter (with a sampling frequency of 250 Hz, a frequency range of [3, 45] for passband and an order of $0.3 \times sampling frequency$) and QRS complex detection. The Pan-Tompkins algorithm [24] was utilized to identify the R peaks accurately. The Q and S peaks were later identified by utilizing the capabilities of the chosen toolbox and the R peak positions. Further analysis was then conducted on the two remaining waves of interest that were still present, the T and P waves.

The localization of the P peaks in all heartbeats posed the most significant challenge during the signal analysis. In order to attain accurate results, modifications were made to the functionality of the BioSPPy toolbox to ensure precise identification of the P peak positions.

For quality control, a visual analysis was conducted on the collected signals to verify the correct placement of the peaks and exclude any outliers exhibiting significantly deviant distances. Figure 3.6 illustrates a portion of the raw signal with the median filter to remove the baseline wander, already implemented in the firmware of the VitalSticker device, and the filtered ECG signal zoomed. The graph prominently displays the distinctive peaks, identified and marked with vertical lines of different colours for each peak. This visual representation serves as a valuable reference, allowing for clear visualization of the relevant points and aiding in understanding the subsequent feature extraction process. Each processing step was meticulously executed, carefully considering relevant parameters to optimize the quality and usability of the signals. Once the precise locations of the key points in the ECG signal were obtained, a set of features was extracted

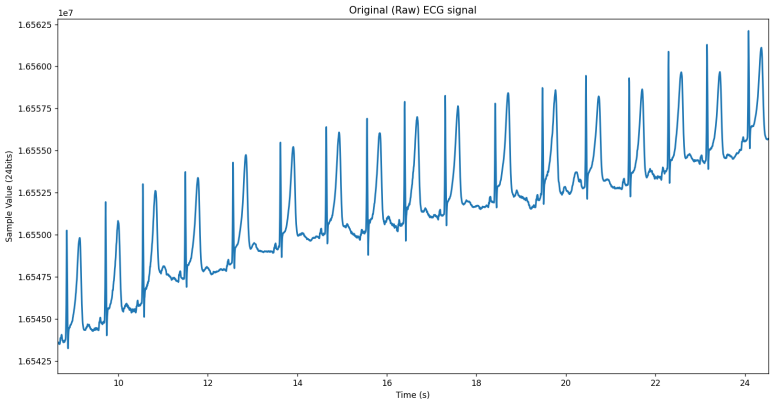

(a) Raw ECG signal

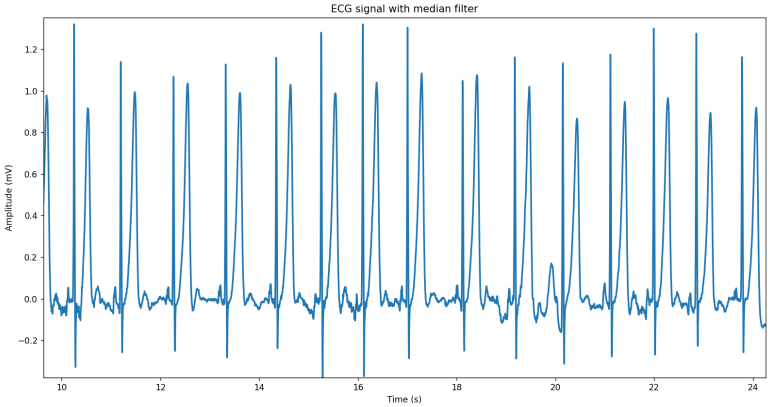

(b) ECG signal with median filter

Figure 3.5: The effect of the median filter

from these positions.

Feature extraction

As mentioned, feature extraction can be performed using fiducial and non-fiducial features. In this study, fiducial points of the ECG signal were utilized to extract features for the identification algorithm. In particular, temporal characteristics were derived from the waveform by utilizing the precise positions of the critical ECG peaks acquired during the signal processing stage. Informative temporal features were derived by calculating various time intervals between fiducial points, such as ST, RT, QT, RR, and others.

These temporal features were selected based on their potential significance in capturing essential characteristics of the ECG waveform related to individual identification [4]. The chosen features allow for the characterization of essential intervals and durations between specific fiducial points, providing insights into the underlying physiological processes of the heart. By incorporating these features into the classification algorithm, distinctive patterns within these time intervals may aid in accurately authenticating individuals.

It is important to note that these specific temporal features were selected based on existing literature and domain knowledge [4] [13] [14]. These justifications provide a strong rationale for

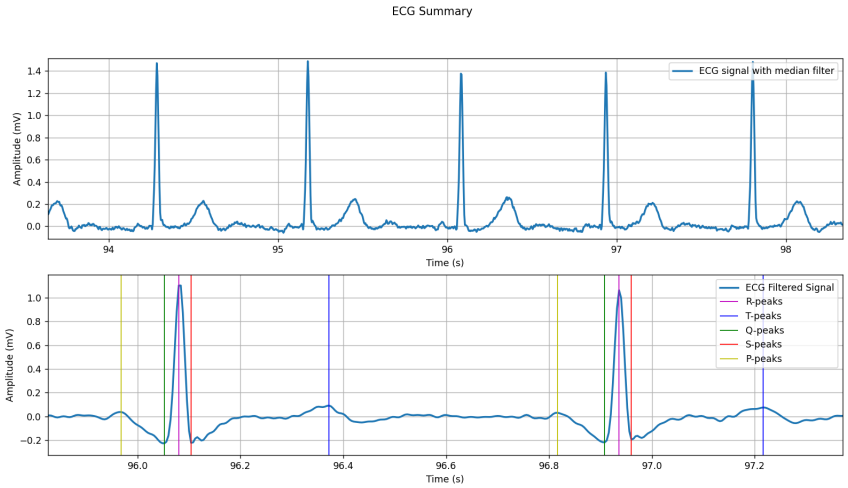

Figure 3.6: Raw ECG signal only with the median filter(top graph) and filtered ECG signal (bottom graph) with the signal peaks identified

including these temporal features in the machine learning classification algorithm.

However, it is essential to acknowledge potential limitations and considerations regarding the chosen features. Variability in the ECG morphology among individuals and potential confounding factors, such as physiological conditions or medication usage, may impact the reliability and generalizability of these temporal features. Careful evaluation and validation of these features are necessary to ensure their robustness and suitability for the authentication classification algorithm.

Strategically extracting temporal features based on fiducial points offers a promising approach for achieving accurate and reliable identification/authentication. By considering the physiological relevance of these features and addressing their limitations, the classification algorithm can effectively use the unique patterns within the time intervals of the ECG waveform to authenticate individuals with a wearable device.

After extracting the relevant features from the acquired ECG signal, the next step involved computing the temporal distances between the key fiducial points, namely Q, R, S, and T, for each individual's heartbeat. These temporal distances were subsequently utilized as features for the classification task. Specific criteria were applied to filter out noisy heartbeats to ensure the reliability of the extracted features. This was achieved by applying a series of conditions to ensure the reliability and accuracy of the selected heartbeats. The following conditions were used to filter out noisy heartbeats [4]:

1. Heartbeats with a temporal distance between the Q and R peaks exceeding 0.075 seconds were excluded from the analysis. This criterion ensured that only heartbeats with a suitable time delay between these fiducial points were considered.

$$QR <= 0.075s \tag{3.1}$$

2. Another constraint was established on the QT interval to RR interval square root ratio.

Heartbeats outside of the 0.200 to 0.360 range for this ratio were considered noisy and eliminated from the data set. This criterion was used to keep the temporal link between these intervals consistent.

$$0.200s < \frac{QT}{\sqrt{RR}} < 0.360s \tag{3.2}$$

3. In addition to the above conditions, particular attention was given to the P peaks, which are often more challenging for the algorithm to detect accurately. To address this, outliers among the P peaks were removed by deleting those with a distance RT considerably different from the mean distance, taking into account the mean distance plus or minus the standard deviation of the varied RT of each person's heartbeats. By doing so, P peaks that deviated significantly from the typical distance were excluded from the dataset, ensuring a more reliable analysis.

The feature vectors associated with noisy heartbeats were efficiently eliminated by applying these severe constraints, ensuring that only high-quality and trustworthy heartbeats were included in the subsequent analysis.

The steps for the ECG signal analysis were based in a already existed pipeline defined in [4]. Figure 3.7 illustrates the pipeline followed for analysing this vital signal, including all the processing steps and the identification process with machine learning algorithms using this signal.

Respiration signal

Signal processing

The respiration signal was subjected to a comprehensive processing procedure similar to the ECG signal, as discussed in the preceding section. The BioSPPy toolbox [43] was employed to facilitate this processing. Initially, a Butterworth filter (with order = 2 and a sampling rate of 250 Hz) was implemented to reduce unwanted noise and artefacts, enhancing the overall signal quality.

The identification of valleys and peaks in the respiration signal involved detecting zero crossings with the help of BioSPPy toolbox, which correspond to points where the signal intersects the zero axis. By utilizing the positions of these zero crossings, the precise locations of the valleys and peaks were derived. Figure 3.8 visually depicts the respiration signal, illustrating both the raw and filtered segments, with vertical lines indicating the presence of valleys and peaks.

Following this, a detailed analysis was conducted for each respiration cycle, focusing specifically on the characteristics associated with individual breaths. Each respiration cycle encompasses a valley, a peak, and another valley. Within each cycle, several parameters were computed to capture essential characteristics. Specifically, the amplitudes of inspiration and expiration, which signify the magnitudes of the inhalation and exhalation phases, were determined. Additionally, the durations of the inspiration and expiration steps were measured, offering valuable insights into the time spent in each phase.

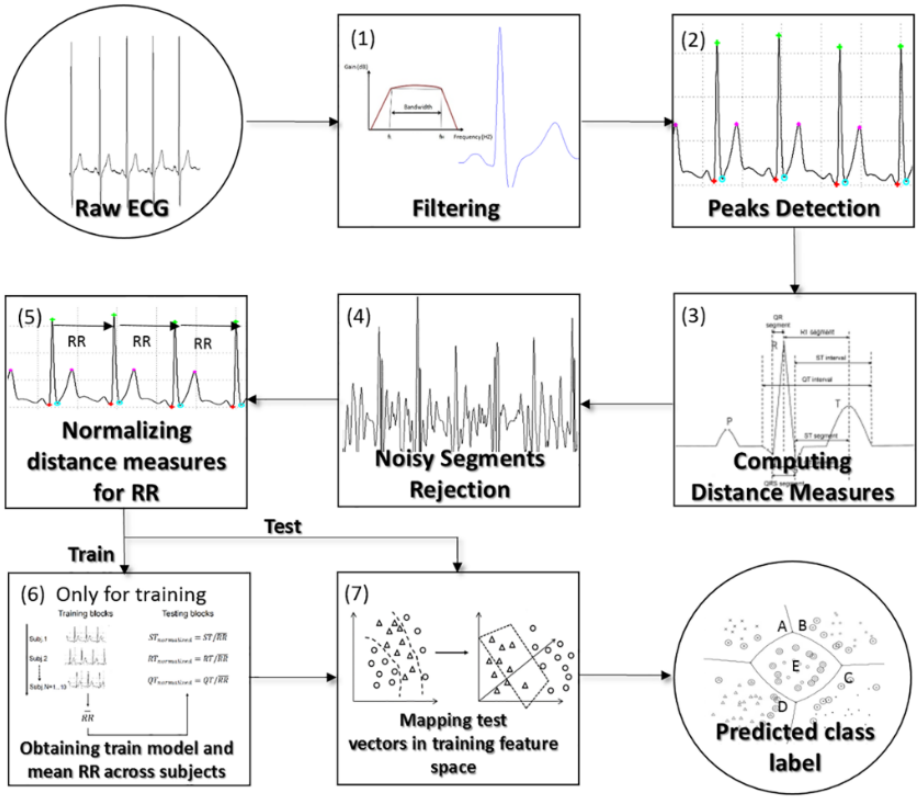

Figure 3.7: Pipeline scheme of the ECG identification algorithm. (1) filter the raw signal;(2) find the fiducial points; (3) distance measure computed; (4) remove noisy heartbeats; (5) normalize features (with the training data); (6) train the data; (7) test phase [4]

By incorporating these computed parameters, a more comprehensive understanding of the respiration signal was attained, enabling the extraction of essential features for subsequent identification purposes [35] [34].

Feature extraction

For the feature extraction of the respiration signal, several parameters were computed for each respiration cycle to capture essential characteristics. The previously mentioned parameters include the inspiration and expiration amplitudes, which indicate the magnitudes of the inhalation and exhalation phases, and the lengths of the inspiration and expiration steps, which provide information about the time spent in each phase. The initial valley, peak, and second valley positions were used to determine these parameters throughout each respiration cycle.

In addition, inspiratory and expiratory velocities [34] were extracted from the respiratory signal. Inspiratory velocity represents the pace of air entering the lungs during inhalation, while expiratory velocity measures the rate of air expelled during exhalation. They were calculated by subtracting the amplitude value of a peak value and dividing the result by half a respiration cycle, depending if it is inhalation or exhalation. These velocities provide valuable insights into breathing patterns and dynamics.

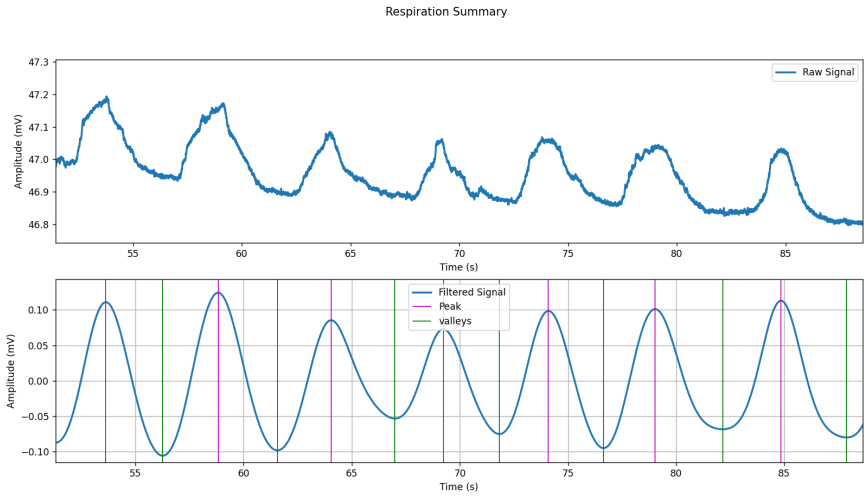

Figure 3.8: Raw and filtered respiration signals

Furthermore, the respiratory rate was calculated by dividing a minute (60s) by the duration of a complete respiratory cycle. This measurement gives an essential indicator of breathing frequency.

These features offer valuable information for respiratory monitoring and assessment and potential applications in human identification processes[35] [34].

In order to ensure the reliability of the extracted features, the following criteria were applied to each respiration cycle:

1. **Elimination based on Amplitude:** If the amplitude of either the inspiration or expiration is too small, specifically less than or equal to 20% of the mean peak-to-valley amplitude, the associated pair of peak and valley is deleted [45]. This criterion helps remove insignificant or noisy cycles from the analysis.

2. **Elimination based on Duration:** Empirical observations showed that the respiration duration could vary significantly, ranging from 0.9 seconds during heavy exercise (such as running) to 12.5 seconds during activities like a conversation. To ensure consistency, only time intervals from valley to valley falling within the range of 0.9 seconds to 12.5 seconds were accepted [46] [45]. Respiration cycles with durations outside this range were ignored.

3. **The ratio of Duration to Amplitude:** After analyzing the waveform and considering the mean ratio of all respiration cycles, a threshold was set to filter out cycles deviating significantly from the expected waveform characteristics. If the ratio of inspiration duration to inspiration amplitude or expiration duration to expiration amplitude ratio was less than 0.003, the corresponding respiration cycle was excluded. This criteria was based in [46] which defends that the ratio of inspiratory to expiratory duration and amplitude should not be more than 1.5.

The reliability and quality of the retrieved characteristics were improved by applying these criteria to each respiration cycle, ensuring that only significant cycles were evaluated for further classification and authentication.

The steps for the respiration signal analysis were based in the ECG signal pipeline defined in [4]. Figure 3.9 illustrates the pipeline followed for analysing this vital signal, including all the processing steps and the identification process with machine learning algorithms using this signal.

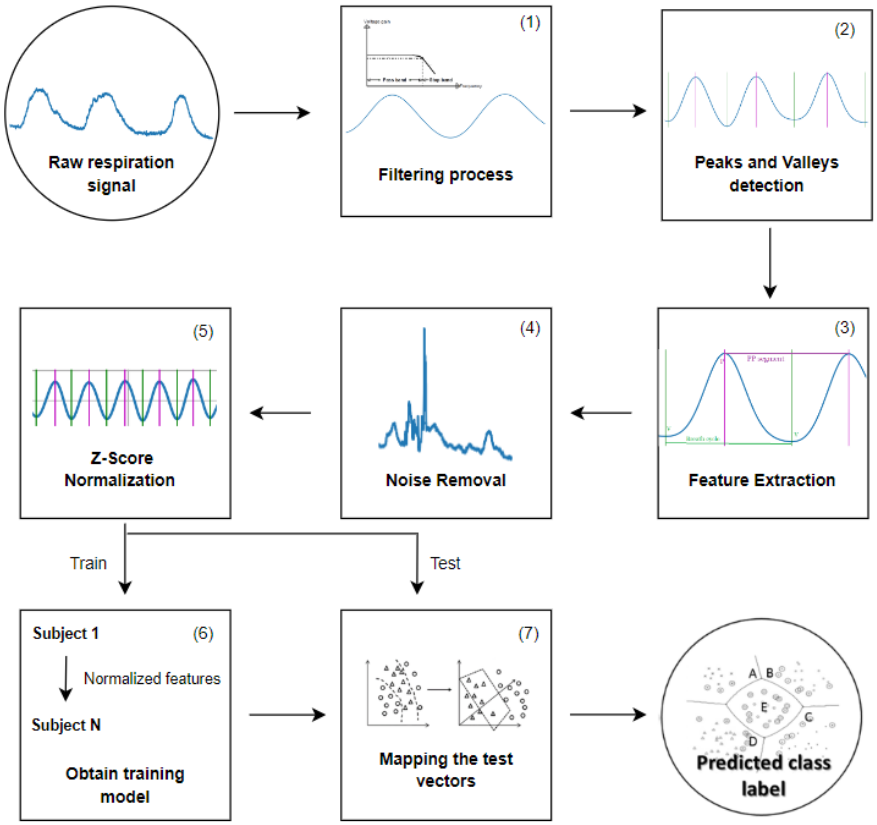

Figure 3.9: Pipeline scheme of the respiration identification algorithm. (1) filter the raw signal;(2) find the fiducial points; (3) distance measure computed; (4) remove noisy breaths; (5) normalize features (with the training data); (6) train the data; (7) test phase [4]

3.3.2 Quality Signal Validation

3.3.2.1 ECG Validation study

The purpose of these experiments is to validate and analyse the signal quality of the ECG data gathered using the wearable device VitalSticker, which served as the primary tool for building the dataset. In the context of the master's thesis, it is essential to ensure the reliability and accuracy of the collected ECG signals.

Validating the signal quality holds significant importance for several reasons. Firstly, accurate ECG measurements are crucial for the reliable diagnosis and monitoring of various cardiac conditions. Secondly, ECG data possesses inherent characteristics that make it a promising biometric authentication modality, capable of uniquely identifying individuals. Therefore, ensuring the precision and fidelity of VitalSticker's signal acquisition is imperative. By doing so, the credibility of the dataset employed in the research can be firmly established, enhancing the reliability and credibility of the identification and authentication methods proposed.

These experiments are performed using both VitalSticker and VitalJacket® [47] (figure 3.10) devices to identify and quantify any potential performance limitations or errors in these devices, allowing for a comprehensive evaluation of the dataset's reliability. VitalJacket®, a medically certified device to the MDD 93/42 EEC for ambulatory cardiology, is utilized alongside VitalSticker to provide a comparative analysis of signal quality.The Vital-Jacket® is designed to enable patients' mobility in cardiology and sports applications. It is a lightweight, comfortable, and flexible jacket worn discreetly underneath clothing. Equipped with sensors, including three electrodes, the VitalJacket® accurately measures vital signs such as heart rate, respiratory rate, blood pressure, and body temperature. These sensors wirelessly communicate the data they collect to a receiver the patient can carry around in their pocket or belt. Subsequently, the receiver can be connected to a computer or mobile device for real-time monitoring and further analysis of the acquired data.

Figure 3.10: The certificated wearable device VitalJacket® [48]

However, as VitalSticker serves as the primary device employed throughout the research, the reliability and validity of its signal directly impact the credibility of the research outcomes. Therefore, a thorough understanding and justification of the importance of validating the ECG signal quality collected with VitalSticker become paramount. By validating the signal quality, the overall credibility of the research findings is strengthened, ensuring robust and reliable conclusions.

In summary, these experiments aim to validate and analyse the signal quality of the ECG data collected with VitalSticker. This validation technique contributes to the overall credibility and integrity of the study results by guaranteeing the reliability and correctness of the collected signals.

3.3.2.2 Experiment A: Comparing VitalSticker and VitalJacket Performance with an ECG Simulator

In this experiment, a comparison was made between the performance of VitalSticker and VitalJacket. The validation process involved using an ECG simulator, the PS-2006 microprocessor-based Patient Simulator 3.11.

The specifications of the ECG simulator include various features such as ECG simulation with four waveforms, constant QRS duration, and six machine performance testing waveforms, including Holter simulation.

The ECG simulator features six patient lead snap connectors and offers the capability to generate ECG signals at different heart rates. For this experiment, signals were generated at two heart rates: 60 beats per minute (bpm) and 120 bpm. The simulator provides a constant ECG signal at the specified heart rates. Figure 3.12 presents a schematic diagram illustrating the experimental setup of Experience A with the three devices used and the five electrodes represented by the blue circles.

Figure 3.11: PS-2006 microprocessor-based ECG Patient Simulator [49]

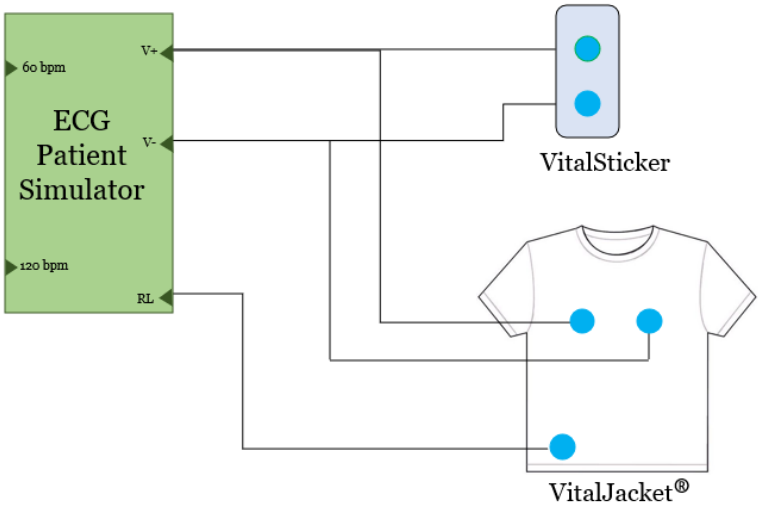

Figure 3.12: Schematic representation of experiment A setup

The known RR intervals for these heart rates were determined to establish a baseline for comparison. With a constant heartbeat, the RR interval can be calculated as the reciprocal of the heart rate. For example, the RR interval at 60 bpm equals 60 seconds divided by 60 bpm or 1 second. Similarly, at 120 bpm, the RR interval equals 0.5 seconds, representing 60 seconds divided by 120 bpm. In order to assess and contrast the RR intervals received from the wearable devices, these known RR intervals were used as a benchmark.Figure 3.13 illustrate the protocol diagram of the analysis done in next section.

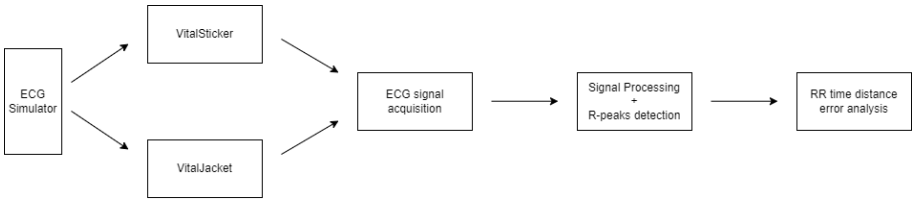

Figure 3.13: Protocol Diagram of experiment A

By utilizing the ECG simulator and establishing the known RR intervals for the heart rates of interest, a reliable baseline was created to evaluate the performance of VitalSticker and VitalJacket. The signals generated by the simulator were regarded as the objective and correct standards to evaluate and contrast the RR intervals obtained by the wearable devices. By comparing the RR values from the wearable devices to the baseline set by the ECG simulator, it was possible to evaluate the precision and dependability of the measures. Figure 3.14 shows three peaks zoomed of VitalSticker and VitalJacket® signal synchronised. The R peaks of both signals are not in the same time position, which causes the errors analysed in the next section.

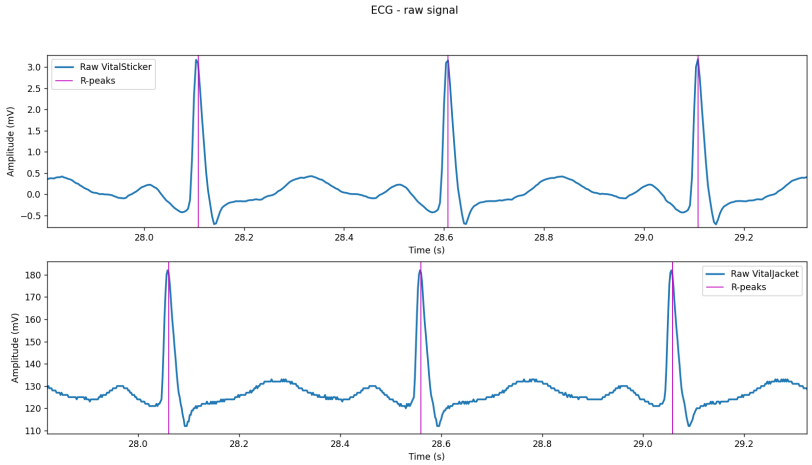

Figure 3.14: VitalSticker and VitalJacket® signals

Error analysis

In this section, the resolution and errors observed for both VitalSticker and VitalJacket will be discussed. The testing took place at heart rates of 60 and 120 beats per minute for 2 minutes corresponding to 120 and 240 heartbeats, respectively.

Starting with the resolution of the devices, VitalJacket has a better sampling frequency of 500 Hz compared to VitalSticker's 250 Hz (sample rate). When analysing the errors, this resolution difference will be taken into consideration.

The results in tables 3.3 and 3.4 show, at 60 bpm, that VitalSticker had 37 inaccuracies over the 2-minute test period at 60 bpm, each with a magnitude of 0.004 seconds, in line with time the resolution of 1/250 Hz = 0.004 seconds, representing the error of one sample. Assuming all the absolute values of the errors, the maximum accumulative error will be calculated multiplied by the 37 times the error occurs by 0.004 seconds. It can be used to determine the VitalSticker's cumulative error, which equals 0.148 seconds. VitalJacket, on the other hand, displayed 117 faults with a resolution of 1/500 Hz = 0.002 seconds and an average magnitude of 0.002 seconds. In the same perspective, the maximum cumulative error of VitalJacket® may be calculated as 117 mistakes multiplied by 0.002 seconds, which results in an error of 0.234 seconds.

Table 3.3: 60bpm analysis

60bpm					
Device	**Time (min)**	**Number of heartbeats**	**Max error (s)**	**Number of RR time distance errors**	**Max Cumulative error (ms)**
VitalSticker	2	120	0,004	37	148
VitalJacket	2	120	0,002	117	234
VitalSticker	5	300	0,004	92	368
VitalJacket	5	300	0,002	264	528

Table 3.4: 120bpm analysis

120bpm					
Device	**Time (min)**	**Number of heartbeats**	**Max error (s)**	**Number of RR time distance errors**	**Max Cumulative error (ms)**
VitalSticker	2	240	0,004	41	164
VitalJacket	2	240	0,002	143	286
VitalSticker	5	600	0,004	106	424
VitalJacket	5	600	0,002	456	712

In addition to the previous analysis, another test was conducted using a simulator to compare the performance of both VitalSticker and VitalJacket over a 5 minutes test duration. The 5 minutes correspond to 300 heartbeats at 60 bpm and 600 at 120 bpm. The results of this performed tests, including the maximum error of the RR interval, the number of errors, and the cumulative error for each device, are summarized in the tables of figures 3.3 and 3.4.

Results discussion

The evaluation of the results reveals critical implications for the overall signal quality and reliability of the collected ECG data. When monitoring ECG signals over a longer duration, the cumulative effects of errors become particularly significant, potentially introducing a time-dependent bias and compromising the accuracy of derived parameters.

A comparison between the VitalSticker and VitalJacket devices brings to light a trade-off between the magnitude and accumulation of errors. While VitalJacket exhibits smaller errors in terms of magnitude, it accumulates a higher number of errors over time. On the other hand, VitalSticker, despite having larger errors, demonstrates fewer cumulative errors. This trade-off emphasizes the importance of carefully considering error resolution and the cumulative effects when evaluating the signal quality of wearable ECG devices.

However, it should be noted that the errors observed in both devices fall within the range of approximately one sample, indicating an intrinsic error inherent to the devices themselves. Consequently, both devices exhibit an expected error that does not exceed the resolution limitations of the respective device.

In conclusion, the comprehensive analysis conducted with the VitalSticker device, along with the evaluation of error magnitude and accumulation, highlights its excellent performance in acquiring ECG signals. This comparative assessment, when considering the already medically validated performance of the VitalJacket device in acquiring ECG signals, underscores the importance of thoroughly assessing the performance of ECG devices.

3.3.2.3 Experiment B: A Comparative Analysis of VitalSticker and VitalJacket® with Real Person ECG Signals

In Experiment B, the signals from three individuals were collected and synchronized to compare the performance of VitalSticker. The collection of signals involved the placement of electrodes on the individuals. With VitalSticker, two electrodes were positioned in the middle of each person's chest. With VitalJacket, three electrodes were utilized, with two electrodes positioned directly above the VitalSticker electrodes in a vertical line. The third electrode of the VitalJacket was placed near the top of the right leg. Both devices simultaneously collected signals from each person for approximately 3 minutes. To ensure accurate synchronization of the signals, an external artefact was created simultaneously on both devices (the person jumped). Figure 3.15 represents the moment where the participant jumped and served as the moment for synchronization of the two signals of the different devices.

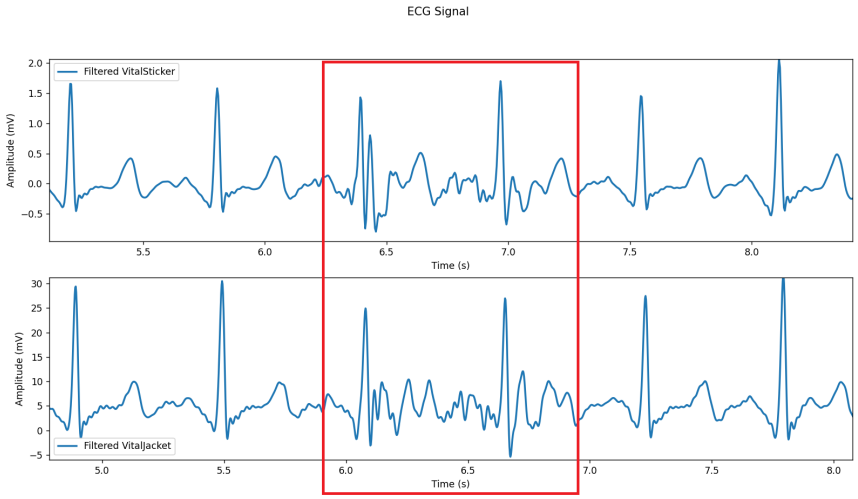

Figure 3.15

The fiducial points (R and T peaks) measured were calculated using the algorithm described in previous sections, which involved processing, filtering, and extracting the peaks of the ECG signal. This experiment focused on the time distance between R peaks in sequential heartbeats and the time distance between the R peak and the T peak within the same heartbeat. Both intervals were compared in the synchronized signals obtained from VitalSticker and VitalJacket.

Given that VitalJacket is a medically certified device, it was chosen as the baseline for assessing the signal quality of VitalSticker. The research aims to assess the accuracy and dependability of VitalSticker in capturing and processing ECG signals by contrasting its performance with that of VitalJacket®.

This experimental setup allowed for a direct comparison between VitalSticker and VitalJacket using synchronized signals collected from real individuals. By using VitalJacket as the baseline, the analysis sought to determine the signal quality of VitalSticker and identify any potential differences or limitations in its performance. Figure 3.16 represents the protocol diagram of this

experiment.

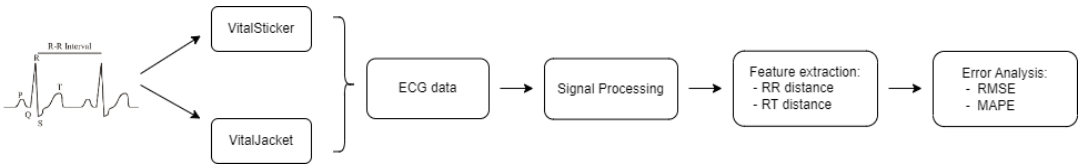

Figure 3.16: Protocol Diagram of experiment B

Error analysis

The error analysis focused on the temporal distances between the R-peaks (RR interval) and the RT intervals, representing the duration between the R-peak and the T-peak, obtained from the ECG signals of VitalSticker and VitalJacket. The signals were lined up by the same starting R-peak to ensure synchronization. The RR and RT measurements were calculated for each heartbeat using individual A, B, and C signals. The aim was to compare the measurements obtained from VitalSticker and VitalJacket and assess the level of error in the signals.

For each subject, the time intervals of RR and RT obtained from VitalSticker and VitalJacket® were compiled into vectors (Figure 3.17).VitalSticker's RR time distance vector was deducted from VitalJacket®'s associated RR time distance vector. Similarly, VitalJacket®'s associated RT time distance vector was removed from VitalSticker's RT time distance vector. These comparisons made it possible to quantify the variations in RR and RT readings between the two devices.

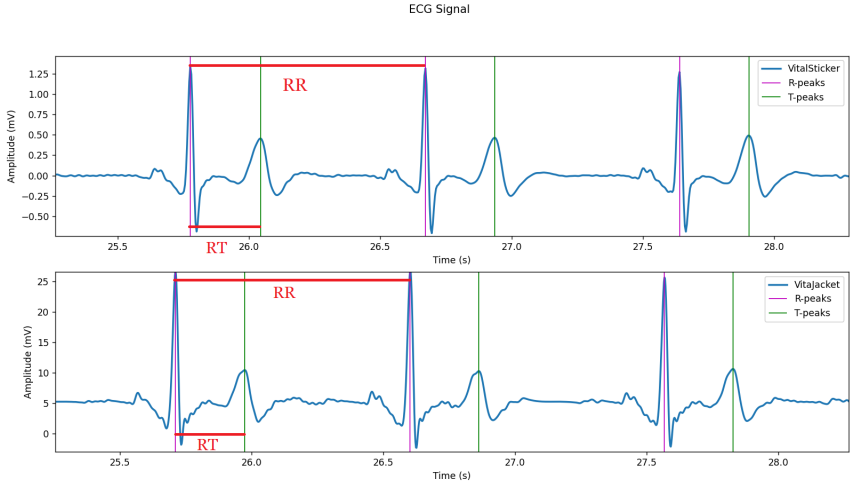

Figure 3.17: Time intervals calculated for the error analysis (RR and RT distance) in both devices

The average difference (AD), standard deviation (σ), root mean square error (RMSE - equation 3.1), and mean absolute percentage error (MAPE - equation 3.2) were all calculated as part of the error analysis [50]. The average difference (AD) and standard deviation (σ) were determined to analyze the discrepancy between the measurements obtained from VitalSticker and VitalJacket.

The RMSE quantified the overall error magnitude, while the MAPE expressed the error as a percentage of the actual value.

$$RMSE = \sqrt{\frac{\sum_{i=1}^{N} ||y(i) - y^*(i)||}{N}} \tag{3.3}$$

$$MAPE = \frac{1}{N} \times \sum_{i=1}^{N} \frac{y(i) - y^*(i)}{y} \tag{3.4}$$

The obtained results for individuals A and B are summarized in following table.

Table 3.5: Experiment B results; AD: average difference; (σ): standard deviation; RMSE: root mean square erro; MAPE: mean absolute percentage error

201 R-peaks	RR interval				RT interval			
Subject	AD (s)	σ (s)	RMSE (%)	MAPE (%)	AD (s)	σ (s)	RMSE (%)	MAPE (%)
A	0,0022	0,0052	0,5630	0,3300	0,0075	0,0132	1,5210	3,4830
B	0,0026	0,0018	0,3150	0,3040	0,0056	0,0033	0,6550	2,1580
C	0,0030	0,0019	0,3530	0,3560	0,0070	0,0058	0,9080	2,6900

The results demonstrate that the RR error for all individuals was below one per cent, illustrating good accuracy in measuring RR intervals. The RT error, on the other hand, was roughly 3%, indicating a significantly higher error level in the measurement of RT intervals. These findings provide insights into the performance and reliability of VitalSticker and VitalJacket® in capturing and analyzing ECG signals.

The error analysis involved a comprehensive comparison of the RR and RT measurements obtained from VitalSticker and VitalJacket®. The results demonstrate the level of error present in the signals and contribute to the evaluation of the signal quality and reliability of both devices.

Results discussion

The analysis of the errors in the context of evaluating VitalSticker signal quality reveals promising findings. The observed errors were relatively small, indicating that VitalSticker exhibits good accuracy and quality in collecting ECG signals. This is significant as it demonstrates the device's ability to capture reliable and precise data.

The small RR error observed in VitalSticker's measurements further reinforces its accuracy. The RR interval, representing the time difference, is critical in analysing heart rate variability and cardiac rhythm. VitalSticker achieved a small RR error comparable to the medically approved VitalJacket suggests that VitalSticker has good accuracy in measuring heart rate and ensuring reliable ECG data collection.

However, it is important to consider the slightly higher RT error observed in the measurements. The RT interval presents challenges due to the T-wave's lower visibility compared to the

prominent R-peak. Consequently, a slightly higher error in the RT interval is comprehensible. While the minor delays or errors in the RT measurements do not necessarily invalidate the usability of the ECG data collected with VitalSticker, they should be considered during data analysis and interpretation.

In conclusion, the comparison of VitalSticker with the medically approved VitalJacket indicates that VitalSticker has the capability to acquire high-quality ECG signals. The minor errors in the RR measures emphasise their reliability and precision. While the slightly higher RT errors require attention, they may be handled through optimisation techniques and are not detrimental to the general usability of the VitalSticker ECG data. These findings contribute to the understanding and validation VitalSticker's signal quality, supporting its potential as a valuable tool for ECG monitoring and analysis in various applications.

3.3.2.4 Conclusions of the ECG quality signal validation

The key findings from both experiments consistently demonstrated that VitalSticker provides a good quality signal when collecting ECG signals. Experiment A, comparing VitalSticker with a certified device (VitalJacket), confirmed the device's comparable signal quality. Experiment B, utilizing real-person ECG signals, revealed small errors in RR and RT measurements, indicating the accuracy and reliability of VitalSticker.

The objective of validating the signal quality of ECG data with VitalSticker has been successfully achieved. These findings have implications for the credibility and precision of ECG data as a biometric method and for monitoring. However, it is critical to recognize the tests' limitations, which include the limited sample size and specific settings. Future research should concentrate on greater sample numbers, diversified groups, and performance investigation under various physiological situations or activities.

In conclusion, the findings of these research studies significantly corroborate the validity and reliability of the ECG data gathered by VitalSticker. The device frequently produced high-quality signals, showing its value in healthcare research. These findings contribute to the advancement of wearable ECG monitoring technology and underscore the importance of VitalSticker in reliable ECG data collection.

3.3.2.5 Respiration Validation study

The purpose of this study was to validate the respiration signal obtained from the VitalSticker device and assess its quality to use it in conjunction with the ECG signal in the classification process to identify a person.

It was essential to compare the VitalSticker device's respiration signal to a well-established baseline to confirm its validity and dependability. This study selected the respiration signal obtained from a CPAP/APAP respiratory machine as the baseline for comparison. The respiratory machine used in this study was the iBreeze CPAP /APAP machine, a medically certified device

commonly employed for measuring respiration signals in individuals, particularly those with sleep apnea.

The advanced algorithms of the iBreeze CPAP/APAP machine allow for the identification and analysis of a wide range of respiratory events, ensuring accurate and gentle regulation of its airflow. This feature contributes to the machine's ability to provide optimal therapy to people suffering from respiratory problems. Furthermore, the iBreeze CPAP/APAP machine enables the preservation of therapy findings on an SD card. This data includes sleep and compliance information, which may be examined on the machine's screen or a Windows computer with the included PC software. The Intelligent Pressure Release (IPR) functionality of the iBreeze APAP machine is a standout feature. During sleep apnea treatment, many individuals may find it difficult to exhale against high air pressure. When IPR is on, the machine provides lower pressure during exhale than during inhalation, improving comfort and satisfaction during continuous positive airway pressure therapy.

By utilizing the CPAP/APAP machine as the ground truth, we aimed to evaluate the performance of the VitalSticker device and gain insights into its ability to capture and represent respiratory patterns accurately. The goal is to examine the fidelity and dependability of the VitalSticker device for capturing respiration signals by comparing the respiration signals received from the VitalSticker device and the CPAP/APAP machine. This assessment was critical in assessing the VitalSticker device's suitability for incorporation into the categorization process used to identify persons.

The validation tests were conducted with participants wearing a nose mask incorporated with the CPAP/APAP machine. This setup ensured that the respiration signals captured by both the VitalSticker device and the CPAP/APAP machine were obtained simultaneously and under similar conditions, simulating a real-life respiratory monitoring scenario.

Validating the respiration signal captured by the VitalSticker device and establishing its reliability would significantly enhance the accuracy and effectiveness of the classification process. As a result, the VitalSticker technology has potential uses in various disciplines, including healthcare, fitness monitoring, and biometric identification.

In the following sections, we will describe the methodology employed for data collection and analysis, present the results of the comparison between the VitalSticker device and the CPAP/APAP machine, and discuss the implications of our findings concerning the validation of the VitalSticker device for respiration signal capture.

Experiment setup

The respiratory validation experiment involved the participation of five individuals who simultaneously used the VitalSticker device and a nose mask connected to a CPAP/APAP machine, figures 3.18a and 3.18b illustrate how the two devices are used. Figure 3.19 illustrates the protocol diagram of this experience. The participants were selected to be healthy and within the age range of 23 to 50.

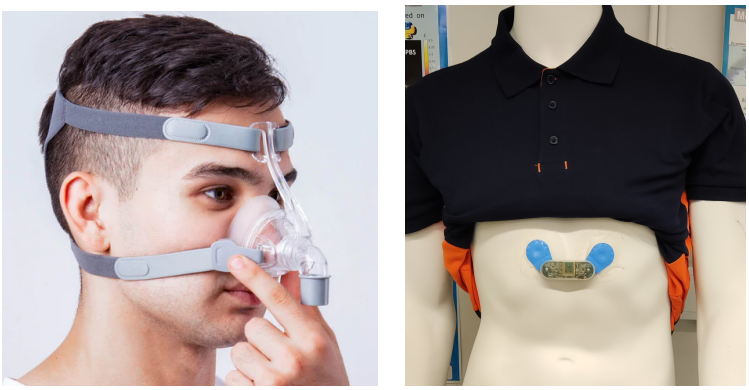

(a) Nose mask of CPAP/APAP machine [51]

(b) VitalSticker with two electrodes

Figure 3.18: Visual illustration of how the two devices were used in the study

In the experiment, the participants were seated and instructed to breathe normally through their nose. The setup involved the placement of the VitalSticker and two electrodes on the chest in capturing the respiratory impedance of the thoracic cavity between them. Simultaneously, the participant used a nose mask CPAP/APAP machine, which delivered constant pressurized air through a mask.

The machine delivered constant pressurized air through the mask, automatically adjusting the positive airway pressure based on the participants' breathing needs. The respiratory signal recorded by the CPAP/APAP machine was obtained directly from the airway of the participants, providing information on their breathing patterns. In contrast, the VitalSticker device captured the respiratory signal by measuring the impedance variation in the thoracic cavity during inhalation and exhalation. This measurement was achieved using two electrodes placed on the participant's chest. When a participant inhaled, the impedance in the thoracic cavity increased, and as they exhaled, it decreased [52]. These impedance changes were converted into voltage fluctuations that formed the respiratory signal of the VitalSticker device.

It is essential to highlight the distinction in the data acquisition processes between the two devices. While the CPAP/APAP machine directly measured the respiratory signal from the airway, the VitalSticker device relied on capturing the impedance changes in the thoracic cavity. This fundamental difference in acquisition methods leads to variations in the amplitude and waveform characteristics of the respiratory signals obtained from each device.

Therefore, it is essential to consider that although the data acquisition was synchronized, the respiratory signals collected by the CPAP/APAP machine and the VitalSticker device may exhibit temporal asynchrony due to the different physiological sources being measured. Additionally, the CPAP/APAP machine's delivery of pressure during inhalation may cause the inspiratory process to be slower compared to the expiratory process. In contrast, the impedance shift measured by the VitalSticker device remains relatively constant throughout both inhalation and exhalation.

It is worth mentioning that all participants provided informed consent before participating in the study. The INESCTEC ethics committee approved the research protocol to ensure the ethical

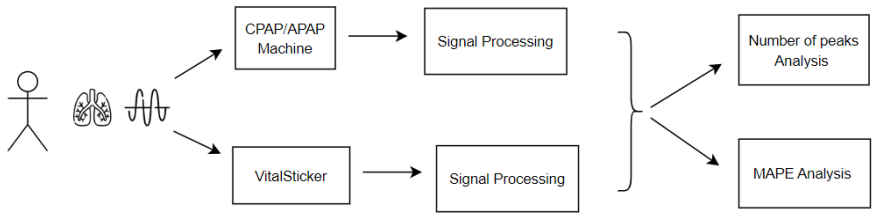

Figure 3.19: Protocol Diagram of the Validation study of the Respiration Signal

considerations and protection of the participant's rights and well-being.

Results

The recorded respiratory signals from the VitalSticker and the CPAP/APAP machine are similar, yet there are also some discrepancies. For the comparison of these signals, two analysis approaches were employed.

Firstly, a specific time duration was analysed for each participant using both devices and counted the number of respiratory cycles representing two valleys and one peak. Table 3.6 contains a table with the comparison between the two devices, indicating that they are generally aligned but occasionally diverge by a maximum of one peak. Typically the VitalSticker tended to exhibit an additional peak compared to the CPAP/APAP machine. Additionally, Using the CPAP/APAP machine as the ground truth, the mean absolute percentage error (MAPE) [50] was determined for the vector comprising the number of breathing cycles from both devices. MAPE error was calculated to be 2.5%.

Table 3.6: Table with the breathing cycles comparison between CPAP/APAP machine and VitalSticker

Person	Analysis time (sec)	Number of breathing cycles	
		CPAP/APAP Machine	VitalSticker
A	187	36	37
B	168	52	51
C	160	43	43
D	155	26	27
E	124	27	28
MAPE (%):		2,45	

In the second analysis, the MAPE was calculated for the differences between the devices in respiration rate, peak duration, and respiration cycle duration. Table 3.7 contains the results of all participants. The respiration rate is calculated by dividing 60 seconds by the time between successive peaks, which is divided by the sampling rate. Moreover, the time disparities between valleys were used to compute the duration of respiratory cycles, whereas time differences between peaks were used to calculate peak duration. Notably, the error in peak duration measurements was

often lower than in valley duration measurements. This discrepancy can be attributed to the distinct data acquisition processes of the two devices. The CPAP/APAP machine measures the respiration signal based on the induced pressure in the patient, resulting in potentially longer inspiratory processes and shorter expiratory processes compared to the VitalSticker device. Although this compensates for synchronisation, the differences in valleys are more prone to error, leading to the observed results.

Table 3.7: Table with MAPE analysis

Person	Mean Absolute Percentage error (%)			Cycles analysed
	Respiration Rate Difference	Respiration Cycle Duration	Peaks Duration Difference	
A	7,42	9,45	7,33	35
B	4,46	6,22	4,44	34
C	9,41	9,13	8,88	43
D	6,21	13,49	6,20	20
E	9,78	12,53	7,56	27

Following this observation, figure 3.20 and 3.21 were generated to illustrate the phenomenon visually; the second figure is an ampliation of the first one to understand better the time differences of both devices and the desynchronization associated with that. Figure 3.21 highlights a distinct pattern between the two devices, particularly evident between the 50th and 100th second. In this interval, the inhalation time recorded by the CPAP/APAP machine appears longer than the VitalSticker device. The observed differences in inhalation duration between the CPAP/APAP machine and the VitalSticker device align with their respective data acquisition processes. The CPAP/APAP machine measures the respiration signal based on induced pressure, potentially resulting in longer inspiratory processes. In contrast, the VitalSticker device captures the respiratory signal through impedance variations, which may lead to shorter inhalation durations. This discrepancy in inhalation times contributes to the variations observed in the valleys of the respiratory signals. Summarising, the figure provides visual evidence supporting the notion that these devices capture respiration signals differently, emphasizing the potential impact of the data acquisition process on the observed variations between them.

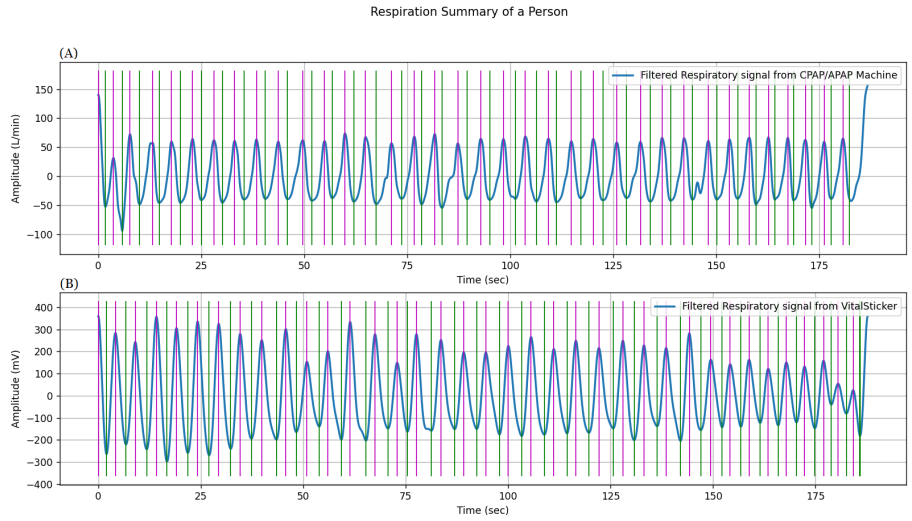

Figure 3.20: Respiratory signal from a participant. (A) signal from CPAP/APAP machine; (B) signal from VitalSticker

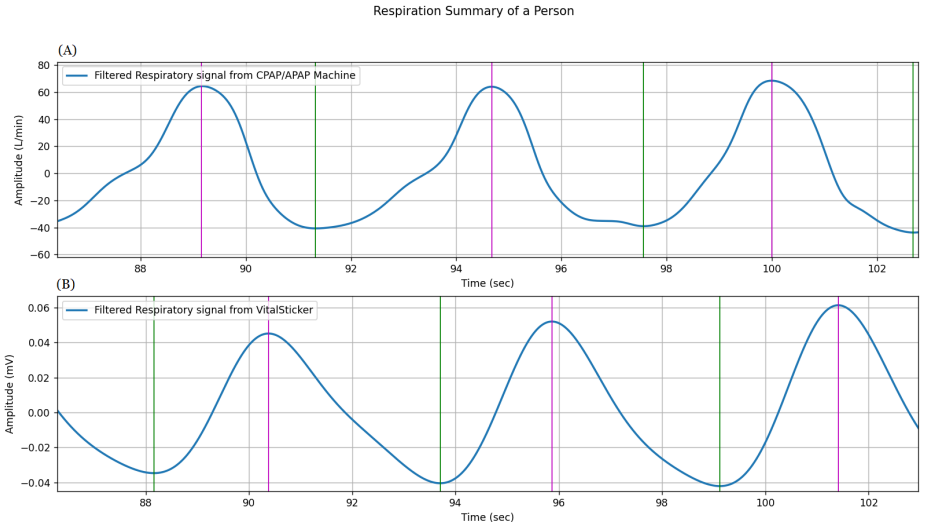

Figure 3.21: Zoomed figure of the respiratory signal. (A) signal from CPAP/APAP machine; (B) signal from VitalSticker

In addition, two Bland-Altman plots were generated to assess between the devices regarding the duration of peaks and respiratory cycles. The Bland-Altman plot illustrates the level of agreement between the two measuring methods by showing the difference between the values against their average. The graphs (in Figures 3.22 and 3.23) for both parameters exhibited most of the data points clustered around the mean difference and within two times the standard deviation of the data. This indicates reasonable agreement between the VitalSticker device and the CPAP/APAP machine.

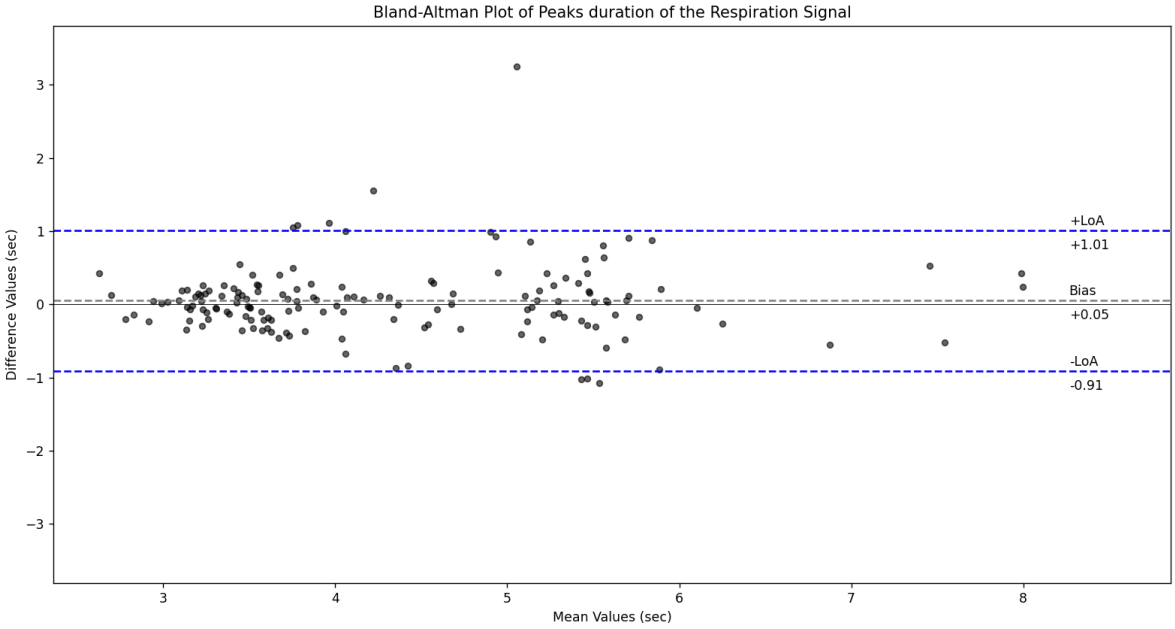

Figure 3.22: Bland-Altman Plot of time duration between peaks

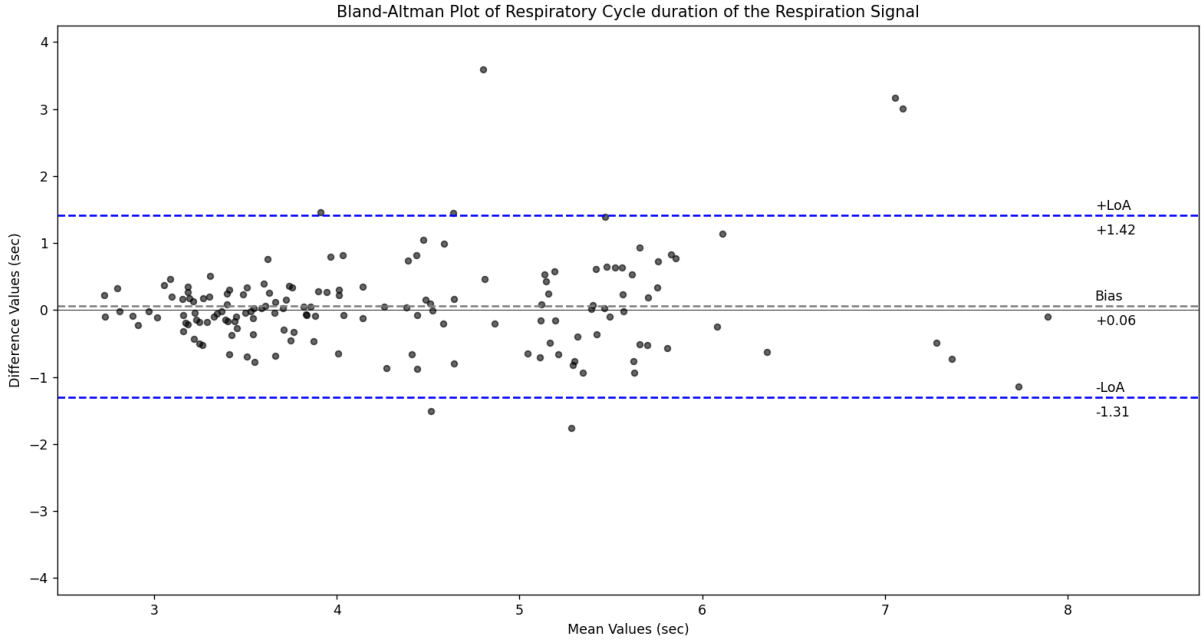

Figure 3.23: Bland-Altman Plot of Respiratory Cycle duration

Discussion

For the cycle count, VitalSticker and CPAP/APAP machine are very similar, thus validating the breathing cycles on the VitalSticker device. For the cycle alignment, the variations in inhalation

and exhalation duration and, consequently, the errors associated can be attributed to the distinct data acquisition processes employed by the devices. The CPAP/APAP machine, which measures respiration based on induced pressure, tends to have longer inspiratory and faster expiratory processes than the VitalSticker device, which captures signals through impedance variations in the thoracic cavity. However, this was expected as the CPAP/APAP machine induces air pressure through the nose mask resulting in longer inspiratory processes, which leads to the difference in the VitalSticker results.

These differences directly impact the valleys and peaks of the respiratory signals. Additionally, participant-related factors, including breathing patterns and anatomical variations, could have contributed to the discrepancies.

3.3.2.6 Conclusions of the Respiration quality signal validation

In conclusion, this study successfully validated the respiration signal collected with the VitalSticker device by comparing it with the CPAP/APAP machine. The VitalSticker device provides a non-invasive and simple approach for measuring breathing, with results equivalent to a CPAP/APAP machine. The study underlines the importance of considering the data acquisition method as well as the potential impact of device-specific characteristics on signal measurements. Overall, this research advances our understanding of respiratory monitoring devices, and the VitalSticker device shows promise as a dependable instrument for recording respiration signals.

Chapter 4

Machine Learning Classifiers for Biometric Identification

The primary goal of this research is to investigate the potential benefits of incorporating respiration data alongside ECG signals in the classification system of the wearable device. Integrating these two physiological signals aims to enhance the accuracy and robustness of biometric identification.

Biometric identification using ECG and respiration signals holds great significance in healthcare and security. As described in previous chapters, ECG signals provide unique patterns that can be used for individual identification. Respiration signals, however, reflect individual breathing patterns and can provide extra information for more exact identification. Combining these two signals can potentially increase biometric identification systems' reliability and accuracy.

This research will explore machine learning approaches for developing a biometric classification method using ECG and respiration signals. The classifiers that will be examined include Support Vector Machines (SVM), K-Nearest Neighbors (KNN), Decision Tree, Gaussian Naive Bayes and Random Forest. These classifiers were chosen for their proven effectiveness in biometric identification tasks and their potential to be implemented in a lightweight algorithm suitable for a wearable device [53] [54], such as a microcontroller integrated into VitalSticker, used in the master's thesis for acquiring the data.

This study seeks to create an efficient and accurate biometric classification algorithm that can be deployed on a wearable device and enable real-time identification of persons based on ECG and breathing signals. A system like this would be helpful in various industries, including healthcare, security, and personalised monitoring.

In the following sections of this chapter, we will show the approach used for training and testing the ML classifiers, review the results and performance analysis, and investigate the possible benefits of adding respiration data in enhancing biometric identification.

4.1 Experiment Setup

This section will provide an overview of the experimental setup, including details about the dataset, the participants involved, feature extraction from ECG and respiratory signals, and the preprocessing steps applied to the data.

4.1.1 Dataset Description

Three ML experiments were carried out with the dataset collected, the detailed explanation about it is in section 3.2. In the first test, we utilized the entire dataset, consisting of 24 individuals. Subsequently, we performed two additional tests with 10 and 5 participants, respectively. This variation in participant numbers is rooted in the context of this study, which focuses on utilizing vital parameters for biometric authentication/identification in hazardous scenarios. In such situations, access to restricted areas is limited, and the number of individuals to be identified is typically small, ranging from 5 to 10 persons.

4.1.2 Feature Extraction from ECG and Respiratory Signals

The methodology described in [4] was followed to extract relevant features from the ECG signals. This study, which achieved an accuracy of 97% using SVM with 10 participants, identified the most significant features of the ECG signal for person identification. Based on their findings, the following features were selected: the duration between fiducial points of an ECG waveform, namely ST, RT, and QT.

Regarding the feature extraction from respiratory signals, it relied on the research conducted in [35] and [34]. These studies also utilized the same features to identify individuals using the respiratory signal. In [35], the authors achieved an accuracy of 100% with 6 participants, employing an SVM classifier. Similarly, in [34], a remarkable accuracy of 97% was achieved using SVM and 87% using KNN classifiers, with 20 participants. It is worth noting that the signal acquisition method in this research differed from the referenced studies (RADAR), as this one utilized a wearable device (VitalSticker). From the signals acquired through this alternative approach, the selected features were the duration of inspiration and expiration, respiration rate, and the speed of inhalation and exhalation as the features for analysis.

Preprocessing Steps

All signals were preprocessed before feature extraction, as outlined in previous chapters. These processes included the essential techniques for cleaning and enhancing the signals, assuring the correctness and dependability of the subsequent feature extraction process.

Following these steps established an experimental setup, enabling an investigation into the potential of utilizing vital parameters for biometric authentication/identification in hazardous scenarios.

4.2 Performance Evaluation of ECG-Driven ML Classifiers

This section presents the results of training and testing machine learning classifiers using only the ECG data from the collected dataset. The following five classifiers were tested: Support Vector Machine (SVM), K-Nearest Neighbor (KNN), Decision Tree, Gaussian Naive Bayes (GNB), and Random Forest. These classifiers are chosen for their lightweight nature, making them suitable for integration into wearable devices. They are particularly well-suited for scenarios with limited data and real-time identification of a small group of individuals.

To evaluate the performance of the classifiers, the entire dataset consisting of 24 individuals was utilized for training and testing. The results were carefully analyzed, and the two classifiers demonstrating the best performance were further evaluated using subsets of 10 and 5 individuals' data. This additional evaluation allowed for the selection of the best ML classifier for ECG data, considering the specific characteristics of this dataset. Figure 4.1 illustrates the schematic of the classficiation steps done.

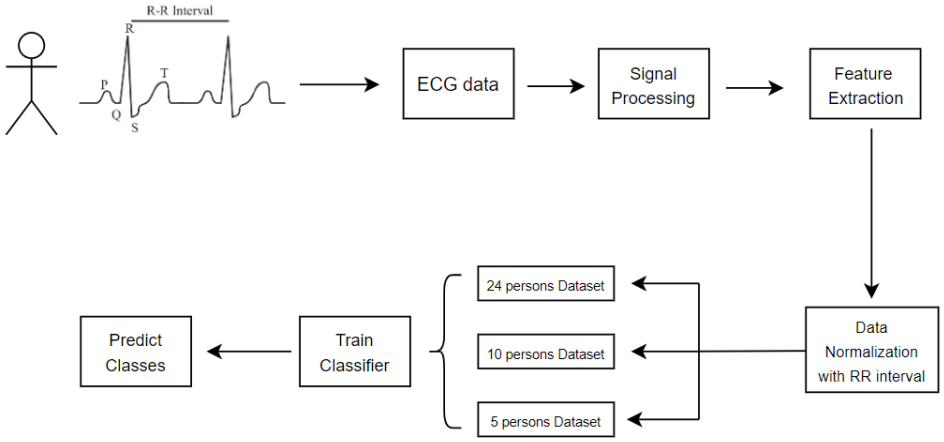

Figure 4.1: Schematic representation of the classification steps using only the ECG signal

4.2.1 Normalization process

The features and pre-processing techniques applied to the ECG signal were discussed in previous chapters. However, in accordance with [4], a normalization method based on the average RR distance across all subjects in the training set was adopted. This approach offers the advantage of providing an independent classification of the subject's heart rate, contrasting with other methods in the literature that employ subject-specific RR values. Consequently, this research utilized the RR distance of the training set to normalize all the ECG data features.

Normalizing the features with the training set's RR distance ensures comparability and consistency across different individuals. This normalization method accounts for individual variations in heart rate, thereby enhancing the classifier's ability to generalize and make accurate predictions across diverse subjects.

4.2.2 Classifiers Training and Evaluation

The ML classifiers chosen for this study demonstrate high effectiveness in classification tasks, particularly for small datasets. The selected classifiers include Support Vector Machine (SVM), K-Nearest Neighbor (KNN), Decision Tree, Gaussian Naive Bayes (GNB), and Random Forest.

1. **Support Vector Machines (SVM):** SVM is a powerful binary classification algorithm that constructs a hyperplane in a high-dimensional feature space. Its objective is to maximise the margin between classes while identifying the optimal separation boundary. SVM handles complex decision boundaries and performs well with small to medium-sized datasets [55]

2. **K-Nearest Neighbors (KNN):** KNN is a non-parametric algorithm that classifies new instances based on the majority vote of their k nearest neighbours in the feature space. Unlike other classifiers, KNN does not assume any specific underlying data distribution and can effectively handle continuous and categorical features [56]

3. **Decision Trees:** Decision Trees are tree-based models that recursively partition the feature space, making decisions at each node based on specific criteria. These classifiers offer interpretability and can capture non-linear relationships within the data. They are well-suited for scenarios where understanding the decision-making process is crucial [57]

4. **Gaussian Naive Bayes:** Gaussian Naive Bayes is a probabilistic classifier that assumes the features follow a Gaussian distribution. Applying Bayes' theorem calculates the posterior probability of each class given the input features, enabling the selection of the class with the highest probability. [58]

5. **Random Forest:** Random Forest is an ensemble learning method that combines multiple decision trees. Bootstrapping and random feature selection create a robust and diverse set of trees. Random Forest is known for handling high-dimensional data, reducing overfitting, and providing reliable predictions [59]

The selection of these ML classifiers aims to leverage their distinct properties and capabilities to achieve accurate and reliable classification results on the ECG dataset used in this study.

Parameter Selection

For each classifier, the parameters that could optimize their performance on the data were selected. The parameter selection involves the knowledge of each one and empirical experimentation. The tool used for parameter selection and the training process was the Python library *scikit-learn*. The library used already includes all the classifiers that were used for this study, as well as multiple parameter options for each classifier [60]. The parameters tested in each classifier are described below:

- **Support Vector Machines:** SVM required tuning parameters such as the regularization parameter (C)- which trades off correct classification of training examples against maximization of the decision function's margin- and the gamma parameter (γ)- how far the influence of a single training example reaches. The kernel used was a radial basis function based on [4]. The experiments include different parameter combinations to find the optimal settings that yield the best classification performance.

- **K-Nearest Neighbors:** The main parameter is k, representing the number of nearest neighbours to consider. It explored different values of k to find the optimal balance between overfitting (low k) and over smoothing (high k). However, it also tested the distance computation metric, the algorithm to compute the nearest neighbour and the Weight function used in prediction.

- **Decision Tree:** The parameters focused on the maximum tree depth, minimum samples required to split, minimum samples required at a leaf node and the function to measure the quality of a split. These parameters help to prevent overfitting and ensure reasonable tree complexity.

- **Gaussian Naive Bayes:** This classifier does not have many tunable parameters that could be beneficially explored for this dataset in specific.

- **Random Forest:**Parameters considered for Random Forest included the number of trees in the ensemble, the maximum number of features to consider at each split, and some others also explored in the Decision Tree classifier. The aim was to balance model complexity and diversity among the constituent trees.

Training Procedure

During the training of all classifiers, cross-validation techniques were employed, specifically k-fold cross-validation, to evaluate the models' generalization capabilities and mitigate the risk of overfitting. Additionally, hyperparameter tuning was conducted to identify each classifier's optimal combination of parameters. The grid search method was utilized for this purpose.

Once each classifier's optimal parameters were determined, the models were trained with 80% of the data and evaluated based on their performance with the rest 20% of the data. This approach ensured that the classifiers were fine-tuned and assessed accurately, enabling to make reliable conclusions about their capabilities and suitability for the classficiation task.

Evaluation Metrics

In order to evaluate the performance of the different classifiers, the metrics used include accuracy, precision, recall, specificity and F1-score. The analyse of these metrics provides quantitative measures to determine the effectiveness of the classifiers and will help to choose the most suitable with ECG data. A more detailed explanation of the metrics is explained next [61]:

- **Accuracy:** This metric is the most used and is defined as the number of correct predictions overall predictions. The result provides a percentage representing the proportion of accurately predicted cases compared to the total number of instances. Mathematically, accuracy is defined as:

$$Accuracy = \frac{Number\_of\_correct\_classified\_intances}{Total\_number\_of instances}$$

- **Precision:** This measure how many positive predicts were correct (true positives). Precision provides insights into the classifier's ability to make accurate optimistic predictions. This metric formula is:

$$Precision = \frac{Number\_of\_correct\_predicted\_positive\_instances}{Number\_of\_total\_positive\_predictions}$$

$$= \frac{True\_positive}{True\_positive + False\_positives}$$

- **Recall/Sensitivity:** Measure how many positive cases the classifier correctly predicted over all the positive cases in the data. The recall is a valuable metric for correctly evaluating the classifier's ability to capture positive instances. Mathematically defined as:

$$Recall = \frac{True\_positive}{True\_positive + False\_negatives}$$

- **Specificity:** This metric measures the proportion of correctly predicted negative instances out of all actual negative instances. It provides insights into a classifier's ability to identify true negatives.

$$Specificity = \frac{True\_Negatives}{True\_negatives + False\_positives}$$

- **F1-Score:** F1-Score is a measure combining both precision and recall into a single value. This composite metric provides a balanced measure of the classified performance and is beneficial when dealing with imbalanced datasets, where precision and recall might have different priorities. The formula to calculate it is:

$$F1\_score = 2 \times \frac{Precision \times Recall}{Precision + Recall}$$

The evaluation metrics mentioned above are widely used in classification tasks and provide valuable insights into the performance of the classifiers and will help decide the best classification method for the dataset used.

4.2.3 Classifiers Results

The evaluation of the classifiers using only ECG data was conducted with datasets consisting of 24, 10, and 5 individuals. The initial analysis focused on the performance metrics described earlier,

utilising the dataset of 24 individuals.

Table 4.1 presents the evaluation metrics for all classifiers using the dataset of 24 individuals. Remarkably, all classifiers had excellent specificity ratings, demonstrating their ability to recognise negative cases reliably. Due to the high specificity of all classifiers, this metric is less critical and will be discarded in the selection process.

Table 4.1: Performance evaluation of a ECG-driven identification algorithm in a 24 people dataset

Classifier	Dataset	Accuracy (%)	Precision (%)	F1-score (%)	Recall (%)	Specificity (%)
SVM	Train	69,0	69,0	68,0	68,0	98,5
	Test	66,0	65,0	63,0	63,0	98,3
KNN	Train	83,0	84,0	84,0	83,0	99,0
	Test	67,0	65,0	65,0	64,0	98,0
Decision Tree	Train	69,0	69,0	68,0	68,0	98,4
	Test	64,0	64,0	61,0	62,0	98,2
GNB	Train	31,0	25,0	28,0	20,0	96,6
	Test	28,0	21,0	26,0	20,0	96,5
Random Forest	Train	70,0	70,0	69,0	69,0	98,5
	Test	64,0	63,0	62,0	62,0	98,3

When analysing the results in Table 4.1, the Gaussian Naive Bayes classifier exhibited the lowest performance compared to the other classifiers on all metrics. Consequently, it was excluded from further consideration as the worst-performing classifier for the given dataset.

The next phase involved evaluating the performance of the four remaining classifiers (SVM, KNN, Decision Tree, and Random Forest) using reduced datasets containing 10 and 5 individuals, respectively. The results of these evaluations are presented in Table 4.2 and Table 4.3.

Table 4.2: Performance evaluation of a ECG-driven identification algorithm in a 10 people dataset

Classifier	Dataset	Accuracy (%)	Precision (%)	Recall (%)	F1-score (%)	Specificity (%)
SVM	Train	85,0	86,0	85,0	85,0	98,0
	Test	86,0	87,0	86,0	86,0	98,0
KNN	Train	93,0	93,0	93,0	93,0	99,0
	Test	86,0	86,0	86,0	85,0	98,0
Decision Tree	Train	85,0	85,0	84,0	84,0	98,2
	Test	84,0	85,0	84,0	84,0	98,0
Random Forest	Train	86,0	86,0	86,0	86,0	98,4
	Test	85,0	86,0	85,0	85,0	98,3

When evaluating performance on the 10-person dataset, the test set evaluation metrics were given more weight than the training set assessment metrics. The SVM classifier outperformed the others, followed by the KNN classifier. Both classifiers produced encouraging results, proving their ability to identify instances within the smaller dataset correctly.

On the other hand, the 5-person dataset produced a slightly different outcome. In this case, the Random Forest classifier outperformed the other evaluation criteria discussed before. Notably, the SVM classifier remained a strong contender, performing only 1% worse than the Random Forest classifier.

Table 4.3: Performance evaluation of a ECG-driven identification algorithm in a 5 people dataset

Classifier	Dataset	Accuracy (%)	Precision (%)	Recall (%)	F1-score (%)	Specificity (%)
SVM	Train	97,0	97,0	97,0	97,0	99,0
	Test	97,0	97,0	97,0	97,0	99,0
KNN	Train	98,0	98,0	98,0	98,0	99,5
	Test	97,0	96,0	97,0	97,0	99,1
Decision Tree	Train	96,0	96,0	96,0	96,0	98,9
	Test	96,0	96,0	96,0	96,0	99,0
Random Forest	Train	97,0	97,0	97,0	97,0	99,3
	Test	98,0	97,0	98,0	98,0	99,4

These findings show that the performance of the classifiers varies according to the size of the dataset. The SVM classifier consistently showed competitive performance, while the KNN classifier demonstrated its potential on larger datasets. In addition, a Random Forest classification performed exceptionally well for smaller datasets showing that it was able to do so efficiently with limited data samples.

The results obtained from these evaluations provide valuable insights into the effectiveness of classifiers across different dataset sizes, enabling better decision-making on which classification model to use alongside respiratory data in future analyses. Based on the performance observed, it is worth noting that the SVM classifier consistently demonstrated competitive results across the various dataset sizes tested. Therefore, considering its strong performance and robustness, the SVM classifier will be selected as the primary classification model when combining the ECG data with respiratory data. This choice ensures the incorporation of a dependable and accurate classifier capable of efficiently leveraging both types of physiological inputs to improve the wearable device's overall performance and prediction capabilities.

Comparison with literature

The research that forms the basis of this ECG-based machine learning classifier for human identification is *BEAT-ID* [4]. Similar to this work, it also utilizes the SVM classifier and ECG data as input. However, the main difference lies in the dataset used. While this work created a new dataset, the referenced paper employs ECG signals from the Physionet database. A comparison of the results from both approaches is presented in Table 4.4, which shows that the accuracy values in this work are slightly lower than those reported in *BEAT-ID* [4]. This discrepancy can be attributed to the differences in the datasets. The ECG signals from the Physionet database have a high level of quality as they are clinical signals acquired with 12-lead electrodes. On the other hand, the ECG signal collected by a wearable device (VitalSticker) using only two electrodes presents more noise, resulting in lower accuracy compared to the literature.

Table 4.4: Accuracy comparison between BEAT-ID [4] and this work of an ECG-driven identification algorithm

	BEAT-ID	This work
Number of persons:	10	10
Classifier used	SVM	SVM
Accuracy (%)	97,5	86,0

4.2.4 Confusion Matrix of the best ECG data classifer

The best classifier based on the evaluation results was the Support Vector Machine (SVM). To provide a comprehensive understanding of its performance, the confusion matrixes of the testing set for the SVM classifier on the ECG data on 24, 10 and 5 persons will be presented. The confusion matrix provides a precise breakdown of the classifier's predictions, allowing us to evaluate it in terms of true positives (TP), true negatives (TN), false positives (FP), and false negatives (FN).

Figure 4.2 depicts the SVM classifier's overall performance in the first test using a dataset of 24 persons. Classifications 0, 1, 3, 7, 8, and 9 had the highest accuracy, with the fewest misclassifications indicated by non-zero values outside the diagonal. In contrast, classes 14, 20 and 21 had a high number of misclassifications due to the fewer data available to them.

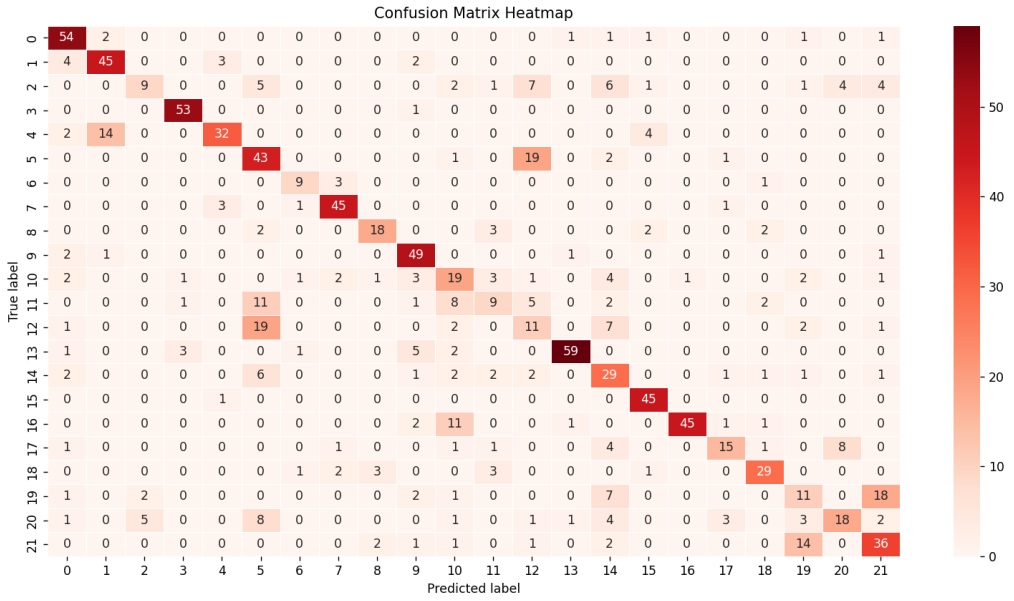

Figure 4.2: Confusion Matrix of 24 persons testing dataset of an ECG-driven identication algorithm

On the 10-person dataset, SVM classier demonstrated a stronger performance (figure 4.3). It correctly classified the majority of instances for each class, indicated by high values along the diagonal. However, there were a few misclassifications, principally in classes 2 and 7.

In the test with five persons dataset, the confusion matrix (figure 4.4) reflects the high accuracy of the classifier in small datasets. Classes 0, 1, 2, 3, and 4 had flawless or near-perfect categorization, with only a few misclassifications in other classes.

On these test sets, the SVM classifier performed well overall, achieving high accuracy in many cases.

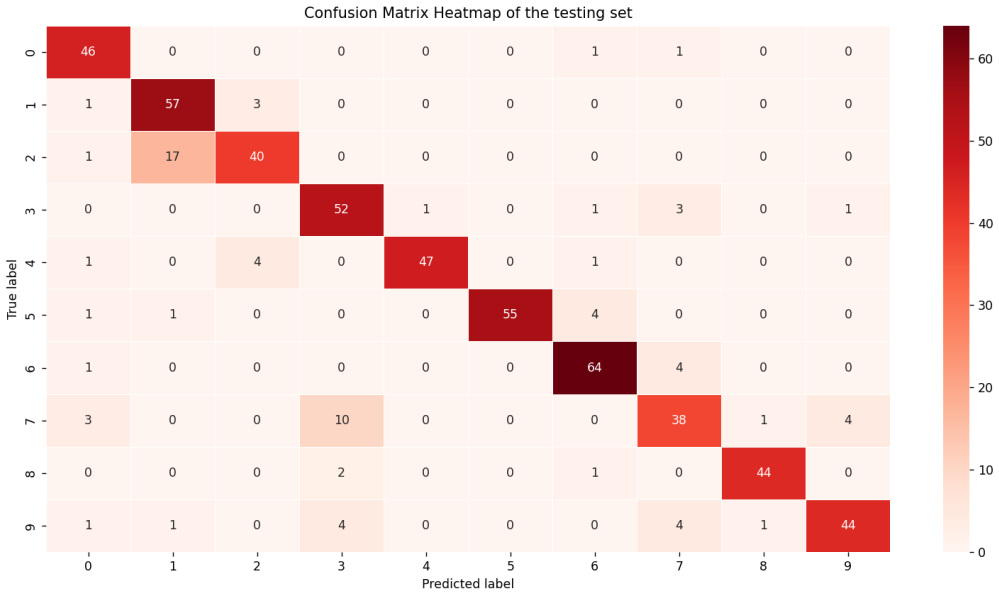

Figure 4.3: Confusion Matrix of 10 persons testing dataset of an ECG-driven identication algorithm

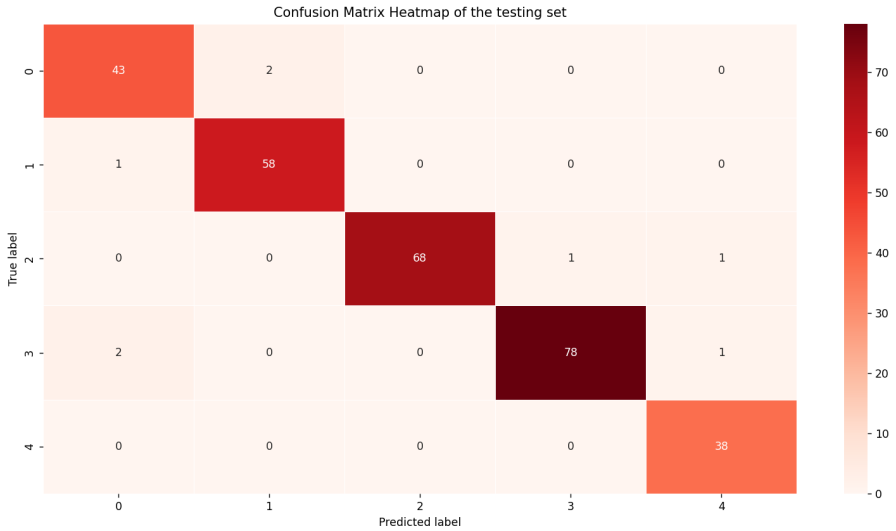

Figure 4.4: Confusion Matrix of 5 persons testing dataset of an ECG-driven identication algorithm

4.3 Performance Evaluation of Combined ECG and Respiratory ML Classifiers

This section focuses on the performance evaluation of machine learning (ML) classifiers using a combined matrix that incorporates ECG and respiratory data. The objective is to analyze the classification performance when these two datasets are integrated.

However, the number of respiratory samples is lower than the number of ECG samples because, based on the collected data, the average duration of a respiratory cycle corresponds to five heartbeats. As a result, the respiration cycles were duplicated in proportion to obtain a square matrix for the classification process. This approach allows us to utilize all the data from the ECG dataset without losing any, which is crucial because ECG features have discriminant characteristics for person identification. By combining these datasets, a more comprehensive analysis can be conducted, specifically regarding classification performance.

While existing literature suggests the potential use of respiratory signals for person identification, their discriminatory capabilities might be inferior to ECG data. However, combining these two signals may significantly improve classification performance. Therefore, the primary focus of this section is to assess whether the integration of ECG and respiratory data enhances the identification process.

By evaluating the performance of ML classifiers on the joint matrix, this study aims to provide insights into the effectiveness and potential limitations of combining these two types of physiological data. The findings will contribute to a deeper understanding of the implications and feasibility of utilizing a joint matrix approach for classification tasks in the context of ECG and respiratory signals. Figure 4.5 illustrates the schematic of the classficiation steps done

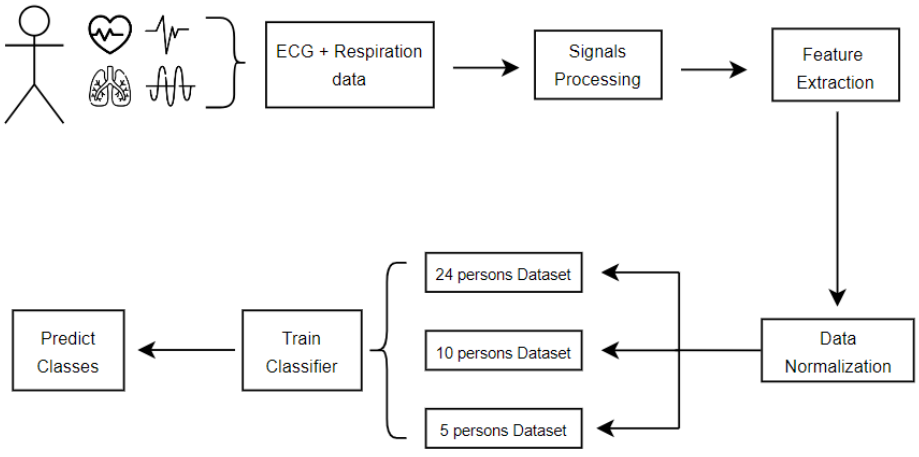

Figure 4.5: Schematic representation of the classification steps using ECG and Respiration signals

4.3.1 Normalization process

After preprocessing the ECG and respiration signals and extracting the relevant features for ML classifiers, the normalization of the data is typically performed. The normalization process is crucial for the following reasons:

1. **Comparable Scale:** The features in the dataset may vary significantly in terms of scale and range. Normalization ensures that all features are brought to a comparable scale, preventing the dominance of certain features and avoiding biases towards specific attributes.

2. **Convergence and Stability:** Normalization can enhance the convergence speed and improve the algorithm's stability during training, leading to more efficient and reliable results.

In the context of this study, where combined data from two vital signals (ECG and respiration) are used, the values often differ in magnitude. To achieve accurate and reliable results, a small study was conducted to determine the most suitable normalization technique for the dataset. The performance of each normalization technique in terms of accuracy, precision, recall, and F1 score was averaged.

The study utilized a reduced dataset comprising 24 individuals for all the classifiers. This reduced dataset included the combined ECG and respiration data without duplicating the respiratory data, and it had fewer samples from the ECG dataset to match the number of respiration samples. Reducing the dataset for normalization analysis offers several benefits, including the elimination of redundant information and resource optimization in terms of computational effort and memory usage.

Furthermore, the study evaluated three normalization techniques: Z-Score, MinMax, and Logarithmic Transformation [62]. The performance of each technique was compared to the dataset without any normalization (raw data), which served as the ground truth for comparison.

The normalization techniques used in this study are as follows:

- **Z-Score Normalization / Standardization:** This technique transforms the data into a mean of zero and a standard deviation of one. Z-Score normalization is widespread as it preserves the distribution shape and effectively handles outliers.

$$x'_{i,n} = \frac{x_{i,n} - \mu}{\gamma}$$

  Where $x_{i,n}$ is the original value, μ is the mean of the data and γ is the standard desviation.

- **MinMax Normalization:** This technique scales the data to 0 and 1. It is particularly useful when the attributes' absolute values or range are crucial. MinMax normalization preserves the relative relationships between data points and is suitable for distance-based classifiers such as KNN.

$$x_{scaled} = \frac{x - x_{min}}{x_{max} - x_{min}}$$

- **Logarithmic Transformation:** This normalization technique is advantageous when the data covers a wide range. The scale is compressed by applying a logarithmic transformation to the data, making it more suitable for classifiers that assume a normal distribution or exhibit improved performance with normalized data.

$$x_{scale} = log(x_i + 1)$$

Where the logaritm have base e

Table 4.5 presents the average values of various evaluation metrics for each normalization technique across the SVM, KNN, Decision Tree, and Random Forest classifiers. The evaluation was conducted on the test set, considered the most crucial set for model evaluation.

Table 4.5: Performance evaluation of the normalization techniques in the (ECG + Respiration) driven identification

Normalization	Dataset	Accuracy (%)	Precision (%)	Recall (%)	F1-Score (%)
without	train	74,00	76,50	73,75	73,50
	test	51,50	52,50	52,25	49,75
Z-score	train	77,50	78,25	78,00	77,50
	test	63,50	64,25	64,75	62,00
MinMax	train	78,75	79,00	78,75	78,00
	test	63,25	62,50	64,75	61,25
Logarithmic	train	71,75	73,00	71,25	70,75
	test	57,25	57,25	58,25	54,75

The analysis reveals that Z-Score normalization performs better than other normalization techniques. It yields higher values for almost all of the evaluated metrics, indicating better classification results. However, it is important to note that the performance difference between Z-Score normalization and Min-Max normalization is relatively tiny. In contrast, the results obtained without normalization exhibit noticeably poorer performance than the normalized approaches. This emphasizes the importance of applying appropriate normalization techniques to ensure reliable and accurate model outcomes. Based on the results obtained, the subsequent steps of the study proceeded with the utilization of Z-Score normalization on the dataset.

4.3.2 Classifiers Training and Evaluation

As previously mentioned, the classifiers SVM, KNN, Decision Tree, and Random Forest were employed for training and evaluation. The parameters for these classifiers were chosen through the Grid Search method, which was also applied in evaluating their performance on the ECG dataset. The evaluation process focuses on several fundamental metrics to comprehensively assess the classifiers' performance, including accuracy, precision, recall and F1-score.

The evaluation was conducted on datasets of 24, 10, and 5 individuals. The first two datasets were used to test all classifiers and to determine the performance of the best classifier — with the highest scores across the generated assessment measures.

The study aims to provide insights into the performance and effectiveness of the selected classifiers on identifying persons by examining these datasets and employing a thorough evaluation methodology, emphasize the ability to classify ECG and respiratory data in different dataset sizes.

4.3.3 Classifiers Results

The evaluation metrics were calculated for each classifier, and the performance of the classifiers is presented in Tables 4.6, 4.7 and 4.8, representing the 24-person, 10-person, and 5-person datasets, respectively.

Table 4.6: Performance evaluation of the 24-persons dataset in the (ECG + Respiration) driven identification; In bold is represented the classifier with the high evaluated metrics

Classifier	Dataset	Accuracy (%)	Precision (%)	F1-score (%)	Recall (%)	Specificity (%)
SVM	Train	82,0	82,0	81,0	81,0	99,1
	Test	74,0	73,0	71,0	71,0	98,7
KNN	Train	100,0	100,0	100,0	100,0	100,0
	Test	73,0	70,0	68,0	68,0	98,7
Decision Tree	Train	87,0	86,0	86,0	86,0	99,4
	Test	71,0	69,0	67,0	68,0	98,6
Random Forest	Train	94,0	94,0	93,0	93,0	99,6
	Test	**78,0**	**76,0**	**75,0**	**75,0**	**98,9**

Table 4.7: Performance evaluation of the 10-persons dataset in the (ECG + Respiration) driven identification; In bold is represented the classifier with the high evaluated metrics

Classifier	Dataset	Accuracy (%)	Precision (%)	F1-score (%)	Recall (%)	Specificity (%)
SVM	Train	93,0	93,0	93,0	93,0	99,3
	Test	88,0	88,0	87,0	88,0	98,6
KNN	Train	100,0	100,0	100,0	100,0	100,0
	Test	86,0	87,0	86,0	86,0	98,4
Decision Tree	Train	94,0	94,0	94,0	93,0	99,3
	Test	82,0	82,0	82,0	82,0	98,0
Random Forest	Train	97,0	97,0	97,0	97,0	99,0
	Test	**91,0**	**91,0**	**91,0**	**91,0**	**99,0**

As it was mentioned before the high values of specificity ratings, demonstrate the classifiers' ability to recognise negative cases reliably. Due to the high specificity of all classifiers, this metric is less critical and will be discarded in the selection process.

Throughout all datasets, the Random Forest classifier consistently displayed the best overall performance based on the examined metrics across all datasets. The SVM classifier had the second-highest values for the 24 and 10-person datasets. KNN and Decision Tree classifiers performed well in the 5-person dataset achieving the second-best value of the evaluation performance. In the 24 and 10-person datasets, the Decision Tree classifier had the worst performance among them.

Table 4.8: Performance evaluation of the 5-persons dataset in the (ECG + Respiration) driven identification; In bold is represented the classifier with the high evaluated metrics

Classifier	Dataset	Accuracy (%)	Precision (%)	F1-score (%)	Recall (%)	Specificity (%)
SVM	Train	97,0	97,0	97,0	97,0	99,3
	Test	96,0	96,0	96,0	96,0	99,0
KNN	Train	100,0	100,0	100,0	100,0	100,0
	Test	97,0	97,0	97,0	97,0	99,3
Decision Tree	Train	98,0	98,0	98,0	98,0	99,5
	Test	97,0	97,0	97,0	97,0	99,0
Random Forest	Train	99,0	99,0	99,0	99,0	99,7
	Test	**99,0**	**99,0**	**99,0**	**99,0**	**99,6**

It is worth mentioning that specific classifiers got 100% evaluation metrics on the training set (the KNN classifier), indicating that overfitting occurs when training the techniques, despite the data previously being normalised to prevent it.

Based on these results, the Random Forest classifier performed the best in identifying individuals using the combined ECG and respiration dataset.

4.3.4 Results discussion

In order to compare the ground truth accuracy of the combined matrix with ECG and respiration data, two datasets were utilized: one containing only ECG data and another containing only respiration data. The classifiers employed for this analysis were SVM and Random Forest, chosen based on their superior evaluation metrics in the ECG-only and combined ECG and respiration datasets, respectively. The objective was to examine the disparities in classification when using the two vital signals separately versus in combination.

Table 4.9 presents the evaluation metrics of SVM and Random Forest using the ECG-only dataset. In contrast, Table 4.10 displays the corresponding evaluation metrics for the same classifiers applied to the respiration-only dataset.

Table 4.9: Performance evaluation of SVM Random Forest classifiers only with ECG data

Classifier	Number of Persons (labels)	Dataset	Accuracy (%)	Precision (%)	Recall (%)	F1-Score (%)
SVM	**24**	Train	69	69	68	68
		Test	**66**	**65**	**63**	**63**
	10	Train	85	86	85	85
		Test	**86**	**87**	**86**	**86**
	5	Train	97	97	97	97
		Test	97	97	97	97
Random Forest	24	Train	70	70	69	69
		Test	64	63	62	62
	10	Train	86	86	86	86
		Test	85	86	85	85
	5	Train	97	97	97	97
		Test	**98**	**97**	**98**	**98**

Table 4.10: Performance evaluation of SVM and Random Forest classifiers only with Respiratory data

Classifier	Number of Persons (labels)	Dataset	Accuracy (%)	Precision (%)	Recall (%)	F1-Score (%)
SVM	24	Train	58	68	57	58
		Test	19	18	17	15
	10	Train	81	86	80	82
		Test	24	21	27	21
	5	Train	100	100	100	100
		Test	51	45	52	47
Random Forest	**24**	Train	48	53	44	43
		Test	**25**	**18**	**23**	**18**
	10	Train	63	68	61	60
		Test	**36**	**33**	**37**	**32**
	5	Train	84	84	83	83
		Test	**64**	**63**	**64**	**62**

The results reveal that when utilizing only the respiration information, either with SVM or Random Forest, the classifiers performed significantly poorer compared to the dataset with ECG data and the combined dataset with both signals. This finding challenges the existing literature, suggesting that the respiration signal alone can reliably identify individuals in this dataset.

Furthermore, when comparing the ECG-only dataset to the combined dataset, the evaluation metrics consistently exhibited higher values for the combined dataset. Regardless of whether we compare the same classifiers or the best classifiers for each dataset, the combined dataset consistently demonstrated better performance. The disparity becomes less pronounced when reducing the number of individuals in the dataset.

Focusing specifically on the 10-person dataset, which approximates the number of individuals typically found in hazardous environments or restricted areas, the combined dataset outperformed the ECG dataset by approximately 5% and the respiration dataset by 57% when employing the best classifier in all cases. This outcome underscores the benefits of incorporating both ECG and respiration signals in the identification process, as adding respiration data to ECG improved the accuracy of human identification.

Overall, these findings emphasize the advantage of utilizing the combined ECG and respiration datasets over the individual datasets, providing valuable insights into the classification differences between these two vital signals when used in isolation or combination.

The confusion matrices corresponding to each dataset are shown in Figures 4.6a and **??**, which use the combined ECG and respiration dataset and ECG-only dataset, respectively. These matrices were generated using the testing set of each 10-persons dataset (20% of the data). The two confusion matrices exhibit similarity, with both displaying a prominently highlighted diagonal region characterized by darker colors, indicating a good classifier performance. However, in the combined ECG and respiration dataset (4.6a), the occurrences of misclassifications are comparatively fewer. In several instances, the colors outside of the diagonal region appear lighter when compared to the dataset containing only ECG data. This observation reaffirms that the integration of both

vital signals yields advantages in the identification process.

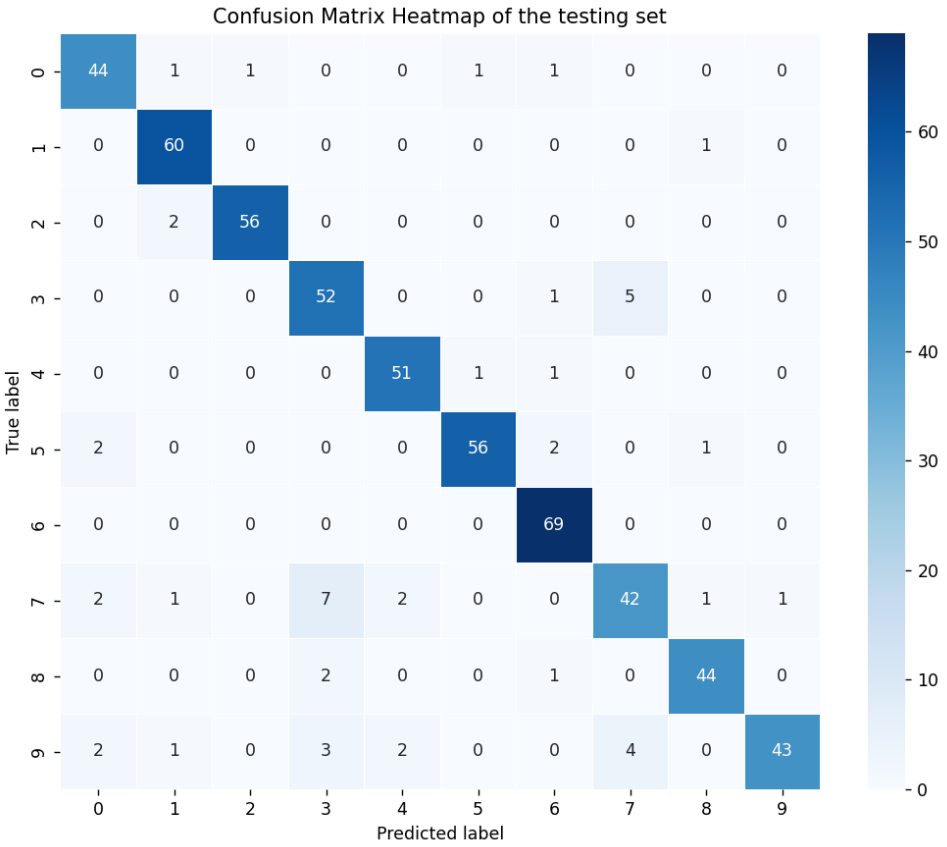

(a) 10 persons dataset with ECG and respiration data and the Random Forest classifier

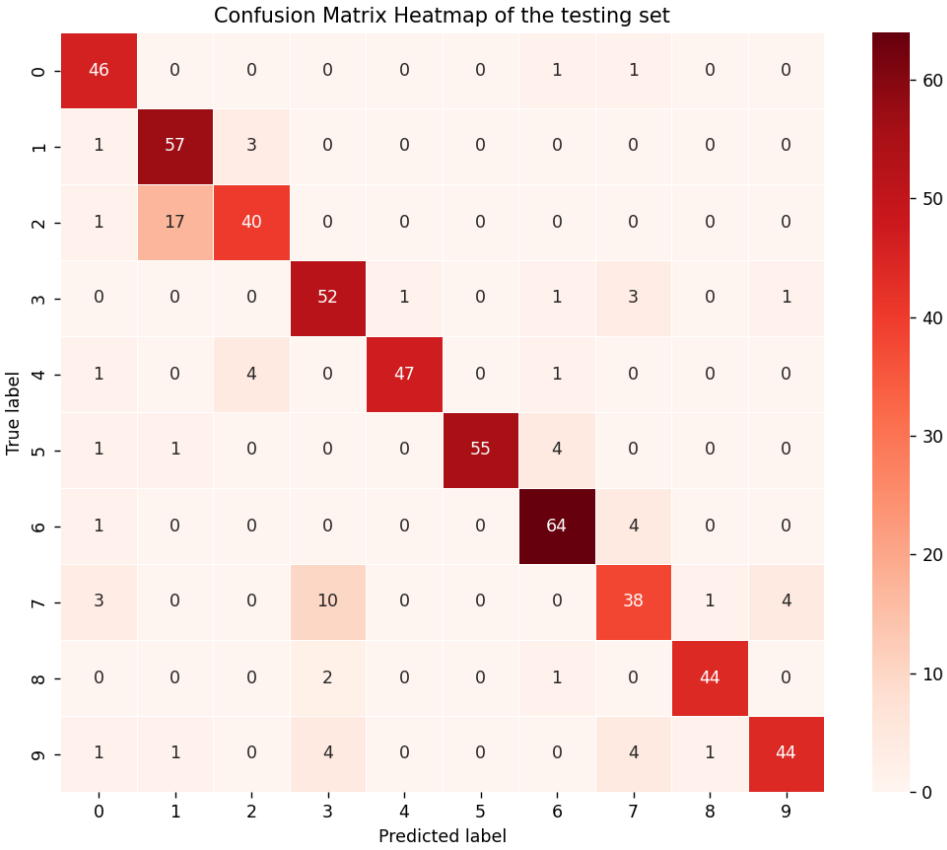

(b) 10 persons dataset with only ECG data and the SVM classifier

Figure 4.6: Confusion Matrix of the test set

Chapter 5

Conclusions and Future Work

In recent years, with the increasing automation and digitization of various aspects of our lives, robust and secure individual recognition methods have become critical and necessary. This has led to interest in the development of biometric-based identification systems, which use a person's unique physiological or behavioural features to identify them. Wearable devices have emerged as a potential technology in this area, enabling the opportunity to capture physiological signals in a non-invasive and easy manner. This research investigates the use of wearable devices for physiological signal collecting and their significance in individual recognition, specifically in health and security situations.

This master's thesis explores the application of wearable devices in acquiring physiological signals for individual recognition. The focus is on utilizing electrocardiogram (ECG) signals as a biometric trait and investigating the integration of respiration signals for improved identification. The wearable device VitalSticker, produced in INESC TEC, was used to acquire the signals. In summary, the main objectives of this master's thesis were achieved, and in order to achieve them, this research passes through several essential steps.

Initially, the study of VitalSticker devices was done. Adhering to the ethical considerations provided by the INESC TEC ethical committee, a dataset of signals from 24 participants was collected. The signals were then carefully processed, and relevant features were extracted for further analysis. Additionally, signal validation was conducted to ensure the accuracy and reliability of the acquired ECG and respiration signals.

Various classifiers (five) were assessed to determine the most suitable models for analyzing the collected vital data. In the evaluation phase, three datasets comprising 24, 10, and 5 individuals were utilized to assess the performance of the developed models. The study's results highlight the effectiveness of the Support Vector Machine (SVM) classifier, which outperformed other methods in ECG dataset and Random Forest in the combined dataset (ECG and respiration signals). Notably, the findings demonstrate that ECG signals alone exhibit a accuracy rate in the identification process of 86% with the 10-person dataset. However, when combined with respiration signals, the accuracy values increases, reaching 91% with the same 10-person dataset. The literature [4], which this work was based, achieve a 97.5% of accuracy in a 10-persons dataset, but with

a different dataset (Physionet database) with high quality signals.

The comparison between the performance of the ECG-only dataset and the combined ECG and respiration dataset revealed that the combined dataset exhibited superior performance. The improvement demonstrated that combining these vital signals is an advantage in a identification process leading to a biometric marker for individual identification.

These findings offer insight into employing ECG and respiration signals as a reliable biometric marker for individual identification. While the findings are encouraging, more studies can be done to increase the classifier's effectiveness by expanding the dataset size, for example.

In conclusion, this work significantly contributes to the field of biometrics and lays the foundation for future research endeavours. It highlights the efficacy of ECG and respiration signals acquired from tiny wearables in accurately identifying individuals and paves the way for further advancements in this field of study. The research outcomes underscore the potential of wearable devices in improving security measures and emphasize the importance of physiological signal collection in various applications, particularly in health and security.

5.1 Future Work

Future work should prioritise the implementation of the ML classifier in the wearable device (A). This implementation holds great potential as it would enable the device to accurately identify the user and serve as an effective authentication method in hazardous scenarios. With additional time and resources, the integration of the ML classifier into the wearable device can be achieved, leading to improved user authentication and enhanced safety measures.

Furthermore, other potential approaches exist to develop the combination between the ECG and respiration signals. One possible example could involve using two classifiers in series, where the ECG data is the first classified, and then a reduced dataset (such as the top 5 persons with the highest probability from the ECG classifier) is used as input for another classifier that utilises respiration data. This approach could be explored to assess if it improves the overall performance of the identification system.

Moreover, further research can focus on optimising the performance and efficiency of the ML classifier, ensuring its seamless integration into the functionality of the wearable device. Addressing these aspects allows a more secure and reliable identification that could be used for authentication systems to be developed for use in hazardous environments.

Appendix A

Edge computing

As it was mentioned in the future work of this research (5.1), the next crucial step is the implementation of a machine learning (ML) classifier within the wearable device. This implementation enables real-time identification and authentication, presenting promising opportunities.

The following section provides an overview of the current state of edge computing in wearable devices, highlighting the existing computational capabilities within these devices where sensors are typically situated.

A.1 Edge computing for wearable devices

Conventional wearable devices typically collect data and transmit it to external servers for off-chip computing and processing. This approach required a high power consumption and operation speed of the sensing systems. In addition, in the case of real-time sensing data, it also results in an intense hardware occupation [7]. Consequently, this method goes against the goals of the general systems.

Wearable devices are constantly trying to balance the trade-off between battery life and computational capacity. Without processing any collected samples (low computation capacity), the amount of raw data sent to external systems will be higher, which results in higher energy consumption. On the other hand, the battery life of the wearable will last longer because it does not include any data analysis. Furthermore, these devices present drawbacks such as being powered by a battery, with a limit energy capacity, and difficulty processing complex algorithms, which might be resolved with edge technology[6].

The modern embedded systems lead us to push computing closer to where the sensors are located gathering data (edge of the network). Edge computing appeared as a more power-efficient technique that reduces the required internet bandwidth. Besides that, it also provides lower latency because raw data does not need to be transferred to other systems for processing, which means decisions can be on real time on the device and for wearable technology [7], [6]. The Edge concept in wearable devices' microcontroller aims to integrate data processing algorithms rather than just the typical tasks of a microcontroller. This means that data is collected and processed

locally, which enables the systems to maximize their performance without compromising their memory budget [7] and also increases its resiliency because it can operate autonomously.

In the context of wearable devices, Edge computing offers more resources without increasing the weight or the size optimising the process of transmitting data, for example. In addition, with the integration of wearable devices and edge computing, the battery life balance of the devices improves and the communication protocols become more energy-efficient [6]. Moreover, with the local processing, the edge approach also ensures that the detailed raw data is not shared with a third-party system, only inference results and metadata, therefore being less susceptible to ethical issues.

All the benefits described above contribute to the decision of developing this dissertation based on an edge computing approach. This approach defends that the classification matrix, developed after training the classifier, should be integrated into the microcontroller. However, this technique could be more deeply explored by integrating the training process of ML classifiers into the MCU as well.

A.1.1 Embedded computing machine learning tools

Embedded computing machine learning techniques are a quickly spreading technology. It finds practical use in wearable health monitoring systems, wireless surveillance systems, and on many Internet of Things (IoT) systems. Besides all the benefits it brings for being based on edge computing, with TinyML, which refers to ML model compression that runs in ultra-low-power microcontrollers, is possible to increase the power autonomy of ML applications.

TinyML combines lightweight ML models with the accuracy of a typical neural network. In addition, this approach allows offline inference without requiring data to be transferred [63]. Lightweight machine learning models aim to reduce memory and latency while retaining the performance of the other ML models. In [63] are presented some of these models like a ProtoNN, which is a lightweight KNN classifier, a lightweight convolution network, or a temporal convolution network (TCNs).

The goal of embedded ML techniques is not only to perform the model execution and inference on embedded devices but also to train the ML models. A develop a recent tool to integrate lightweight ML models to run on microcontrollers (MCU) is the TensorFlow Lite. This framework provides the necessary tools for running neural networks effectively on embedded devices with a few kilobytes of memory. Besides having the possibility of running on multiple MCU cores, its interpreter is flexible and easy to adapt to new applications and features[64]. In this way, TensorFlow Lite tries to address the major issues of TinyML, such as the hardware and software heterogeneity (making it a challenge for TinyML to adopt a given learning method) and the lack of benchmarking tools (in case of inference modes that consume a great amount of memory) [65].

Appendix B

Ethics Approval

B.1 Ethics Approval Documentation

In order to ensure the integrity and ethical conduct of research (3.2.1), it is essential to critical to follow the established guidelines and obtain the necessary approvals. This section presents the documentation that validates the ethical considerations undertaken for the current study. The three essential files for the approval were:

- **Informed Consent of the Participants:** This document stands as a testament to the voluntary participation of individuals, acknowledging their autonomy and ensuring that they have been adequately informed about the research purpose, procedures, and associated risks or benefits. In order to meet ethical norms and respect participants' rights to make informed decisions regarding their engagement, this informed consent must be obtained.
- **Data Collection Protocol:** Document that describes the approach employed for this study. It details the methods, procedures, and instruments used to collect data, reflecting transparency and adherence to ethical guidelines.
- **Email of Ethics Approval:** This approval is the official documentation approving the research project's adherence to ethical principles. This email confirms that the study methodology has undergone rigorous evaluation and received approval from the ethics committee at INESCTEC. It attests to the research's ethical integrity and provides credibility for the study.

CONSENTIMENTO INFORMADO PARA PARTICIPAR EM ESTUDO

Por favor, leia com atenção a seguinte informação. Se achar que algo está incorreto ou pouco claro, não hesite em pedir mais informações através do email: (mafalda.a.ferreira@inesctec.pt)

Se deseja participar no estudo solicitamos que preste o seu consentimento, assinando o documento no final.

A participação no estudo é voluntária, podendo o participante em qualquer altura cessar a sua participação sem qualquer tipo de consequência, bastando para isso contactar o responsável através do e-mail acima.

1.DESCRIÇÃO DO ESTUDO

Título: Aquisição de dados fisiológicos de indivíduos

Entidade Responsável: INESC-TEC

Responsável Direto: *Nome:* ***Duarte Dias*** *Telemóvel:* ***919182933***

Descrição Geral: Este estudo decorre no âmbito do desenvolvimento de uma tese de mestrado do curso de Engenharia Eletrotécnica e de Computadores para o ano letivo 2022/2023. O objetivo incide na recolha de dados fisiológicos de um indivíduo, através de elétrodos inseridos numa banda torácica usada na altura do peito e uma máscara facial colocada na região do nariz. Com este estudo pretende-se melhorar a facilidade na identificação de um indivíduo, em situações em que outros métodos não são viáveis, e a segurança no controlo de acesso a áreas reservadas.

2.TRATAMENTO DE DADOS PESSOAIS

Procedimentos gerais: Ser-lhe-á pedido que use uma banda torácica ou elétrodos certificados no peito durante duas atividades distintas e use uma máscara facial durante apenas uma delas, conforme o protocolo definido. As atividades serão repetidos duas/três vezes ao longo de um dia durante aproximadamente 3 a 5 minutos. Na primeira deverá estar sentado a trabalhar naturalmente, enquanto usa a banda/elétrodos e durante parte dela utilizará a máscara na região do nariz. No decorrer do uso da máscara sobre a zona do nariz, deverá apenas respirar por essa via. A segunda consistirá numa caminhada contínua por um percurso definido utilizando o dispositivo. O percurso incluirá a abertura/fecho de portas e deve manter uma velocidade baixa e natural que usa para se deslocar normalmente. Aquando da execução do protocolo, a aquisição de sinais fisiológicos será realizada (Eletrocardiograma (ECG), respiração e temperatura corporal) de forma contínua e não invasiva, assim como a aquisição de valores inerciais. Para além disso, será feita a gravação da sessão para efeitos de sincronização, de notar que a gravação não permitirá qualquer identificação do participante. Todas as instruções de utilização ser-lhe-ão explicadas pelo investigador.

Riscos: Os riscos e desconforto causado não serão maiores dos que está sujeito normalmente no seu dia a dia, na utilização de qualquer equipamento médico de ECG e respiração. Para melhorar a condutividade do sinal adquirido será aplicado uma pasta condutora sobre a pele, assim como adesivos para ajudar à fixação dos elétrodos, de modo a reduzir o ruído causada pela deslocação destes. Salienta-se que a utilização de elétrodos ou a máscara facial podem causar alguma irritação na pele.

Benefícios: A sua participação neste estudo será de extrema importância para melhorar o estado da arte na área de engenharia biomédica, pois contribuirá para entender o papel dos dados fisiológicos na autenticação e verificação de indivíduos no acesso a áreas reservadas.

Compensações e/ou custos: Não há qualquer compensação financeira, nem custos associados a participação neste estudo.

Finalidade do tratamento:
Os dados recolhidos serão tratados de acordo com a legislação nacional e da UE aplicável e apenas serão usados pelos investigadores para os fins de investigação científica.

Responsável pelo Tratamento:
INESC TEC – Instituto de Engenharia de Sistemas e Computadores, Tecnologia e Ciência, Campus da FEUP, Rua Dr. Roberto Frias, 4200 - 465 Porto.

Confidencialidade: Todos os dados adquiridos serão analisados para fins científicos no âmbito do estudo em causa; todos os envolvidos neste estudo têm um compromisso de confidencialidade e de não divulgação de dados ou informação de carácter pessoal dela retirada; os dados recolhidos serão tratados de forma pseudo-anónima e em conjunto, de forma a não ser identificada a sua participação individual no estudo. Alguns passos serão tomados para proteger a sua identidade individual, nomeadamente: a) a cada participante será atribuído um código; b) todos os dados recolhidos serão guardados num servidor local do INESC TEC (instituição acolhedora do estudo) com acesso restrito e limitado apenas aos membros do grupo de investigação envolvidos; c) qualquer vídeo contendo imagens que identifiquem os participantes serão guardados de forma segura e apenas é permitido o seu acesso a investigadores autorizados. No entanto, os participantes podem, ou não, permitir esta partilha anónima de dados a investigadores terceiros, indicando "SIM" ou "NÃO" na frase seguinte:
- Compreendo que os investigadores possam querer utilizar alguma parte de um vídeo para questões ilustrativas, apenas para fins científicos e/ou educativos. Dou autorização para tal, desde que o meu nome e rosto não sejam visíveis. Nestes casos, a imagem original será devidamente destruída.

Por favor indique: _____SIM _____ NAO

Partilha de Dados Pessoais: Os dados/resultados anónimos e em conjunto poderão ser divulgados/publicados no âmbito de publicações científicas, podendo envolver equipas de investigação de diversas instituições. Após a anonimização destes dados, os documentos de base, que possuam alguma relação com uma possível identificação, serão destruídos num prazo de 6 meses.

Encarregado de Proteção de Dados: Para quaisquer questões, exercício de direitos do titular dos dados pessoais, pedidos ou reclamações relativas ao tratamento de dados pessoais, contacte por favor, o nosso encarregado de proteção de dados, através do contacto: dpo@inesctec.pt

Adicionalmente, se algum problema ou anomalia fisiológica for detetada nos dados recolhidos, deseja ser informado dessa situação?

Por favor indique: _____SIM _____ NÃO

Caso responda positivamente indique o seu contacto (email ou tel):_____

Direitos do Titular dos Dados: Enquanto titular dos dados, a lei reconhece-lhe os seguintes direitos: Informação, Acesso, Retificação, Apagamento, Oposição e Portabilidade. No caso de desistência não há prejuízo no tratamento de dados recolhidos até então, sendo estes tornados totalmente anonimizados. Para o exercício de algum dos seus direitos utilize o seguinte endereço de e-mail: duarte.f.dias@inesctec.pt.

O exercício dos direitos poderá ver-se afastado ou limitado, no respeito pelos termos e condições previstos na legislação nacional e da UE aplicável, na medida em que tal exercício seja suscetível de tornar impossível ou prejudicar gravemente a obtenção dos objetivos do tratamento para fins de investigação e apenas na medida do necessário para a prossecução daqueles fins.

A lei confere-lhe, igualmente, o direito de apresentação de queixas perante uma Autoridade europeia de supervisão, sendo que em Portugal a Autoridade competente é a Comissão Nacional de Proteção de Dados (www.cnpd.pt).

3.TERMO DE CONSENTIMENTO INFORMADO

1. Li e compreendi a informação sobre o estudo, incluindo a identidade do Responsável, o tipo de dados que vai ser recolhido, o objetivo da recolha e do respetivo tratamento.	☐
2. Li e compreendi a informação sobre como os dados serão armazenados e durante quanto tempo, incluindo o que acontecerá aos meus dados no caso de desistir de participar no estudo.	☐
3. Foi-me dada a oportunidade de fazer perguntas e de esclarecer todas as dúvidas sobre este estudo.	☐
4. Compreendo que posso desistir desta participação em qualquer momento, sem necessitar de dar justificações e sem que sofra penalizações ou que questionem as minhas razões.	☐
5. Percebi de que forma poderei comunicar a minha desistência, bem como exercer os meus direitos enquanto titular dos dados.	☐
1.	

<u>O Participante:</u>

Declaro ter lido e compreendido este documento, bem como as informações verbais que me foram fornecidas previamente. Desta forma, aceito participar neste estudo e permito a utilização dos dados que forneço de forma voluntária.

Nome: …

Assinatura: … Data: …… /…… /……..

Considerações no âmbito do estudo para a recolha de dados para melhoria de algoritmos de biometria

Âmbito

O estudo em causa decorre no âmbito da identificação biométrica de indivíduos a partir de sinais fisiológicos dos mesmos usando técnicas de processamento de sinal e modelos de aprendizagem computacional.

Este estudo de autenticação biométrica surgiu da necessidade de melhoramento do controlo de acesso a áreas reservadas. Apresenta como objetivo facilitar esse acesso e garantir um melhor controlo de segurança. A recolha de dados de indivíduos saudáveis ajudará a desenvolver os métodos biométricos que vão ser utilizados no processo de identificação.

Método para recrutamento de voluntários

Com o objetivo de angariar voluntários, pretende-se apresentar este estudo, de uma forma clara e objetiva, aos colaboradores do INESC TEC e membros da comunidade da FEUP. Será disponibilizado aos participantes o contacto do investigador responsável pelo estudo – Duarte Dias, para que os potenciais interessados possam demonstrar o seu interesse em participar no estudo de uma forma totalmente voluntária e informada. Pretende-se recolher dados de aproximadamente 20 a 30 indivíduos, sendo que este serão totalmente anonimizados. A gestão dos dados recolhidos está descrita no consentimento.

Critérios de exclusão

- Doenças cardíaca ou respiratórias

Material

- Elétrodos e Banda torácica e aplicação respetiva
- VitalSticker (protótipo proprietário do INESC TEC de aquisição de sinais vitais)
- Computador para aquisição dos dados localmente.
- Máscara facial Auto-CPAP / APAP
- Câmara e suporte
- Consentimento informado para a participação no estudo
- Questionário demográfico

Local do estudo

O estudo será realizado no INESC TEC, numa sala de trabalho e num corredor do edifício que possibilite uma caminhada de 3 a 5min.

Protocolo

Os dados requeridos englobam:

1) a recolha de dados demográficos, nomeadamente o género e a idade;

2) a recolha de dados inerciais, sinais de eletrocardiograma (ECG) e respiratórios no contexto de análise dos movimentos do participante, sendo que estes contextos serão os seguintes: a) sentado; b) de pé; c) em andamento; d) em andamento (atividade normal) a realizar a ação de abrir portas.

3) Esta recolha será realizada durante 3 vezes ao dia: manhã, almoço e tarde.

[PROCESSOS] Processo Propostas de Projeto PP2023-0030: Aprovado

sig-suporte@inesctec.pt

seg 13-02-2023 19:28

Para: Duarte Filipe Dias <duarte.f.dias@inesctec.pt>; Susana Cristina Rodrigues <susana.c.rodrigues@inesctec.pt>; Mafalda Alexandra Ferreira <mafalda.a.ferreira@inesctec.pt>;

A seguinte proposta está pendente de uma ação sua:

Número Processo: PP2023-0030
Nome: PP2023-0030: Biometrics
Estado Atual: Aprovada
Consultar em: https://intranet.inesctec.pt/atividades/proposta-projeto/cber/PP2023-0030

Cumprimentos,
SIG

Appendix C

Accepted paper

In this section is presented the accepted paper mention in contibution section 1.4.

VitalSticker: A novel multimodal physiological wearable patch device for health monitoring

Francisco Manuel Pinto Vieira
C-BER, INESC Technology and Science
Porto, Portugal
francisco.m.vieira@inesctec.pt

Mafalda Alexandra Ferreira
C-BER, INESC Technology and Science
Porto, Portugal
mafalda.a.ferreira@inesctec.pt

Duarte Dias
C-BER, INESC Technology and Science
Porto, Portugal
duarte.f.dias@inesctec.pt

João Paulo Silva Cunha,
Senior Member, IEEE
INESC Technology and Science,
Faculty of Engineering, University of Porto. Porto, Portugal
jcunha@ieee.org

Abstract - **Wearable Health Devices (WHDs) are increasingly becoming an integral part of daily life and significantly contributing to self-monitoring in healthcare. WHDs have a wide range of applications, ranging from sports to clinical settings, where the monitoring of cardiovascular health, particularly through ECG, plays a crucial role. This study introduces a unique WHD called VitalSticker, which exhibits distinctive features such as having a comfortable tiny patch form-factor to be attached to the chest, collecting multiple vital signs with medical-grade quality (ECG, respiration, temperature and actigraphy) and seamlessly sending data to a companion app. This paper encompasses a detailed description of the hardware, firmware, and case design of the WHD. A study was conducted to assess the quality of the ECG signal acquired by VitalSticker, comparing it with the signal obtained from a CE medical-grade certified ambulatory device. The results demonstrate that our VitalSticker achieves similar medical-grade quality when compared to the reference device, surpassing its counterpart in several specifications. Furthermore, this study presents the successful implementation of an ECG baseline wander correction filter that runs on the tiny on-board wearable microcontroller without introducing any artifacts into the ECG signal, reducing the need for further processing for this outside the wearable patch.**

Keywords - Wearable Health Devices, Hardware, Firmware, Vital Signs, Electrocardiogram, Baseline wander.

I. INTRODUCTION

Wearable Health Devices (WHDs) are an emerging technology with proven impact in the healthcare area namely in telecare monitoring and personalized health applications. The combination of wearable technology with the Internet of Things (IoT) is leading to the fast adoption of wearable devices at a global scale with expected 14% annual market growth from 2023 to 2030 [1,2]. WHDs aim to measure, monitor and analyze physiological signals from the human body, to screen, diagnose (certified medical device) or just self-monitor for possible diseases. WHDs have a large area of applicability (clinical, sports, occupational health, etc.) and different requirements according to the use case, such as comfort, size, medical certification, battery duration, and signal quality, among others [3]. Current technology trends are making these devices smaller, with lower power consumption, wireless connectivity, and accuracy levels dependent on their application [4]. For example, in the area of cardiovascular monitoring, one of the most advanced devices is the Chest Monitor from Biobeat® [3], which is a medical-certified device (for some physiological metrics) and needs a high level of accuracy on signal acquisition; on the other hand, for example, the Garmin Vívoactive® 4 [5] watch is a sport/fitness WHD that aims to monitor the human physiology but does not need clinical accuracy [3].

WHDs most popular wireless transmission is Bluetooth and Bluetooth Low-Energy (BLE). Although this protocols only have a maximum range of about 100m, the data rate of it is in the range of 1-3Mbps, and the power consumption is significantly low (about 2.3-100mW) compared with Wi-Fi and ZigBee – two common wireless protocols in IoT technologies [3]. Using these wireless technologies, WHDs have an advantage in real-time health monitoring, making it possible to monitor a human during their daily activities from anywhere using an internet connection. The signals acquired by the user can be easily transmitted via Bluetooth to a gateway (portable devices, smartphones, computers, etc.) for visualization and further analysis [3]. Processing physiological signals in real-time on the WHDs raises constraints in terms of power efficiency, fast response, and accuracy in data processing. The solution to this problem is to find a balance between energy consumption and computational capacity [4].

The signal pre-processing in this work is focused on the ECG [7]. The ECG raw signal may present low-frequency noise, such as baseline drift due to human activity and high-frequency noises such as electromagnetic interference and muscular activity [8]. The baseline wonder is one of the most common noise types which can be removed with some techniques that include high-pass, moving-average, wavelet, or median filters [9].

This study introduces a unique WHD called *VitalSticker*, which exhibits distinctive features such as having a comfortable tiny patch form-factor to be attached to the chest, collects multiple vital signs with medical-grade quality (ECG, respiration, temperature and actigraphy) and seamlessly send data to a companion app. We present the full development of VitalSticker, namely its design, hardware, firmware workflow, energy consumption, ECG signal quality analysis, a successful implementation of an ECG baseline wander correction filter that runs on the tiny on-board wearable microcontroller and power consumption reduction approaches that offers our patch a top-notch specification set for log-term ambulatory cardiovascular monitoring scenarios.

This project has received funding from the European Union's Horizon 2020 research and innovation programme under grant agreement No 101037419.

II. *VitalSticker* Design & Development

The development of *VitalSticker* was based on more than 20 years of research in embedded physiological data acquisition systems, which had already resulted in the first medically certified wearable device – VitalJacket® [10]. Based on this accumulated knowledge, research needs and existing systems on the market, a new system was designed. This was achieved through incremental developments of different versions leading to the one that is presented in this work. The device presented is the final working version and allows for the acquisition of the ECG and respiration signal with a medical-grade level of accuracy. Besides this, it also allows for the acquisition of skin temperature and inertial movements of the individual wearing it. The device development compromises the hardware, the firmware and the case design.

A. Hardware

VitalSticker was developed based on a hardware module containing a MicroController Unit (MCU) capable of Bluetooth 5.2 Low Energy (BLE) communication supported by a secondary radio subsystem MCU that manages Bluetooth related operations allowing the main MCU to run more complex applications having more time for processing. The module has its own built-in antenna certified for medical applications and an Integrated Development Environment (IDE) which integrates Bluetooth Generic ATTribute profile (GATT) configuration tools.

Regarding the sensors integrated in the *VitalSticker*, they allow the acquisition of motion and vital signals at a specific rate (TABLE I). Motion signals are measured using an Inertial Measurement Unit (IMU), allowing the acquisition of accelerometer, gyroscope, and magnetometer data. The surface body temperature device requires the use of a Negative Temperature Coefficient (NTC) thermistor that is then placed outside the case for skin contact and temperature reading. ECG and respiration measurements were made using a peripheral with programable gain amplifiers and high-resolution 24-bit Analog-to-Digital Converters (ADC). This peripheral contains a programmable virtual Right Leg (RL) driver reference allowing the measurement of high-quality one Lead ECG with only two contacts. It also has a respiration impedance measurement module allowing the acquisition of respiration waveform.

VitalSticker Printed Circuit Board (PCB) was designed with the Altium Designer PCB CAD. This software allows for the simulation of every aspect needed by using 3D models of every component which was a key developing tool since the main objective was to obtain the most compact possible device without compromising the intended functionality and autonomy. The size of the wearable was determined by the size of the Bluetooth module and the snap connectors needed for attaching the electrodes meaning that the final width achieved was 20 mm, the length of 62 mm and 8.2 mm height (Fig.1). Almost every component was placed on the top layer and the components were chosen to be lower than the height of the Bluetooth module - this led to the need of using a mid-layer USB type-C connector to reduce the thickness of the final device. A button was implemented to turn ON/OFF the device and also to be used as a push-button. The height of this component was chosen per the Bluetooth module, enabling it to be pressed easily in the final assembly. In the bottom layer only a few components were placed, leaving most of the space for the battery between the snap connectors. All the components were soldered at INESC TEC making use of the Ersa i-tool and rework soldering station. It was possible to design a 2-layer PCB integrating every component and following safe design rules and good signal isolation where needed. In terms of ground planes, there were three isolated plans, one for the battery/charging, another one for the digital signals, and another one for the analog signals. These plans were isolated using ferrite inductors to reduce high-frequency noise significantly impacting the analogic signals acquired.

The battery had a limited available space being limited by the height and distance between the snaps (38 mm) and the PCB width. A lithium polymer battery with a capacity of 150mAh and respective protective circuits was used measuring 30 (L) * 20 (W) * 3 (H) mm. This battery combined with power management based on efficient switching power regulators allowed for the autonomy of up to 27 hours of consecutive active use (acquiring all the sensors data and sending it by Bluetooth), leading to an average current consumption of 5,49 mA. This value was acquired using the Nordic® Power Profiler Kit II and the respective software provided by Nordic®.

A limiting factor in terms of hardware was the ECG and respiration peripheral since it required an ultra-low-noise regulator leading to the use of a low-dropout regulator which is less efficient. Nevertheless, careful and efficient firmware was designed and developed to help improve the autonomy of the device by adjusting the acquisition and transmission frequencies of the peripherals' data.

TABLE I. SIGNALS ACQUISITION SPECIFICATIONS

Signal	Measurement Frequency	Measurement Range
ECG	250 Hz	24-bits ADC (+/- 350 mV)
Respiration	250 Hz	24-bits ADC (+/- 350 mV)
Accelerometer Gyroscope Magnetometer	25 Hz	-4 to 4 g -2000 to 2000 º/s -4900 to 4900 µT
Body temperature	0,5 Hz	0 to 70 ºC

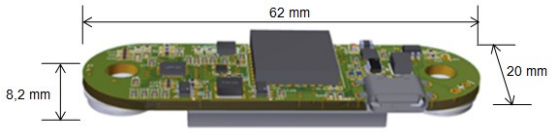

Fig. 1. Altium Designer 3D model generated of the PCB finished design.

B. Firmware

Simplicity Studio 5, the IDE from Silicon Labs, was used to develop the firmware. A pre-configuration of the Bluetooth communication protocol was used, so the major effort in this protocol implementation was on the reconfiguration of the GATT by creating our own service and characteristics needed for the intended data transmission, having each one a generated Universally Unique IDentifier (UUID).

The firmware was designed to be as low power as possible, making a compromise between data sensor acquisition frequency and Bluetooth transmission frequency. This compromise led to a reduced acquisition frequency of some sensors to give priority to the ECG acquisition. When the device is turned on (Fig. 2) it starts the initialization of all the components of the system and the configuration of each peripheral. Then it starts the Bluetooth advertising (every second), and the system stays on standby waiting for a

connection and the request for data notifications. If a connection is established it enters the sensor data processing loop in which data from the different sensors is periodically acquired, using a specific timer for each sensor. This data is placed on a buffer that is sent via Bluetooth whenever it is full. To avoid data loss, this buffer is copied into an auxiliary one for the Bluetooth Stack, making the main buffer immediately available to receive new data from the sensors.

The sensor data processing loop is suspended whenever the system detects an external interruption, or if it is necessary to process any Bluetooth event. ECG/Respiration peripheral is configured to work in a continuous data acquisition mode and whenever data is ready to be acquired an interruption is generated. The MCU was configured to prioritize the external interruptions so that it could be possible to acquire the signals in real-time without losing any data. In terms of the Bluetooth events, the system must have time to process them to maintain stable and reliable communication, which is not a problem because data is buffered/copied so that they can have a lower priority.

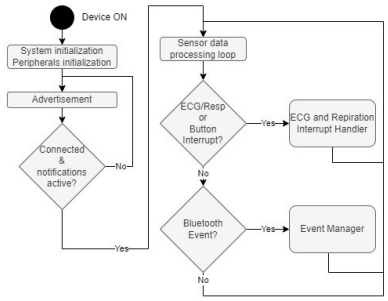

Fig. 2. Simplified firmware fluxogram of the developed system.

To improve the device autonomy, it was necessary to test different measurement frequencies for the IMU and body temperature sensors to guarantee a good data flow and sampling rate according to human movement and to reduce battery consumption. Another important factor that significantly affected the power consumption was the Bluetooth data transmission, so a small study was made to analyze the best balance between transmission frequency and data buffer size for each sensor signal. The best results obtained for the buffer size and transmission frequency are present in TABLE II

C. *Case personalized design*

A personalized case was designed to ensure a minimal thickness but high robustness. There were five main concerns considered during the design of the case: 1) the material used could not be porous or toxic to be able to be in contact with the skin; 2) minimal possible thickness to be as much comfortable as possible; 3) allow the use of the button through the case, the connection on the USB type-C port and easy visualization of the light from the LEDs; 4) keep all electronic components, including the battery, safe and well-secured, without moving inside the case; 5) connection of the case with the snap buttons to ensure that the force exerted on the device does not go into the PCB but to the snaps. Fig. 3 shows the result obtained through SLA 3D-printed manufacturing process using formlabs clear resin which fills all the concerns above. The last concern was possible to achieve by designing a personalized socket for the snap buttons to fit in, allowing to secure them to the case. The case's final dimensions are 65 (L) * 23 (W) * 10 (H) mm.

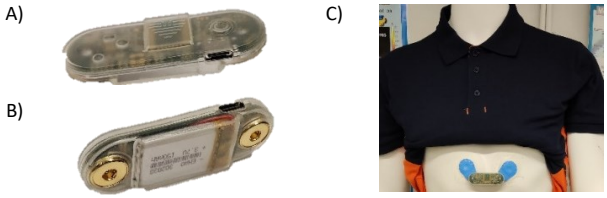

Fig. 3. *VitalSticker* case printed in formlabs clear resin. A) front view; B) back view; C) representation of the device in use.

TABLE II. SIGNALS BUFFER SIZE AND TRANSMISSION FREQUENCY USED ON THE BLUETOOTH TO REDUCE CURRENT CONSUMPTION TO 5.49 MA

Signal	Buffer size	Transmission frequency
ECG	99 bytes (33 samples)	7.6 Hz
Respiration	99 bytes (33 samples)	7.6 Hz
Accelerometer Gyroscope Magnetometer	180 bytes (5 samples per sensor per dimension)	5 Hz
Body temperature	2 bytes (1 sample)	0.5 Hz

III. ECG SIGNAL QUALITY ANALYSIS AND DISCUSSION

A study was performed to compare the ECG signals obtained from the *VitalSticker* and from a medical-grade CE-certified ECG signal and actigraphy in real time called VitalJacket®. For the comparative study, the ECG signal of an individual was recorded using both devices simultaneously with a duration of five minutes.

A. *Signal Acquisition & Comparative Study*

ECG, represented in Fig. 4, was one of the signals acquired from both devices. These devices have two main differences: *VitalSticker* has a sampling frequency of 250Hz and a 24-bit resolution, while VitalJacket's sample frequency is 500Hz and has an 8-bit resolution. Usually, with less resolution, the acquired signal has less quality and information because the ECG signal has a low voltage amplitude variation (in the millivolt scale).

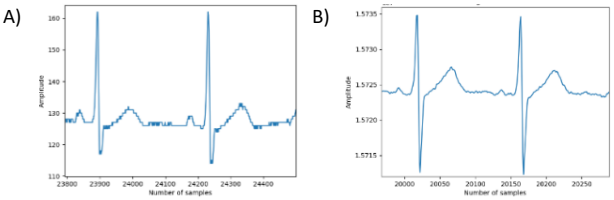

Fig. 4. Raw ECG signal from VitalJacket (A) and *VitalSticker* (B). Amplitude in mV. Sampling frequency: A - 500Hz; B - 250Hz.

Analyzing VitalJacket® (Fig. 4-A) and the *VitalSticker* (Fig. 4-B) signals it is noticeable that the prominent differences in the graphs are related to technological advancements. The amplitudes of the different waves are due to the location of the electrodes on the chest, leading to ECG waveform different amplitude distribution.

VitalSticker quality was analyzed statistically by comparing it with VitalJacket® (ground truth). The analysis focused on the temporal distances between the R-peaks (RR interval) and the RT intervals. To ensure synchronization, the signals were aligned by the same initial R-peak. The temporal RR distance and the RT distance for each heartbeat in both devices were calculated for two subjects using our ECG fiducial points detector algorithm reported in [7].

Subsequently, the difference between the signal of both devices was calculated: each interval (RR and RT) of *VitalSticker* was subtracted from the corresponding interval of the VitalJacket®. This comparison was performed for two subjects (A and B) computing for each one the Average Difference (AD), standard deviation (σ), relative error (δ), and Root Mean Square (RMS) error for both RR and RT time distances (TABLE III).

TABLE III. STATISTICAL ANALYSIS OF THE *VITALSTICKER* SIGNAL QUALITY USING VITALJACKET® SIGNAL HAS THE GROUND TRUTH. (TEMPORAL RESOLUTION: VITALJACKET®= 0.002s; *VITALSTICKER=0.004s)*

	RR interval diff.				RT interval diff.			
Subject	AD (s)	σ (s)	δ (%)	RMS	AD (s)	σ (s)	δ (%)	RMS
A (130 R peaks)	0.002	0.006	0.38	0.007	0.008	0.016	3.67	0.018
B (130 R peaks)	0.002	0.002	0.29	0.003	0.009	0.006	3.70	0.011

B. *Baseline wander filter*

Although being more precise and with a high-resolution signal, *VitalSticker* measurements present baseline noise due to movement and respiration of the user - low-frequency artifact in the ECG [9]. This effect can be observed in the raw signal acquired from *VitalSticker* (Fig. 5-A). Additionally, the use of an internal RL virtual reference in the ECG/respiration module without readjustment to baseline changes contributes to this low-frequency baseline noise. To address this issue, a low-pass filter was integrated into the MCU firmware. In this work, it was implemented and compared a median and an average filter to correct the baseline wander, both with a window of 150 samples (0.6 seconds) – a window chosen after different heart rate samples analysis. A study was conducted considering artifacts created by the filter, time usage by the filter on the MCU, and power consumption of the device. While the median filter exhibited higher computational timing (0.715µs > 0.02µs) and current consumption increment (0.97mA > 0.8mA) compared with the average filter, it did not introduce any artifact to the ECG signal as shown in Fig. 5-D. The artifact in Fig. 5-C (average filter) exemplifies the signal distortion caused by his type of filtering (P-wave is distorted). Taking this into account the *VitalSticker* firmware was upgraded with a median filter (Fig. 5-B) on the "Sensor data and processing loop" block (Fig. 2), with a real-time visualization delay of 0.3 seconds. As a result of the baseline wander correction, the ECG signal size was reduced from a 24-bit unsigned integer to a 16-bit signed integer. This reduction made it possible to reduce the payload of the Bluetooth transmission associated with the ECG signal from 99 bytes to 66 bytes and this helped compensate for the power consumption increase associated with the filter.

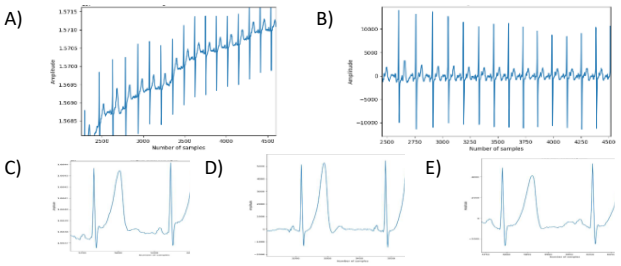

Fig. 5. ECG signal from the *VitalSticker*: A) ECG raw signal with no filtering; B) ECG signal with median filter for baseline wander correction; C) ECG raw signal zoom in; D) ECG signal zoom in with median filter; E) ECG signal zoom in with mean filter.

IV. CONCLUSIONS AND FUTURE WORK

This research presented the developments of a wearable capable of acquiring real-time vital signs with a focus on high-quality ECG. This work also provided a hardware flexible platform to research and develop new signal pre-processing and analysis based on each individual signal (respiration, body temperature, and inertial data) or on a multimodal approach. Some of these research lines are already being conducted by our laboratory, such as the computation of core temperature and integration of movement analysis.

The signal comparison of VitalSticker with VitalJacket® supports the fact that our device can acquire high-quality ECG signals by achieving ~1 samples error (0.38 % max error) in RR interval and ~2 samples error (3.70 % max error) in the RT interval. Although this level of error is considered good, it shows that further research can be conducted with more subjects to understand the consistency of the results. The implementation of the baseline wander correction filter was successfully integrated, ensuring real-time performance, and improving signal output stability. The smaller signal bitwise achieved by this integration helped compensate for the power consumption increase associated its computation.

Furthermore, more tests are being conducted with a bigger population to validate the ECG and perform a validation of the respiration waveform that *VitalSticker* is also acquiring simultaneously.

REFERENCES

[1] "Wearable Technology Market Size, Trends, Growth, Report 2030." https://www.precedenceresearch.com/wearable-technology-market (accessed Mar. 01, 2023).

[2] "Wearable Technology Market Share & Trends Report, 2030." https://www.grandviewresearch.com/industry-analysis/wearable-technology-market (accessed Mar. 01, 2023).

[3] D. Dias and J. P. Cunha, "Wearable Health Devices—Vital Sign Monitoring, Systems and Technologies," Sensors, vol. 18, p. 2414, Jun. 2018, doi: 10.3390/s18082414.

[4] E. Covi et al., "Adaptive Extreme Edge Computing for Wearable Devices," Front Neurosci, vol.15, 2021, doi: 10.3389/fnins.2021.611300.

[5] "Products | Biobeat." https://www.bio-beat.com/products (accessed Mar. 05, 2023).

[6] "Garmin vívoactive® 4 | Smartwatch com GPS | Fitness." https://www.garmin.com/pt-PT/p/643382#specs (accessed Mar. 05, 2023).

[7] J. S. Paiva, D. Dias, and J. P. S. Cunha, "Beat-ID: Towards a computationally low-cost single heartbeat biometric identity check system based on electrocardiogram wave morphology," PLoS One, vol. 12, no. 7, pp. 1–32, Jun. 2017, doi: 10.1371/journal.pone.0180942.

[8] H. S. Bıçakcı, M. Santopietro, and R. Guest, "Activity-based electrocardiogram biometric verification using wearable devices," IET Biom, vol. 12, no. 1, pp. 38–51, Jan. 2023, doi: 10.1049/BME2.12105.

[9] F. Perdigón Romero, L. Romaguera, C. R. Seisdedos, C. Filho, M. Costa, and J. Neto, "Baseline wander removal methods for ECG signals: A comparative study." Jun. 2018. doi: 10.13140/RG.2.2.12523.03361/1.

[10] J. P. S. Cunha, B. Cunha, A. S. Pereira, W. Xavier, N. Ferreira, and L. Meireles, "Vital-Jacket®: A wearable wireless vital signs monitor for patients' mobility in cardiology and sports," in 2010 4th International Conference on Pervasive Computing Technologies for Healthcare, 2010, pp. 1–2. doi: 10.4108/ICST.PERVASIVEHEALTH2010.8991.

Bibliography

[1] European Commission. Directorate General for Research and Innovation., *Industry 5.0: towards a sustainable, human centric and resilient European industry.* en. LU: Publications Office, 2021. [Online]. Available: https://data.europa.eu/doi/10.2777/308407 (visited on 01/09/2023).

[2] M. Zviran and Z. Erlich, "Identification and Authentication: Technology and Implementation Issues", en, *Communications of the Association for Information Systems*, vol. 17, 2006, ISSN: 15293181. DOI: 10.17705/1CAIS.01704. [Online]. Available: https://aisel.aisnet.org/cais/vol17/iss1/4 (visited on 07/03/2023).

[3] W. N. Zealand, *Protective clothing*, en-NZ, Aug. 2021. [Online]. Available: https://www.worksafe.govt.nz/topic-and-industry/personal-protective-equipment-ppe/protective-clothing/ (visited on 06/27/2023).

[4] J. S. Paiva, D. Dias, and J. P. S. Cunha, "Beat-ID: Towards a computationally low-cost single heartbeat biometric identity check system based on electrocardiogram wave morphology", en, *PLOS ONE*, vol. 12, no. 7, e0180942, Jul. 2017, Publisher: Public Library of Science, ISSN: 1932-6203. DOI: 10.1371/journal.pone.0180942. [Online]. Available: https://journals.plos.org/plosone/article?id=10.1371/journal.pone.0180942 (visited on 10/20/2022).

[5] F. M. P. Vieira, M. A. Ferreira, D. Dias, and J. P. S. Cunha, "VitalSticker: A novel multimodal physiological wearable patch device for health monitoring", en, *7th ENBENG 2023 IEEE Portuguese Meeting in Bioengineering, Accepted for publication*,

[6] X. Jin, L. Li, F. Dang, X. Chen, and Y. Liu, "A survey on edge computing for wearable technology", en, *Digital Signal Processing*, Sensing, Signal Processing and Computing for the Era of Wearables, vol. 125, p. 103 146, Jun. 2022, ISSN: 1051-2004. DOI: 10.1016/j.dsp.2021.103146. [Online]. Available: https://www.sciencedirect.com/science/article/pii/S1051200421001858 (visited on 12/18/2022).

[7] E. Covi, E. Donati, X. Liang, *et al.*, "Adaptive Extreme Edge Computing for Wearable Devices", *Frontiers in Neuroscience*, vol. 15, 2021, ISSN: 1662-453X. [Online]. Available: https://www.frontiersin.org/articles/10.3389/fnins.2021.611300 (visited on 12/18/2022).

[8] Y. Khan, A. E. Ostfeld, C. M. Lochner, A. Pierre, and A. C. Arias, "Monitoring of Vital Signs with Flexible and Wearable Medical Devices", en, *Advanced Materials*, vol. 28, no. 22, pp. 4373–4395, Jun. 2016, ISSN: 09359648. DOI: 10.1002/adma.201504366. [Online]. Available: https://onlinelibrary.wiley.com/doi/10.1002/adma.201504366 (visited on 01/07/2023).

[9] D. Dias and J. Paulo Silva Cunha, "Wearable health devices—vital sign monitoring, systems and technologies", *Sensors*, vol. 18, no. 8, p. 2414, 2018, Publisher: MDPI.

[10] C. L. VanPutte, J. L. Regan, and A. F. Russo, *Seeley's essentials of anatomy & physiology*, en, Ninth edition. New York, NY: McGraw-Hill Education, 2016, ISBN: 978-0-07-809732-4.

[11] L. Ortiz Martin, P. Picazo-Sanchez, P. Peris-Lopez, and J. Tapiador, "Heartbeats Do Not Make Good Pseudo-Random Number Generators: An Analysis of the Randomness of Inter-Pulse Intervals", *Entropy*, vol. 20, p. 94, Jan. 2018. DOI: 10.3390/e20020094.

[12] P. Kligfield, F. Badilini, I. Rowlandson, *et al.*, "Comparison of automated measurements of electrocardiographic intervals and durations by computer-based algorithms of digital electrocardiographs", en, *American Heart Journal*, vol. 167, no. 2, 150–159.e1, Feb. 2014, ISSN: 0002-8703. DOI: 10.1016/j.ahj.2013.10.004. [Online]. Available: https://www.sciencedirect.com/science/article/pii/S0002870313007102 (visited on 05/22/2023).

[13] S. H. Jambukia, V. K. Dabhi, and H. B. Prajapati, "Classification of ECG signals using machine learning techniques: A survey", in *2015 International Conference on Advances in Computer Engineering and Applications*, Mar. 2015, pp. 714–721. DOI: 10.1109/ICACEA.2015.7164783.

[14] N. M. Hameed and J. M. Al-Tuwaijari, "A survey on various machine learning approaches for human electrocardiograms identification", *International Journal of Nonlinear Analysis and Applications*, vol. 13, no. 1, pp. 4017–4035, Feb. 2022, Publisher: Semnan University, ISSN: 2008-6822. DOI: 10.22075/ijnaa.2022.6223. [Online]. Available: https://ijnaa.semnan.ac.ir/article_6223.html (visited on 05/22/2023).

[15] T. Noto, G. Zhou, S. Schuele, J. Templer, and C. Zelano, "Automated analysis of breathing waveforms using BreathMetrics: A respiratory signal processing toolbox", en, *Chemical Senses*, vol. 43, no. 8, pp. 583–597, Sep. 2018, ISSN: 0379-864X, 1464-3553. DOI: 10.1093/chemse/bjy045. [Online]. Available: https://academic.oup.com/chemse/article/43/8/583/5050471 (visited on 01/09/2023).

[16] J. R. Pinto and J. S. Cardoso, "ECG Biometrics", en, in *Encyclopedia of Cryptography, Security and Privacy*, S. Jajodia, P. Samarati, and M. Yung, Eds., Berlin, Heidelberg: Springer Berlin Heidelberg, 2021, pp. 1–4, ISBN: 978-3-642-27739-9. DOI: 10.1007/978-3-642-27739-9_1517-1. [Online]. Available: http://link.springer.com/10.1007/978-3-642-27739-9_1517-1 (visited on 10/22/2022).

[17] J. Ribeiro Pinto, J. S. Cardoso, and A. Lourenço, "Evolution, Current Challenges, and Future Possibilities in ECG Biometrics", *IEEE Access*, vol. 6, pp. 34 746–34 776, 2018, Conference Name: IEEE Access, ISSN: 2169-3536. DOI: 10.1109/ACCESS.2018.2849870.

[18] G. Wübbeler, M. Stavridis, D. Kreiseler, R.-D. Bousseljot, and C. Elster, "Verification of humans using the electrocardiogram", en, *Pattern Recognition Letters*, vol. 28, no. 10, pp. 1172–1175, Jul. 2007, ISSN: 0167-8655. DOI: 10.1016/j.patrec.2007.01.014. [Online]. Available: https://www.sciencedirect.com/science/article/pii/S0167865507000463 (visited on 01/05/2023).

[19] Y. Li, Y. Pang, K. Wang, and X. Li, "Toward improving ECG biometric identification using cascaded convolutional neural networks", en, *Neurocomputing*, vol. 391, pp. 83–95, May 2020, ISSN: 0925-2312. DOI: 10.1016/j.neucom.2020.01.019. [Online]. Available: https://www.sciencedirect.com/science/article/pii/S0925231220300485 (visited on 01/08/2023).

[20] H. S. Bıçakcı, M. Santopietro, and R. Guest, "Activity-based electrocardiogram biometric verification using wearable devices", en, *IET Biometrics*, vol. 12, no. 1, pp. 38–51, 2023, _eprint: https://onlinelibrary.wiley.com/doi/pdf/10.1049/bme2.12105, ISSN: 2047-4946. DOI: 10.1049/bme2.12105. [Online]. Available: https://onlinelibrary.wiley.com/doi/abs/10.1049/bme2.12105 (visited on 03/03/2023).

[21] B. Singh, P. Singh, and S. Budhiraja, "Various Approaches to Minimise Noises in ECG Signal: A Survey", in *2015 Fifth International Conference on Advanced Computing & Communication Technologies*, ISSN: 2327-0659, Feb. 2015, pp. 131–137. DOI: 10.1109/ACCT.2015.87.

[22] S. Fatemian and D. Hatzinakos, "A new ECG feature extractor for biometric recognition", in *2009 16th International Conference on Digital Signal Processing*, ISSN: 2165-3577, Jul. 2009, pp. 1–6. DOI: 10.1109/ICDSP.2009.5201143.

[23] K. N. Plataniotis, D. Hatzinakos, and J. K. M. Lee, "ECG Biometric Recognition Without Fiducial Detection", in *2006 Biometrics Symposium: Special Session on Research at the Biometric Consortium Conference*, Sep. 2006, pp. 1–6. DOI: 10.1109/BCC.2006.4341628.

[24] J. Pan and W. J. Tompkins, "A Real-Time QRS Detection Algorithm", *IEEE Transactions on Biomedical Engineering*, vol. BME-32, no. 3, pp. 230–236, Mar. 1985, Conference Name: IEEE Transactions on Biomedical Engineering, ISSN: 1558-2531. DOI: 10.1109/TBME.1985.325532.

[25] A. D. C. Chan, M. M. Hamdy, A. Badre, and V. Badee, "Wavelet Distance Measure for Person Identification Using Electrocardiograms", *IEEE Transactions on Instrumentation*

and Measurement, vol. 57, no. 2, pp. 248–253, Feb. 2008, Conference Name: IEEE Transactions on Instrumentation and Measurement, ISSN: 1557-9662. DOI: 10.1109/TIM.2007.909996.

[26] M. Li and S. Narayanan, "Robust ECG Biometrics by Fusing Temporal and Cepstral Information", in *2010 20th International Conference on Pattern Recognition*, ISSN: 1051-4651, Aug. 2010, pp. 1326–1329. DOI: 10.1109/ICPR.2010.330.

[27] A. Page, A. Kulkarni, and T. Mohsenin, "Utilizing deep neural nets for an embedded ECG-based biometric authentication system", in *2015 IEEE Biomedical Circuits and Systems Conference (BioCAS)*, Oct. 2015, pp. 1–4. DOI: 10.1109/BioCAS.2015.7348372.

[28] Q. Zhang, D. Zhou, and X. Zeng, "HeartID: A Multiresolution Convolutional Neural Network for ECG-Based Biometric Human Identification in Smart Health Applications", *IEEE Access*, vol. 5, pp. 11 805–11 816, 2017, Conference Name: IEEE Access, ISSN: 2169-3536. DOI: 10.1109/ACCESS.2017.2707460.

[29] G. Wang, D. John, and A. Nag, "Low Complexity ECG Biometric Authentication for IoT Edge Devices", in *2020 IEEE International Conference on Integrated Circuits, Technologies and Applications (ICTA)*, Nov. 2020, pp. 145–146. DOI: 10.1109/ICTA50426.2020.9332012.

[30] V. F. Parreira, C. J. Bueno, D. C. França, D. S. R. Vieira, D. R. Pereira, and R. R. Britto, "Padrão respiratório e movimento toracoabdominal em indivíduos saudáveis: Influência da idade e do sexo", en, *Revista Brasileira de Fisioterapia*, vol. 14, no. 5, pp. 411–416, Oct. 2010, ISSN: 1413-3555. DOI: 10.1590/S1413-35552010000500010. [Online]. Available: http://www.scielo.br/scielo.php?script=sci_arttext&pid=S1413-35552010000500010&lng=pt&nrm=iso&tlng=pt (visited on 01/06/2023).

[31] M. Ragnarsdóttir and E. K. Kristinsdóttir, "Breathing Movements and Breathing Patterns among Healthy Men and Women 20–69 Years of Age", en, *Respiration*, vol. 73, no. 1, pp. 48–54, 2006, ISSN: 0025-7931, 1423-0356. DOI: 10.1159/000087456. [Online]. Available: https://www.karger.com/Article/FullText/87456 (visited on 01/06/2023).

[32] J. Liu, Y. Chen, Y. Dong, Y. Wang, T. Zhao, and Y.-D. Yao, "Continuous User Verification via Respiratory Biometrics", in *IEEE INFOCOM 2020 - IEEE Conference on Computer Communications*, ISSN: 2641-9874, Jul. 2020, pp. 1–10. DOI: 10.1109/INFOCOM41043.2020.9155258.

[33] Z. Guo, X. Zhu, L. Gui, B. Sheng, and F. Xiao, "BreathID: Respiration Sensing for Human Identification Using Commodity Wi-Fi", *IEEE Systems Journal*, pp. 1–12, 2022, Conference Name: IEEE Systems Journal, ISSN: 1937-9234. DOI: 10.1109/JSYST.2022.3191647.

[34] S. M. M. Islam, O. Borić-Lubecke, and V. M. Lubecke, "Identity Authentication in Two-Subject Environments Using Microwave Doppler Radar and Machine Learning Classifiers", *IEEE Transactions on Microwave Theory and Techniques*, vol. 70, no. 11, pp. 5063–5076, Nov. 2022, Conference Name: IEEE Transactions on Microwave Theory and Techniques, ISSN: 1557-9670. DOI: 10.1109/TMTT.2022.3197413.

[35] S. M. M. Islam, A. Rahman, N. Prasad, O. Boric-Lubecke, and V. M. Lubecke, "Identity Authentication System using a Support Vector Machine (SVM) on Radar Respiration Measurements", in *2019 93rd ARFTG Microwave Measurement Conference (ARFTG)*, Jun. 2019, pp. 1–5. DOI: 10.1109/ARFTG.2019.8739240.

[36] R. K. Raji, M. Adjeisah, X. Miao, and A. Wan, "A novel respiration pattern biometric prediction system based on artificial neural network", *Sensor Review*, vol. 40, no. 1, pp. 8–16, Jan. 2020, Publisher: Emerald Publishing Limited, ISSN: 0260-2288. DOI: 10.1108/SR-10-2019-0235. [Online]. Available: https://doi.org/10.1108/SR-10-2019-0235 (visited on 12/18/2022).

[37] S. Kim, B. Kim, Y. Jin, and J. Lee, "Human Identification by Measuring Respiration Patterns Using Vital FMCW Radar", English, *Journal of Electromagnetic Engineering and Science*, vol. 20, no. 4, pp. 302–306, 2020, ISSN: 2671-7255. DOI: 10.26866/jees.2020.20.4.302.

[38] B. Hu, T. Zhao, Y. Wang, *et al.*, "BioTag: Robust RFID-based continuous user verification using physiological features from respiration", in *Proceedings of the Twenty-Third International Symposium on Theory, Algorithmic Foundations, and Protocol Design for Mobile Networks and Mobile Computing*, ser. MobiHoc '22, New York, NY, USA: Association for Computing Machinery, Oct. 2022, pp. 191–200, ISBN: 978-1-4503-9165-8. DOI: 10.1145/3492866.3549718. [Online]. Available: https://doi.org/10.1145/3492866.3549718 (visited on 12/18/2022).

[39] S. M. M. Islam, A. Sylvester, G. Orpilla, and V. M. Lubecke, "Respiratory Feature Extraction for Radar-Based Continuous Identity Authentication", in *2020 IEEE Radio and Wireless Symposium (RWS)*, ISSN: 2164-2974, Jan. 2020, pp. 119–122. DOI: 10.1109/RWS45077.2020.9050013.

[40] V. V. Tipparaju, D. Wang, J. Yu, *et al.*, "Respiration pattern recognition by wearable mask device", en, *Biosensors and Bioelectronics*, vol. 169, p. 112 590, Dec. 2020, ISSN: 0956-5663. DOI: 10.1016/j.bios.2020.112590. [Online]. Available: https://www.sciencedirect.com/science/article/pii/S0956566320305807 (visited on 12/18/2022).

[41] J. Park, J. An, J. Kim, *et al.*, "Study on the use of standard 12-lead ECG data for rhythm-type ECG classification problems", en, *Computer Methods and Programs in Biomedicine*, vol. 214, p. 106 521, Feb. 2022, ISSN: 0169-2607. DOI: 10.1016/j.cmpb.2021.

106521. [Online]. Available: https://www.sciencedirect.com/science/article/pii/S0169260721005952 (visited on 06/28/2023).

[42] L. K. Bawua, C. Miaskowski, S. Suba, *et al.*, "Agreement between respiratory rate measurement using a combined electrocardiographic derived method versus impedance from pneumography", en, *Journal of Electrocardiology*, vol. 71, pp. 16–24, Mar. 2022, ISSN: 0022-0736. DOI: 10.1016/j.jelectrocard.2021.12.006. [Online]. Available: https://www.sciencedirect.com/science/article/pii/S0022073621003010 (visited on 06/09/2023).

[43] *Welcome to BioSPPy — BioSPPy 0.6.1 documentation*. [Online]. Available: https://biosppy.readthedocs.io/en/stable/ (visited on 06/27/2023).

[44] H. Ramalingam and N. H R, "Review on bio-signal processing software packages", Oct. 2020.

[45] K. Hovsepian, M. al'Absi, E. Ertin, T. Kamarck, M. Nakajima, and S. Kumar, "cStress: Towards a Gold Standard for Continuous Stress Assessment in the Mobile Environment", *Proceedings of the ... ACM International Conference on Ubiquitous Computing . UbiComp (Conference)*, vol. 2015, pp. 493–504, Sep. 2015. DOI: 10.1145/2750858.2807526. [Online]. Available: https://www.ncbi.nlm.nih.gov/pmc/articles/PMC4631393/ (visited on 05/15/2023).

[46] L. Coelho, C. Veiga, D. Dias, and J. P. Cunha, "On the Development of an Algorithm for Automatic Estimation of the Respiratory Rate using Wearable Electrocardiography", Dec. 2017.

[47] J. P. S. Cunha, B. Cunha, A. S. Pereira, W. Xavier, N. Ferreira, and L. Meireles, "Vital-Jacket®: A wearable wireless vital signs monitor for patients' mobility in cardiology and sports", en, in *Proceedings of the 4th International ICST Conference on Pervasive Computing Technologies for Healthcare*, Munchen, Germany: IEEE, 2010, ISBN: 978-963-9799-89-9. DOI: 10.4108/ICST.PERVASIVEHEALTH2010.899. [Online]. Available: http://eudl.eu/doi/10.4108/ICST.PERVASIVEHEALTH2010.899 (visited on 06/09/2023).

[48] S. Rodrigues, J. S. Paiva, D. Dias, and J. P. S. Cunha, "Stress among on-duty firefighters: An ambulatory assessment study", en, *PeerJ*, vol. 6, e5967, Dec. 2018, Publisher: PeerJ Inc., ISSN: 2167-8359. DOI: 10.7717/peerj.5967. [Online]. Available: https://peerj.com/articles/5967 (visited on 06/09/2023).

[49] *BC Biomedical PS-2006*. [Online]. Available: https://www.bcgroupstore.com/Biomedical-BC_Biomedical_PS-2006.aspx (visited on 06/30/2023).

[50] T. O. Hodson, "Root-mean-square error (RMSE) or mean absolute error (MAE): When to use them or not", English, *Geoscientific Model Development*, vol. 15, no. 14, pp. 5481–5487, Jul. 2022, Publisher: Copernicus GmbH, ISSN: 1991-959X. DOI: 10.5194/gmd-

15-5481-2022. [Online]. Available: https://gmd.copernicus.org/articles/15/5481/2022/ (visited on 06/30/2023).

[51] *Nasal Mask*, en. [Online]. Available: https://getwellue.com/products/ibreeze-nasal-mask (visited on 06/29/2023).

[52] C. Redmond, "Transthoracic Impedance Measurements in Patient Monitoring", en, *Analog Devices*, p. 5, [Online]. Available: https://www.analog.com/en/technical-articles/transthoracic-impedance-measurements-in-patient-monitoring.html.

[53] G. De Leonardis, S. Rosati, G. Balestra, *et al.*, "Human Activity Recognition by Wearable Sensors : Comparison of different classifiers for real-time applications", in *2018 IEEE International Symposium on Medical Measurements and Applications (MeMeA)*, Jun. 2018, pp. 1–6. DOI: 10.1109/MeMeA.2018.8438750.

[54] J. Kim, K. B. Lee, and S. G. Hong, "Random forest based-biometric identification using smart shoes", in *2017 Eleventh International Conference on Sensing Technology (ICST)*, ISSN: 2156-8073, Dec. 2017, pp. 1–4. DOI: 10.1109/ICSensT.2017.8304518.

[55] T. Evgeniou and M. Pontil, "Support Vector Machines: Theory and Applications", vol. 2049, Sep. 2001, pp. 249–257, ISBN: 978-3-540-42490-1. DOI: 10.1007/3-540-44673-7_12.

[56] K. Taunk, S. De, S. Verma, and A. Swetapadma, "A Brief Review of Nearest Neighbor Algorithm for Learning and Classification", in *2019 International Conference on Intelligent Computing and Control Systems (ICCS)*, May 2019, pp. 1255–1260. DOI: 10.1109/ICCS45141.2019.9065747.

[57] L. Rokach and O. Maimon, "Decision Trees", in *The Data Mining and Knowledge Discovery Handbook*, vol. 6, Journal Abbreviation: The Data Mining and Knowledge Discovery Handbook, Jan. 2005, pp. 165–192. DOI: 10.1007/0-387-25465-X_9.

[58] J. Ren, S. Lee, X. Chen, B. Kao, R. Cheng, and D. Cheung, "Naive Bayes Classification of Uncertain Data", Dec. 2009, pp. 944–949. DOI: 10.1109/ICDM.2009.90.

[59] L. Breiman, "Random Forests", en, *Machine Learning*, vol. 45, no. 1, pp. 5–32, Oct. 2001, ISSN: 1573-0565. DOI: 10.1023/A:1010933404324. [Online]. Available: https://doi.org/10.1023/A:1010933404324 (visited on 06/27/2023).

[60] *1. Supervised learning*, en. [Online]. Available: https://scikit-learn/stable/supervised_learning.html (visited on 06/29/2023).

[61] M. Sokolova, N. Japkowicz, and S. Szpakowicz, "Beyond Accuracy, F-Score and ROC: A Family of Discriminant Measures for Performance Evaluation", vol. Vol. 4304, Jan. 2006, pp. 1015–1021, ISBN: 978-3-540-49787-5. DOI: 10.1007/11941439_114.

[62] D. Singh and B. Singh, "Investigating the impact of data normalization on classification performance", en, *Applied Soft Computing*, vol. 97, p. 105 524, Dec. 2020, ISSN: 1568-4946. DOI: 10.1016/j.asoc.2019.105524. [Online]. Available: https://www.sciencedirect.com/science/article/pii/S1568494619302947 (visited on 06/26/2023).

[63] S. S. Saha, S. S. Sandha, and M. Srivastava, "Machine Learning for Microcontroller-Class Hardware: A Review", *IEEE Sensors Journal*, vol. 22, no. 22, pp. 21 362–21 390, Nov. 2022, Conference Name: IEEE Sensors Journal, ISSN: 1558-1748. DOI: 10.1109/JSEN.2022.3210773.

[64] R. David, J. Duke, A. Jain, *et al.*, "TensorFlow Lite Micro: Embedded Machine Learning on TinyML Systems", en,

[65] P. P. Ray, "A review on TinyML: State-of-the-art and prospects", *Journal of King Saud University - Computer and Information Sciences*, vol. 34, no. 4, pp. 1595–1623, 2022, ISSN: 1319-1578. DOI: https://doi.org/10.1016/j.jksuci.2021.11.019. [Online]. Available: https://www.sciencedirect.com/science/article/pii/S1319157821003335.